

**THE IMPACTS OF GRINDING BALL SIZE DISTRIBUTION
ON ENERGY CONSUMPTION, PRODUCT SIZE AND
MEDIA WEAR WITHIN THE DRY STIRRED MILL**

**KURU KARIŐTIRMALI DEĐİRMENDE BİLYA BOYU
DAĐILIMININ ENERJİ, ÜRÜN TANE BOYU VE BİLYA
AŐINMASI ÜZERİNDEKİ ETKİLERİNİN ARAŐTIRILMASI**

TOLGA SERT

Assoc.Prof.Dr. OKAY ALTUN

Supervisor

Submitted to

Graduate School of Science and Engineering of Hacettepe University

As a Partial Fulfillment to the Requirements

for the Award of the Degree of Master of Science

in Mining Engineering.

2021

ABSTRACT

THE IMPACTS OF GRINDING BALL SIZE DISTRIBUTION ON ENERGY CONSUMPTION, PRODUCT SIZE AND MEDIA WEAR WITHIN THE DRY STIRRED MILL

Tolga SERT

Master of Science, Mining Engineering

Supervisor: Assoc. Prof. Okay ALTUN

(January, 2021, 89 pages)

In today's conditions, it is desired to use water resources more efficiently due to environmental factors. Therefore, it can be said that researches on dry grinding applications, which can replace wet grinding systems with high water consumption, are of increasing importance. Improvements in the field of cement grinding allow for the improvement of the dry grinding process and the development of new equipments. The knowledge accumulated here is transferred to different applications. The mineral industry being one of them, it is aimed to make liberalization in fine sizes more energy efficient. In this context, the importance of dry stirred mills is increasing day by day.

As one of the traditional grinding systems, spherical shaped grinding media with different sizes are used in the ball mills, and grinding performance can be increased by choosing the appropriate grinding media size distribution. It is thought that a similar approach can be applied for dry-stirred mills. Thus, it is predicted that there may be effects on grinding performance and product quality by choosing different grinding media size compositions in dry stirred mills. Although there has been an increasing number of researches on dry stirred mills in recent years, there are still some missing points. Discussing the effect of grinding media size distribution is one of these shortcomings.

Within the scope of this thesis study, the effect of the ball size distribution, which is a variable that directly affects the performance of mills with a grinding medium, on the grinding performance of a vertical dry stirred mill was investigated by batch grinding tests. For this purpose, in the first part of the study, the bi-modal and tri-modal compositions of the media sizes which were selected by using the material size-ball size ratio values developed in the literature were mixed in with different ratios for the vertical stirred mill. The data obtained as a result of the tests performed at different stirrer speeds for calcite, clinker, and copper ores were evaluated in terms of energy, the shape of the size distribution, and the obtained size reduction ratios.

In the following section of the study; The effects of using the grinding media distribution of different sizes on the dry stirred mill with a vertical chamber are discussed.

The findings from this study are expected to be beneficial to dry vertical stirred mill technology, which is expected to become increasingly widespread. In addition, as a result of detailed wear measurements, it will be possible to shed light on companies that can supply spherical shaped grinding media to these mills.

Keywords: Grinding, fine grinding, stirred mill, optimization

ÖZET

KURU KARIŐTIRMALI DEĐİRMEDE BİLYA BOYU DAĐILIMININ ENERJİ, ÜRÜN TANE BOYU VE BİLYA AŐINMASI ÜZERİNDEKİ ETKİLERİNİN ARAŐTIRILMASI

TOLGA SERT

Yüksek Lisans, Maden MühendisliĐi

Tez DanıŐmanı: Doç. Dr. Okay ALTUN

(Ocak 2021, 89 sayfa)

Günümüz koŐullarında, çevresel faktörler sebebiyle, su kaynaklarının daha verimli kullanılması istenmektedir. Bu nedenle de su tüketiminin yüksek olduĐu yaŐ öğütme sistemlerinin yerine geçebilecek kuru öğütme uygulamaları üzerine yapılan araŐtırmaların artan bir öneme sahip olduĐu söylenebilir. Çimento öğütme alanındaki gelişmeler kuru öğütme işleminin iyileŐtirilmesini ve yeni ekipmanların gelişimine olanak sağlamaktadır. Buradan elde edilen bilgi birikimi farklı uygulamalara da aktarılmaktadır. Mineral endüstrisi bunlardan biri olup, ince boylarda serbestleşmenin daha enerji verimli yapılabilmesi amaçlanmaktadır.

Bu bağlamda kuru karıŐırtırmalı değirmanlar üzerine yapılan çalışmaların öneminin günden güne arttıĐı düşünölmektedir.

Geleneksel öğütme sistemlerinden bilyalı değirmenlerde, farklı boylara sahip bilyalar kullanılmakta olup, uygun dağılımın seçimi ile öğütme performansı arttırılabilmektedir. Benzer yaklaşımın kuru karıştırmalı değirmenler için de uygulanabileceği düşünülmektedir. Böylelikle, kuru karıştırmalı değirmenlerde farklı bilya boyu kompozisyonu tercih edilmesi ile öğütme performansı ve de ürün kalitesi üzerinde etkilerin olabileceği öngörülmektedir. Kuru karıştırmalı değirmenlerle ilgili son yıllarda artan sayıda araştırma olmasına karşılık, halihazırda eksik olan bazı noktalar da bulunmaktadır. Bilya boyu dağılımı etkisinin tartışılması bu eksikliklerden bir tanesidir.

Bu tez çalışması kapsamında, öğütücü ortama sahip değirmenlerin performansını doğrudan etkileyen bir değişken olan bilya boyu dağılımının, dik hazneli kuru karıştırmalı değirmenin öğütme performansı üzerine etkisi, kesikli öğütme testleri ile incelenmiştir. Bu amaçla, çalışmanın ilk kısmında, literatürde geliştirilen malzeme boyu ve bilya boyu oranı değerleri kullanılarak seçilen bilya boylarının, dik karıştırmalı değirmen için, ikili ve üçlü bileşimleri farklı oranlarda karıştırılmıştır. Kalsit, klinker ve bakır cevherleri için farklı karıştırma hızlarında yapılan testler sonucunda elde edilen veriler, enerji, boyut dağılımının şekli ve elde edilen boyut indirgeme oranları yönlerinden değerlendirilmiştir.

Çalışmanın ilerleyen kısmında; dik hazneli kuru karıştırmalı değirmende, farklı boyutlara sahip bilya dağılımının kullanılmasının, bilya aşınma değerleri üzerindeki etkileri tartışılmıştır.

Bu çalışmadan elde edilen bulguların, giderek yaygınlaşması beklenen kuru yatay karıştırmalı değirmen teknolojisi üzerinde faydalı olacağı düşünülmektedir. Ayrıca, detaylı aşınma ölçümlerinin yapılması neticesinde bu değirmenlere bilya tedariki yapabilecek firmalara da ışık tutması sağlanabilecektir.

Anahtar Kelimeler: Öğütme, ince öğütme, karıştırmalı değirmen, optimizasyon

ACKNOWLEDGEMENTS

For the received support and assistance throughout the writing of this thesis, I owe a debt of sincere thanks to;

The Head of Hacettepe University Mining Engineering Department who helped me to benefit from the department's resources,

My supervisor, Assoc.Prof.Dr. Okay ALTUN, who guided me during my undergraduate and graduate studies with his knowledge, experience, and motivational support,

Dr. Alper TOPRAK and Dr. Deniz ALTUN who helped me in experimental studies and helped this thesis to develop,

To my colleagues Cumhuriyet Erdem KARAHAN, Seda ÖZÇELİK, Mesut RUSTAMI, Emre YILDIZ, Hakan ŞANIVAR, for their valuable contributions during experimental studies,

Department technicians Mustafa YILMAZ, Işın ASLIYÜKSEK and Cem VURAL, department secretary Sıddık YILMAZOĞLU,

To my mother Meryem SERT and my father Osman SERT, for their financial and moral support, Efe SERT, my precious brother who has stood by me with his mental stamina, Defne Irmak ÇOKER, for her patience and care, Yakup SENEM, who always supports me with his wisdom, and all my beloved friends who always stood by me with their support.

I would also like to thank Hacettepe University Research Foundation Unit (Project No: 119M850) for their financial support.

TABLE of CONTENT

ABSTRACT.....	i
ACKNOWLEDGEMENT.....	v
TABLE of CONTENT.....	vi
FIGURES.....	ix
TABLES.....	xiii
1. INTRODUCTION	1
2. GENERAL INFORMATION.....	4
2.1. Stirred Mills.....	4
2.1.1. Development of The Stirred Mills in The Minerals Industry.....	6
2.1.2. Operating Parameters of Stirred Mill and Their Influences on Grinding Performance	7
2.1.2.1. Stirrer Speed.....	8
2.1.2.2. Media Size and Density.....	9
2.1.2.3. Media Filling	11
2.1.2.4. Feed Rate	11
2.1.2.5. Feed Size	12
2.1.2.6. Mill Geometry.....	13
2.1.3. Modelling of Stirred Mills.....	14
2.1.3.1. Stressing Models.....	14
2.1.3.1.1. Estimation of Stress Intensity.....	16
2.1.3.1.2. Estimation of Number of Stress Events.....	17
2.1.3.2. Population Balance Model.....	21
2.2. Grinding Media and Multi-Model Distribution.....	23
2.2.1. Grinding Media.....	23

2.2.2. Grinding Media Motion in Stirred Mills.....	26
3. EXPERIMENTAL STUDIES and INITIAL TESTWORKS.....	31
3.1. Laboratory Equipments and Test Procedures.....	31
3.1.1. Laboratory Scale Dry Vertical Stirred Mill.....	31
3.1.2. Sympatec Helos Laser	32
3.2. Laboratory Studies.....	33
3.2.1. Experimental Test Matrice.....	33
3.2.2. Preparation of Samples.....	34
3.2.2.1. Calcite	34
3.2.2.2. Clinker	35
3.2.2.3. Copper	35
3.2.3. Media Wear Tests.....	36
3.2.4. Energy Consumption Tests.....	36
3.2.5. Grinding Aid Dosage	37
3.2.6. Rosin Rammler Size Distribution.....	37
4. RESULTS and DISCUSSIONS.....	38
4.1 Batch Test Results.....	38
4.1.1. Results of Calcite Grinding.....	38
4.1.1.1. Monosized Composition Tests.....	38
4.1.1.2. Bi-Modal Composition Tests.....	42
4.1.1.3. Tri-Modal Composition Tests.....	48
4.1.2. Results of Clinker Grinding.....	52
4.1.2.1. Monosized Composition Tests.....	52
4.1.2.2. Bi-Modal Composition Tests.....	55
4.1.2.3. Tri-Modal Composition Tests.....	60

4.1.3. Results of Copper Grinding.....	64
4.1.3.1. Monosized Composition Tests.....	64
4.1.3.2. Bi-Modal Composition Tests.....	68
4.1.3.3. Tri-Modal Composition Tests.....	73
4.2. Wear Tests	76
5. CONCLUSION	78
REFERENCES.....	80
CURRICULUM VITAE	88

FIGURES

Figure 1. The Specific Energy Input Values of Different Mills	4
Figure 2. Schematic Drawing of Continuous Attrition Mill.....	5
Figure 3. The Classification of Stirred Media Mills.....	6
Figure 4.1. Effect of Stirrer Speed.....	8
Figure 4.2. Effect of Stirrer Speed.....	8
Figure 4.3. Effect of Stirrer Speed 1.7-1.2 and 0.85-0.6 mm Media.....	8
Figure 4.4. Effect of Media Size.....	9
Figure 4.5.1. Effect of Media Size For Short and Long Grinding Times.....	10
Figure 4.6. Effect of Media Size on Breakage Rate.....	10
Figure 4.7. Effect of Mill Charge on Grinding Performance.....	11
Figure 4.8. Effect of Feed Rate on Surface Area of The Product.....	12
Figure 4.9. Grinding Performance of The Dry Stirred Mill at Varying Feed Size.....	12
Figure 4.10. Effect of Feed Size on Dry Stirred Mill Performance.....	13
Figure 4.11.1 Effect of Mill Geometry on The Torque and The Product Fineness....	13
Figure 5. Active Volume.....	15
Figure 6. Product Fineness as a Function of Stress Intensity and Specific Energy..	17
Figure 7.1. Relation Between Stress Intensity and Specific Energy.....	19
Figure 7.2. Relation Between Stress Intensity and Stress Number.....	19
Figure 8. Typical Grinding Costs for Grinding Mill.....	23
Figure 9.1. Motion of a Single Media.....	26
Figure 9.2. Particle Trajectory as a Function of Re.....	26
Figure 10. Circumferential Grinding Bead Velocity Distributions.....	27
Figure 11.1. Media Distribution in a Vertical Slice of The Isamill for The 80% Operating Conditions with Media Sizes of (a) 9 mm, (b) 15 mm, And (c) 25 mm.....	29

Figure 11.2. Variation of The Media Distribution and Speed for Three Fill Levels, (a) 70%, (b) 80%, And (c) 90% For 15 mm Media.....	29
Figure 11.3. Variation of Power Draw With Fill Level for Three Different Media Sizes.....	30
Figure 12. Laboratory Scale Vertical Stirred Mill and Stirrer Geometry.....	31
Figure 13. Sympatec Helos Lazer.....	32
Figure 14. Particle Size Distribution of Calcite Feed.....	35
Figure 15. Particle Size Distribution of Clinker Feed.....	35
Figure 16. Particle Size Distribution of Copper Feed.....	36
Figure 17. Particle Size Distribution Plots of Calcite Tests with C1.....	39
Figure 18. Particle Size Distribution Plots of Calcite Tests with C2.....	39
Figure 19. Particle Size Distribution Plots of Calcite Tests with C3.....	40
Figure 20. Specific Energy and Reduction Ratio Relationship of C1, C2, and C3 for Calcite	40
Figure 21. Particle Size Distribution Plots of Calcite Tests with C4.....	42
Figure 22. Particle Size Distribution Plots of Calcite Tests with C5.....	43
Figure 23. Particle Size Distribution Plots of Calcite Tests with C6.....	43
Figure 24. Specific Energy and Reduction Ratio Relationship of C4, C5, C6 for Calcite, and The Void Rates.....	44
Figure 25. Specific Energy and Reduction Ratio Relationship of C2, C3, and C4 for Calcite	45
Figure 26. Specific Energy and Reduction Ratio Relationship of C1, C3, and C5 for Calcite	46
Figure 27. Specific Energy and Reduction Ratio Relationship of C1, C2, and C6 for Calcite	47

Figure 28. Particle Size Distribution Plots of Calcite Tests with C7.....	48
Figure 29. Particle Size Distribution Plots of Calcite Tests with C8.....	49
Figure 30. Specific Energy and Reduction Ratio Relationship of Tri-modal and Monosized Compositions for Calcite and the Void Rates of C7 and C8.....	49
Figure 31. Specific Energy and Reduction Ratio Relationship of All Compositions.....	51
Figure 32. Particle Size Distribution Plots of Clinker Tests with C1.....	52
Figure 33. Particle Size Distribution Plots of Clinker Tests with C2.....	53
Figure 34. Particle Size Distribution Plots of Clinker Tests with C3.....	53
Figure 35. Specific Energy and Reduction Ratio Relationship of C1, C2, and C3 for Clinker.....	54
Figure 36. Particle Size Distribution Plots of Clinker Tests with C4.....	55
Figure 37. Particle Size Distribution Plots of Clinker Tests with C5.....	56
Figure 38. Particle Size Distribution Plots of Clinker Tests with C6.....	56
Figure 39. Specific Energy and Reduction Ratio Relationship of C4, C5, C6 for Clinker, and the Void Rates.....	57
Figure 40. Specific Energy and Reduction Ratio Relationship of C2, C3, and C4 for Clinker.....	58
Figure 41. Specific Energy and Reduction Ratio Relationship of C1, C3, and C5 for Clinker.....	59
Figure 42. Specific Energy and Reduction Ratio Relationship of C1, C2, and C6 for Clinker.....	59
Figure 43. Particle Size Distribution Plots of Clinker Tests with C7.....	61
Figure 44. Particle Size Distribution Plots of Clinker Tests with C8.....	61
Figure 45. Specific Energy and Reduction Ratio Relationship of Tri-modal and Monosized Compositions for Clinker and the Void Rates of C7 and C8.....	62
Figure 46. Specific Energy and Reduction Ratio Relationship of All Compositions for Clinker.....	63
Figure 47. Particle Size Distribution Plots of Copper Tests with C1.....	65

Figure 48. Particle Size Distribution Plots of Copper Tests with C2.....	65
Figure 49. Particle Size Distribution Plots of Copper Tests with C3.....	66
Figure 50. Specific Energy and Reduction Ratio Relationship of C1, C2, and C3 for Copper	66
Figure 51. Particle Size Distribution Plots of Copper Tests with C4.....	68
Figure 52. Particle Size Distribution Plots of Copper Tests with C5.....	68
Figure 53. Particle Size Distribution Plots of Copper Tests with C6.....	69
Figure 54. Specific Energy and Reduction Ratio Relationship of C4, C5, C6 for Copper, and the Void Rates.....	69
Figure 55. Specific Energy and Reduction Ratio Relationship of C2, C3, and C4 for Copper	70
Figure 56. Specific Energy and Reduction Ratio Relationship of C1, C3, and C5 for Copper	71
Figure 57. Specific Energy and Reduction Ratio Relationship of C1, C2, and C6 for Copper	71
Figure 58. Particle Size Distribution Plots of Copper Tests with C7.....	73
Figure 59. Particle Size Distribution Plots of Copper Tests with C8.....	73
Figure 60. Specific Energy and Reduction Ratio Relationship of Tri-modal and Monosized Compositions for Copper and the Void Rates of C7 and C8.....	74
Figure 61. Specific Energy and Reduction Ratio Relationship of All Compositions for Copper	75
Figure 62. Wear rates of C2, C3, and C4.....	76

TABLES

Table 1. Arranged Rinding Media Size Configurations	2
Table 2.1 Details about The Materials which has been Used in The Experiments ..	3
Table 2.2 Test Matrice.....	3
Table 3. Relations Between Media Diameter and Mill Parameters.....	27
Table 4. Technical Characteristics of Dry Stirred Mill.....	32
Table 5. Experimental Study Test Matrice.....	33
Table 6. Dry Stirred Mill Stirrer Speed Information.....	33
Table 7. Media to Material Void Ratios.....	34
Table 8. Grinding Aid Dosage Amount.....	37
Table 9. <i>n</i> Values of C1, C2, and C3 for Calcite.....	41
Table 10. <i>n</i> Values of Monosized and Bi-modal Compositions for Calcite.....	47
Table 11. <i>n</i> Values of Monosized and Tri-modal compositions for Calcite.....	50
Table 12. <i>n</i> Values of C1, C2, and C3 for Clinker.....	54
Table 13. <i>n</i> Values of Monosized and Bi-modal Compositions for Clinker.....	60
Table 14. <i>n</i> Values of Monosized and Tri-modal compositions for Clinker.....	62
Table 15. <i>n</i> Values of C1, C2, and C3 for Copper.....	67
Table 16. <i>n</i> Values of Monosized and Bi-modal Compositions for Copper.....	72
Table 17. <i>n</i> Values of Monosized and Tri-modal compositions for Copper.....	75

1. INTRODUCTION

The grinding process is energy-intensive and known as very inefficient regarding the energy transfer to the particles. While more than 50% of the energy is spent in size reduction processes, only 2 - 20% is transferred [1]. The remaining part is dissipated as heat, sound, and vibrations caused by the intergranular and internal friction between the particles and the mill elements.

Many researchers and machine manufacturers are focusing on simulation, machine designs, etc. to improve energy efficiency [2]. Moreover, with the need for efficiency in water usage in industrial processes, the dry-grinding process has recently started to attract more attention in the mineral industry compared to traditional grinding systems [2,3]. In order to improve the efficiency of the process, process parameters of the milling section are being improved, or energy-efficient grinding technologies are being developed. The dry stirred mills can be considered as one of the efficient machines that can be employed in fine grinding duties [3].

Stirred mills are named as a proven technology in wet applications on account of its provided benefits in mineral processing operations i.e., increased grade and recovery. For the wet operations in mineral processing, fine grinding technology is utilized particularly in the regrinding stage to increase the degree of liberation or for surface cleaning purposes. Dry stirred milling technology provides a distinctive possibility for online control and a chance for optimizing the regrind product particle size as well. The technology is already in use for the paint, pharmaceutical, and food industries. In addition, recent researches focused on its application in cement grinding circuits.

Grinding media is a vital part of the grinding machine owing to its significant influence on the grinding efficiency as well as the operating costs. An optimal mixture of media with different sizes provides an efficient increase in the number of contacts, for a given volume of grinding zones. Additionally, the size distribution of the media may have an improved effect both on the economy of the grinding operations and product quality.

Within the scope of the thesis, the influences of the ball size distribution on the operation of dry stirred mills are to be investigated that have not been performed so far. In this context, the grinding media samples with sizes between 1.5 mm to 4 mm were used within a laboratory-scale vertical batch operated dry stirred mill. Within the study, the grinding media compositions arranged and operated as monosized or a combination of 2 or 3 different size intervals (bi-modal or tri-modal distributed). Therefore, a thorough investigation was undertaken. Table 1 summarizes the grinding media size configurations used within the thesis study.

Table 1. Arranged Grinding Media Size Configurations

Type	Code	1.5 mm	2.5 mm	4 mm	Average
Monosized	C1	100%	0%	0%	1.5 mm
Monosized	C2	0%	100%	0%	2.5 mm
Monosized	C3	0%	0%	100%	4 mm
Bi-modal	C4	0%	50%	50%	3.25 mm
Bi-modal	C5	50%	0%	50%	2.75 mm
Bi-modal	C6	50%	50%	0%	2 mm
Tri-modal	C7	33%	33%	33%	2.66 mm
Tri-modal	C8	10%	25%	65%	3.375 mm

Certainly, the variations in the size of the grinding media have influences on the comminution results of the mill. Such a change not only affects the grind size but also the wear within the mill. Consequently, detailed studies are recommended to investigate these phenomena. The wear mechanism is composed of abrasion, impact, and corrosion.

These mechanisms are based on both interactions between the grinding media itself and the characteristics of samples processed i.e. abrasion, grindability, chemical composition, etc.

The wear measurement procedure includes weighing the grinding media after every grinding process hence cumulative weight losses were measured. The obtained data from each of the grinding media discussed to investigate the effects of the composition and milling conditions on media wear.

Within the scope of the thesis 3 different materials were tested; calcite, clinker, and copper ore. Table 2.1 Summarizes the origin and the d_{80} and d_{50} values of the feed particle sizes. The tests were performed at different grinding times and tip speeds. Test matrice as given in Table 2.2

Table 2.1 Details about The Materials which has been Used in The Experiments

Mineral Type	Origin	d_{80} (μm)	d_{50} (μm)
Calcite	Niğtaş	222	101
Clinker	Bursa Cement	237	101
Copper	Acacia Mining	99	12

Table 2.1 Test matrice

C1	RPM	1"	5"	10"
	4.48 m/s			
	4.06 m/s			
	3.36 m/s			

The findings from this study are expected to be utilized in discussing the optimization alternatives of stirred milling. Such discussions may enlighten some of the points as the dry stirred mills are expected to have widespread use in the near future. Besides, as a result of detailed wear measurements, it will be possible to provide data to manufacturers who produce grinding media to these mills.

2. GENERAL INFORMATION

2.1. Stirred Mills

The purpose of comminution is to reduce the size of a particular material to the desired level for the downstream or end-use. This process is affected by macroscopic and microscopic features of a given material that affects the resistance to grinding. In industrial applications, there are various types of mills available for comminution purposes. Napier-Munn classified the mills according to the operating size ranges and energy consumption levels [4] (Figure 1).

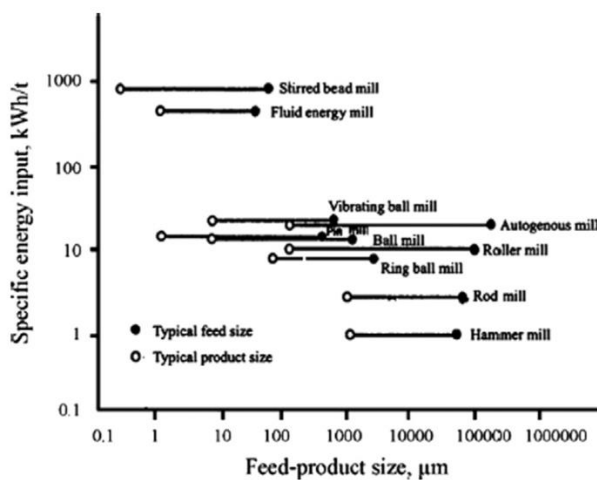


Figure 1. The Specific Energy Input Values of Different Mills [4]

For conventional grinding processes, tumbling mills are often used. In this regard, rod and ball mills are generally preferred for grinding the particle down to 100 μm . Either for rod or ball-shaped grinding media, cataract and cascade type of motions are dominant [5].

Fine and ultra-fine terms can define different sizes that depend on the process. Fine grinding defines the operations with a required product particle size with P_{80} values (80% passing) of 100 μm [6] and ultrafine grinding terms are valid for below P_{80} value of 20 μm [7]. As the grind size gets finer, more surface of grinding media is required. Therefore the small diameter of grinding media are used to improve the number of contacts [8].

The required momentum for small beads (1 – 6 mm) is hard to achieve with gravity. Stirred media mills can generate the required momentum for the media by its rotating impeller which provides high collision intensities due to its speed. The amount of accelerations can be as high as several thousand m/s^2 [9] and have high power densities with a range between 40 and 300 kW/m^3 (compared to 20 kW/m^3 for a ball mill) [10] which can considerably reduce the required plant space at a given throughput. Due to this energy efficiency, stirred milling technology has been firmly established over the past twenty years as superior to ball mills for fine and regrind operations [11]. Stirred mills are now widely used in many mining sectors [12], although they have been used for many years in other industries [5]. This technology has been shown to be more energy efficient with considerably more possibilities for the optimization of fine and coarse grinding in the future [13]. The schematic drawing of a vertical stirred mill can be seen in Figure 2 [14].

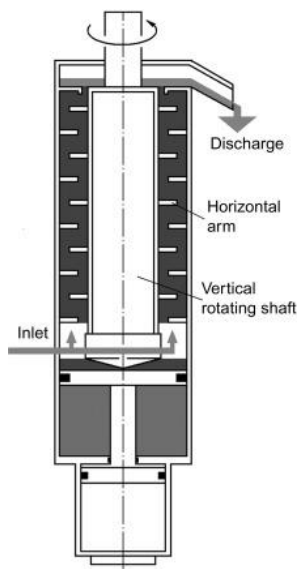


Figure 2. Schematic Drawing of Continuous Attrition Mill [14].

The stirred media mills can be classified as given in Fig. 3. [15]. Operational differences are the main reason for choosing either vertical or horizontal orientation. Because of the higher media fillings (up to 85%), higher agitator speeds (6-22m/s), and small grinding media size (1mm), horizontal stirred mills make the operations more energy efficient over the vertical stirred mills [16].

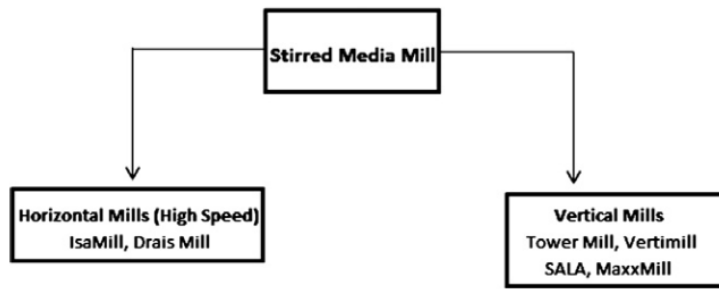


Figure 3 The Classification of Stirred Media Mills [15].

In addition to energy efficiency, the scaling-up of the mills is also an important parameter for selecting a suitable configuration. The vertical stirred mills have scale-up problems to larger sizes because of the start-up torque [16]. Manufacturers pointed out that the mechanical design of the vertical mill was dominated by the start-up torque on the bottom stirrer after a shut-down. On the other hand, in horizontal mills, many stirrers are available to stir the settled load thus the scale-up procedure was easier compared to vertical mills [16].

2.1.1. Development of The Stirred Mills in The Minerals Industry

In 1922, Szegvari stirred a gallon with gravels for a rapid disperse of a sulfur suspension, which is the first example of an agitated vessel and media for comminution [17]. This led to the invention of the first stirred mill by Klein and Szegvari in 1928 [18]. In the following decades, different stirred media mill designs have been developed.

In the 1950's, Tower mill was the first gravity-induced stirred mill invented by the Japan Tower Mill Company. In the 1980s, Metso has developed the Vertimill with an improvement to this technology [19]. The media motion is generated by the rotation of a stirrer in these mills. The speed is not enough to entirely suspend the media. Because of that, at the top of the helix, the beads cascades downwards with gravity. The media stays in an intimate contact for efficient grinding because of the settling. It provides a settled zone of filling above the media which can be extracted as product without a need for screens [20]. The media should be relatively large, with a diameter range between 12 mm to several cm to ensure settling [21].

In the 1960s, the SMD was developed by English China Clay. In these mills, sand was used as media originally. However, in recent decades it was replaced with ceramic grinding beads with small diameters. SMDs have been used in calcium carbonate and kaolin grinding applications, producing particle sizes down to 1-2 μ m [22], for the last 45 years [19]. The design with a vertical octagonal tank with a multi-layer high-speed pin impeller to fluidize the media[21], is similar in concept to the Attritor mill which originated from the high-speed sand grinder that was invented in 1948 by Du Pont for pigment grinding that utilized the sand as grinding media [23].

The IsaMill which has a horizontal disc mill, developed by Netzsch and Mount Isa Mines Ltd. and commercialized for ultra-fine grinding in 1999 [24]. With a horizontal cylindrical chamber and a series of perforated discs connected to a central shaft as an agitator, it was thought to be a high-speed fluidized mill. IsaMill can produce very fine product sizes with p_{80} values as low as 7 μ m [20] with relatively fine grinding media, at around 1-8mm in diameter [25]. Besides the similar operating conditions with SMD's, IsaMill has a narrower particle size distribution due to a lower tendency for coarse particle bypassing, which is beneficial for efficient leaching of precious metals [26].

2.1.2. Operating Parameters of Stirred Mill and Their Influences on Grinding Performance

There are several parameters that can affect the grinding results of a stirred mill. These parameters affect performance hence specific energy consumption and size-reduction relationship [27, 28, 29, 30, 31]. The design and operating conditions of the mill, slurry rheology should be taken into consideration while evaluating the milling performance. For instance, it is possible to achieve a saving of up to 27% in energy consumption in dry horizontal stirred mills when operating conditions are adjusted properly [32].

The following sections discuss the influences of some of the operating parameters briefly.

2.1.2.1. Stirrer Speed

The collision probability between the media and particles is related to the high energy intensity environment and can mainly be increased by the stirrer speed. The studies showed that increasing the stirrer speed increased energy consumption and lowered the product size [4, 5, 31, 32, 33, 34, 35, 36].

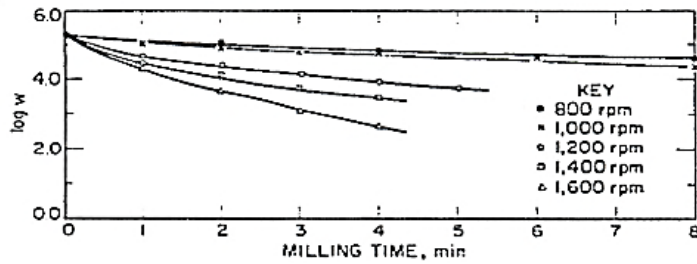


Figure 4.1. Effect of Stirrer Speed [37]

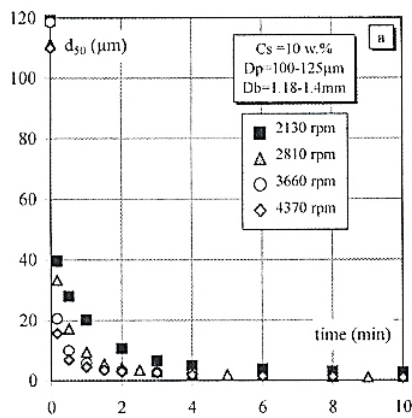


Figure 4.2. Effect of Stirrer Speed [35]

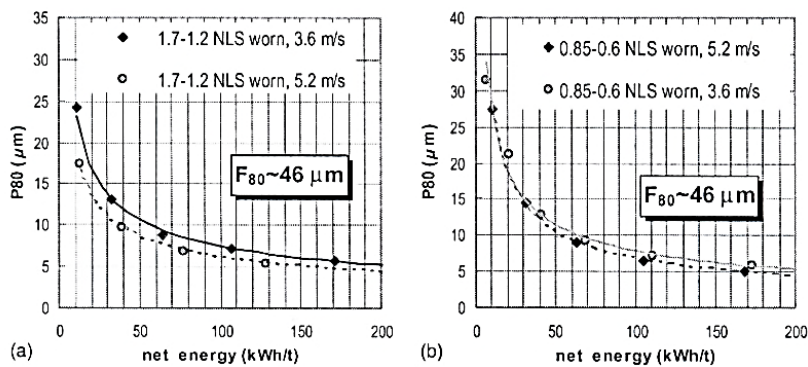


Figure 4.3.1. Effect of Stirrer Speed 1.7-1.2 mm Media Figure 4.3.2. 0.85 - 0.6 mm Media [5]

In 2018, Prziwara reported that the stirrer speed was defined as a more critical operating parameter than other values like media size and material with the continuous tests on a dry horizontal stirred mill.

Since the deflector wheel is coupled with the central shaft, the stirrer speed does not only affects the stressing energy of the media, but also the retention behavior of the wheel classifier at the end of the mill. Additionally, the axial transport velocity is directly affected by the mixing intensity provided by the stirring unit [38].

2.1.2.2. Media Size and Density

The efficiency of the grinding process can be improved with the selection of the proper size of grinding media. Reduction of the energy consumption due to the fluidity of the bulk media and the particle size of the product can be achieved with the use of smaller bead sizes in a stirred mill operation [31, 39]. The limitations of the lowest media size need to be considered to avoid inefficiency (Figure 4.4). The product size distribution became finer and less energy was utilized when media size got finer [5, 35, 40, 41, 42, 43, 44, 45].

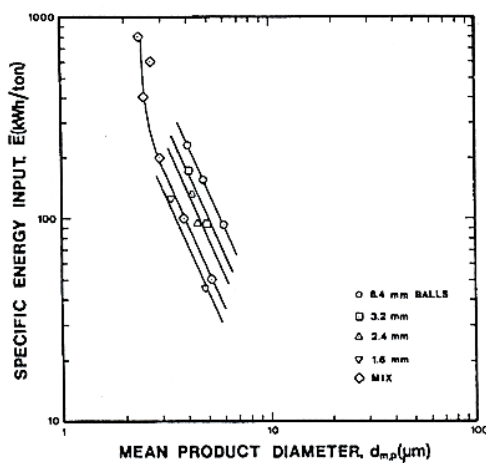


Figure 4.4. Effect of Media Size [40]

The grinding performance of beads depends both on the feed size and target size of the product. Smaller size media should be preferred as the feed size to the mill gets finer [35] (Figure 4.5.1, Figure 4.5.2).

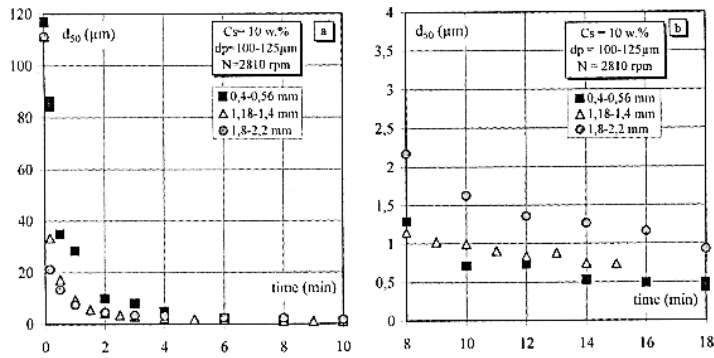


Figure 4.5.1. Effect of Media Size For Short and Long Grinding Times [35].

Mankosa [40] investigated the breakage rate of the grinding action to find the optimum ratio of $D_{\text{ball}}/D_{\text{particle}}$ (Figure 4.6). The breakage rate increased with increasing $D_{\text{ball}}/D_{\text{particle}}$ ratio up to a point that (20:1) media became too small to nip the particles. In addition, another approach has made the optimum ratio of $D_{\text{ball}}/D_{\text{particle}}$ as 12:1 to obtain efficient grinding performance by Zheng et al. [46]. In 2013, Altun investigated the effects of the media size with a dry horizontal stirred mill with a cement grinding purpose and reported that the use of finer media was advantageous over the coarser one and 27% energy saving was achievable. Additionally, 4 mm media size was the lowest limit as no difference in size reduction and energy efficiency were observed compared to 3 mm media size [32].

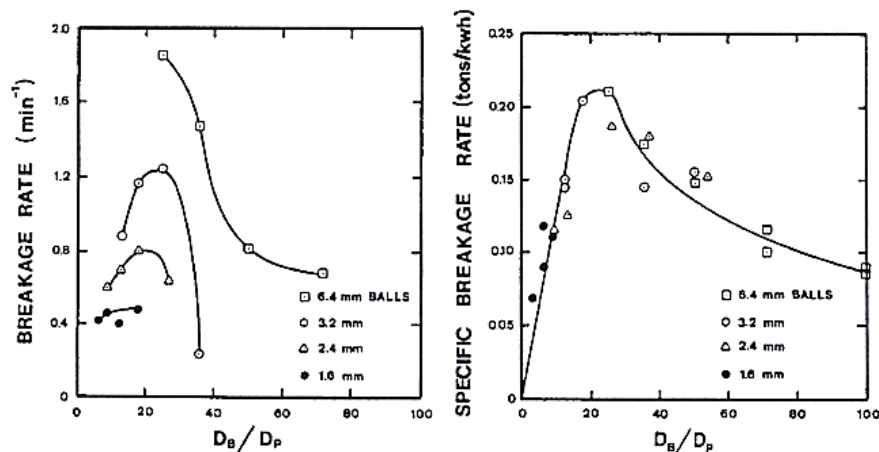


Figure 4.6. Effect of Media Size on Breakage Rate [40]

In stirred milling, most of the energy is used to stir the charged beads. Therefore the change in media density directly affects energy consumption. In general, the use of denser grinding media results in more energy consumption compared to the lighter ones [46]. Various materials like steel, slag, ceramic, glass, etc. can be used as grinding media. The differences between the steel and glass beads were investigated by Zheng et al. [31]. The use of steel balls resulted in obtaining better grinding performance by consuming nearly double of the energy. In a similar study by Mankosa et al. [40], the steel balls produced finer materials.

2.1.2.3. Media Filling

Media filling affects the ball to material amount ratio, thus the fineness of the product. In addition, the main effect of the media filling is observed on the power draw and specific energy consumption. Lower media fillings created an inefficient grinding environment. In other words, higher specific energies were required for lower media fillings to obtain higher size reduction values [32].

It is recommended that mills run at maximum media fill due to their improved grinding performance [37, 43, 47].

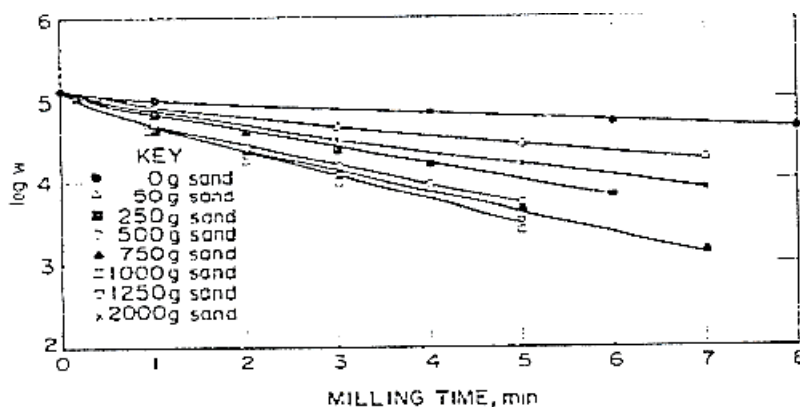


Figure 4.7. Effect of Mill Charge on Grinding Performance [37]

2.1.2.4. Feed Rate

Specific energy which is the function of power draw and feed rate is one of the most important parameters related to the fineness of the product in any kind of grinding operation. For the same media filling, decreasing the feed rate is expected to increase the surface area of the product [33, 36]. Altun also proved that increasing

feed rate decreased specific energy consumption thus coarser product was obtained [32].

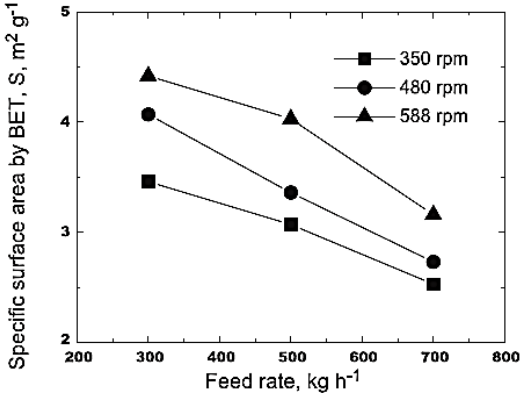


Figure 4.8. Effect of Feed Rate on Surface Area of The Product [33]

2.1.2.5. Feed Size

The dry horizontal stirred mill performance at varying feed size distribution was also investigated by Altun. The test results implied that obtained size reduction was much more rapid for coarse grinding when compared with relatively fine feed (Figure 4.9). As a result of the test studies, F₅₀ of 25 μm was determined as the optimum feed size that efficient grinding was undertaken (Figure 4.10). The top size of the material (150 μm) divided by the media size used in grinding tests (4 mm), was stated as optimal level (27:1) of D_{ball}/D_{particle} [32].

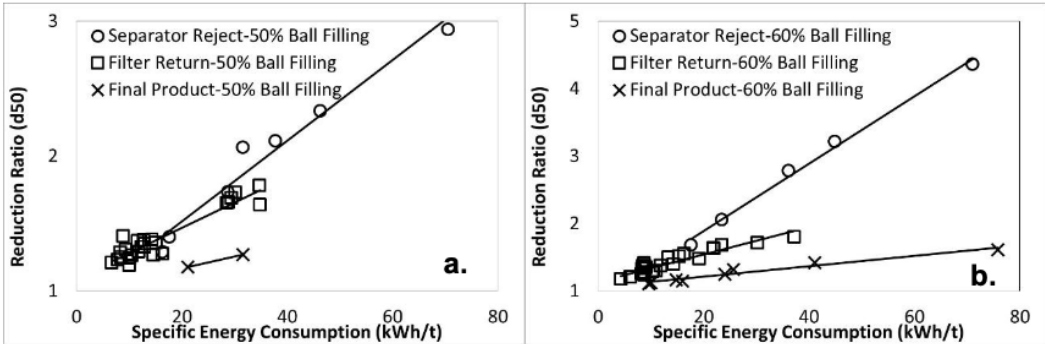


Figure 4.9 Grinding Performance of The Dry Stirred Mill at Varying Feed Size [32]

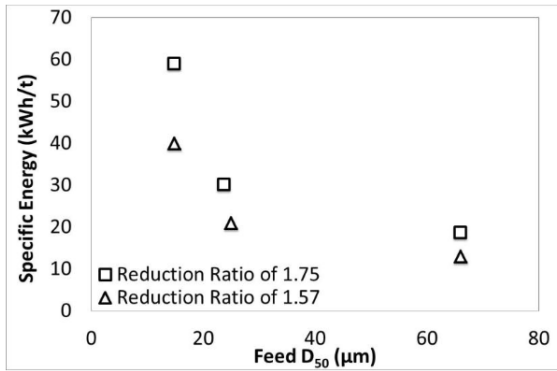


Figure 4.10. Effect of Feed Size on Dry Stirred Mill Performance [32]

2.1.2.6. Mill Geometry

The environment where grinding takes place has influences on the performance. Some research studies have been reported in the literature investigating the effects of mill geometry on stirred media mill performance. There are several studies on developing the relationship between mill geometry and operating conditions [31, 48]. These studies revealed that the diameter of the stirrer affected the torque directly (Figure 4.11.1). Furthermore, reducing the stirrer diameter to mill diameter ratio resulted in obtaining a coarser product (Figure 4.11.2).

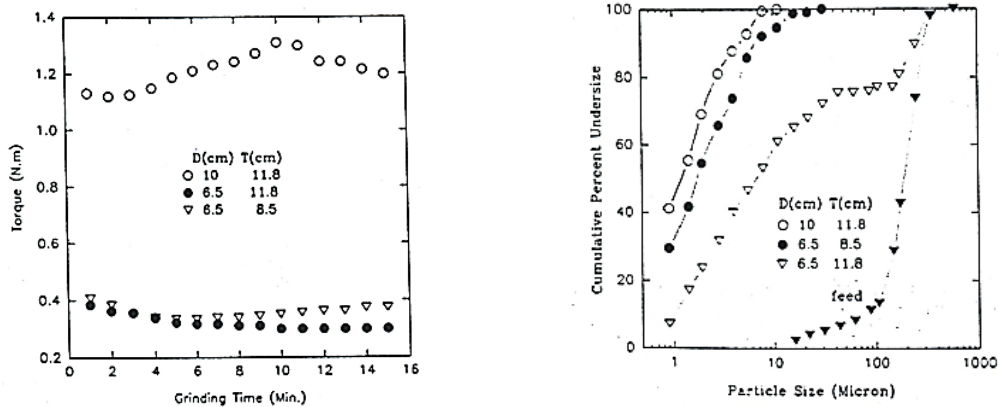


Figure 4.11.1 Effect of Mill Geometry on The Torque and The Product Fineness [31]

2.1.3. Modeling of Stirred Mills

2.1.3.1. Stressing Models

The specific energy input is obtained by dividing the applied energy by the total particle mass or volume. It has long been known that this is one of the parameters that have the highest impact on product particle size [48]. As observed in many studies, changing the particulate solids concentration at a given energy input within certain limits does not have a significant effect on product size [49, 50, 51, 52]. The increase in the number of particles in the grinding environment reduces media-media contact interactions. This way, the fraction of energy transferred to the particles increases. The particles are stressed between the media. The interactions in the void between two colliding media can be defined with the active volume concept. The capturing efficiency is represented by the number of particles stressed per collision. These concepts were developed by Kwade to define the stress intensity theory [53].

Most of the energy available for comminution can be absorbed by the particles that first bridge the gap between two colliding media, either by being larger particles or by being close to the point of minimum separation between the media. The capturing efficiency is less than 1 at low solids contents, so in some collisions the energy is wasted and there are no particles to stress. In the optimum solids content region, it is unlikely to bridge the gap between the media at the same time with several particles. Most of the energy is transferred into a single particle. In this situation, the capturing efficiency is nearly 1, and efficiency is maximized.

Several particles can be stressed simultaneously at excessively high solid contents (capturing efficiency is higher than 1). In this situation, the energy is distributed over a larger area, reducing the likelihood of comminution. In addition, media motion dampening by viscous dissipation can be considered [44].

The solids contents range in which product size appears to follow the input of specific energy can be explained with the wide range of solids contents between avoiding collisions where multiple particles are stressed at once and also with no particles.

Specific energy input is proportional to the stress number (SN), and the stress-energy (SE). The average number of collisions per particle in a certain grinding time

defines the stress number and the measure of the average energy of the collisions defines stress energy. Grinding occurs between two grinding media where the particles are stressed in a stirred mill. However, the particles need to be captured by the media and not get carried away by the fluid to stress. Particles can be stressed in three different ways.

- Single particle stressing.
- Multiple particles are captured and all of them are stressed. Largest particle is subjected to the maximum stress.
- A particle bed is captured and stressed.

Kwade [55] stated that the number of particles captured between two media was a function of solids concentration and particle size (x) and determined by the ratio of the diameter of active volume between two grinding media (d_{act}) (Figure 5) and the average distance between two particles in suspension.

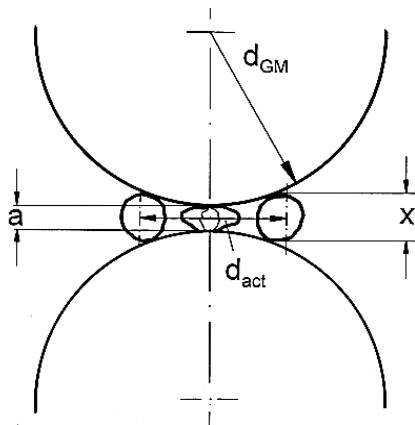


Figure 5. Active Volume [55]

The number of stress events and the intensity of stress parameters comes forward in stressing models of the stirred mill. Mathematical expressions of these parameters are explained in the next section.

2.1.3.1.1. Estimation of Stress Intensity

Kwade and Stender [56] reported that the motion of grinding media which directly influences the grinding performance of the mill influences the stress intensity parameter. Grinding action mainly takes place around stirrers and in the zone of the chamber wall because of the centrifugal action created by the stirrer. Media gain kinetic energy as a result of this movement and the theory relates stress intensity with kinetic energy.

Kwade [41] calculated stress intensity parameters as a function of circumferential speed of the discs, size, and density of the media (Equation 1).

$$S I = D_b^3 * (\rho_b - \rho) * v_d^2 \quad (1)$$

Where;

D_b (m) : Size of the media

v_d (m/s) : Circumferential speed of the discs

ρ_b (t/m³) : Density of the media

ρ : Density of the material

Kwade et al. [41] performed several studies with limestone at different stress intensities (SI) and specific energy inputs to reveal the effects of stress intensity on grinding performance. In Figure 6, a change in median particle size as a function of different operating conditions is presented. The trend of the curve does not change with applied energy as can be seen from the figure. The median size has a reverse correlation with SI and it reaches a minimum point at a certain level. The material starts to get coarser due to high energy losses after this point, therefore it is at the optimum value of stress intensity where an efficient operation is performed [41, 48, 55, 57, 58, 59].

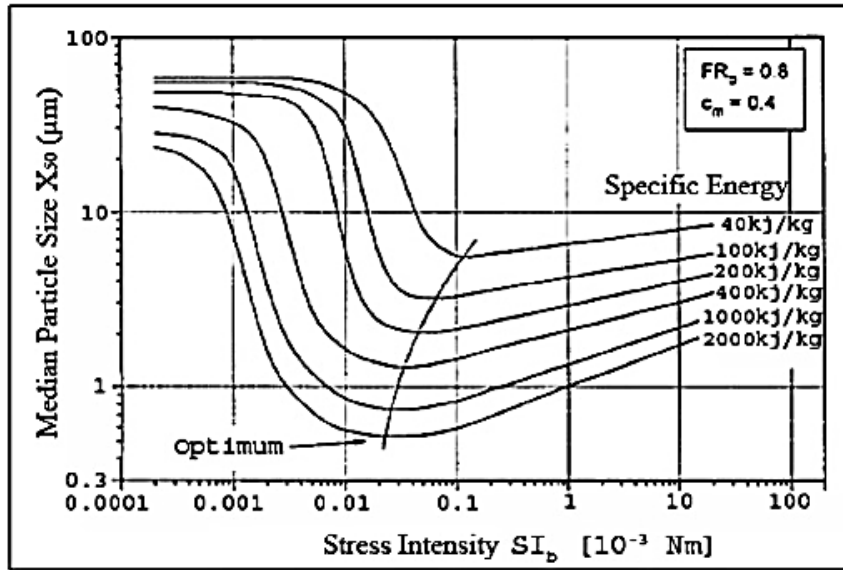


Figure 6. Product Fineness as a Function of Stress Intensity and Specific Energy [41]

2.1.3.1.2. Estimation of Number of Stress Events

The number of stress events (SN) which is given in Equation 2.1 as a function of the media contacts' number (N_c), the probability that a particle is caught and stressed (P_s), and the number of product particles inside of the mill (N_p) was estimated by Kwade [58] with the mathematical expressions of each parameter.

$$SN = \frac{N_c P_s}{N_p} \quad (2.1)$$

The number of media contacts (N_c) which is given in Equation 2.2 is proportional to the number of revolutions of the stirrer and number of grinding media in the chamber (NGM).

$$N_c \propto nt N_{GM} \propto nt \frac{V_{GC} \phi_{GM} (1-\epsilon)}{\frac{\pi}{6} d_{GM}^3} \quad (2.2)$$

Where;

n (s^{-1}): the number of revolutions of the stirrer per unit time

t (s): the milling time

VGC (m^3): the volume of the grinding chamber

\emptyset_{GM} : the filling ratio of the grinding media

ϵ : the porosity of the bulk of grinding media

d_{GM} (m): the diameter of the grinding media

The capturing and sufficient stress probability of a particle by grinding media (P_s) depend on the material and the type of the grinding process. In the case of crystalline material grinding the probability is proportional to the active volume between two grinding media which is affected by the diameters of them (Equation 2.3) [58].

$$P_s \propto d_{GM} \quad (2.3)$$

As given in Equation 2.4, the number of product particles inside the mill (N_p) is proportional to the overall volume of them that is expressed as;

$$N_p \propto V_p = V_{GC}(1 - \emptyset_{GM}(1 - \epsilon))c_V \quad (2.4)$$

When the equations of each parameter is put into Equation 2.1, Equation 2.5 is obtained;

$$SN \propto n \cdot t \cdot \frac{\emptyset_{GM}(1-\epsilon)}{(1-\emptyset_{GM}(1-\epsilon))c_V} \frac{x^3}{d_{GM}^2} \quad (2.5)$$

Where;

x : mean product size

In stirred milling, the energy consumption (E) of grinding operation correlates with stress intensity and the number of stress events parameters (Equation 2.6). Kwade and Stender [56] stated that a constant grinding result, which is beneficial for the scaling-up of the mill, was achievable if the two of these parameters were kept constant. Relations between these parameters are illustrated in Figure 7.1 and Figure 7.2.

$$E \propto SI \cdot SN$$

$$(2.6)$$

Stress intensity-dependent change in energy utilization is shown in Figure 7.1. The points of signature plots produced at different stress intensity and energy levels for given median particle size ($2 \mu\text{m}$) shows that energy consumption decreases until a certain value of stress intensity then it starts to increase [58]. The minimum value of the curve is called the optimum energy requirement for the specified product size. The correlation between stress intensity and stress number parameters is illustrated in Figure 7.2. Two parameters are inversely proportional to each other as indicated. At very small stress intensities the trend tends go to infinity indicating that no evident comminution takes place.

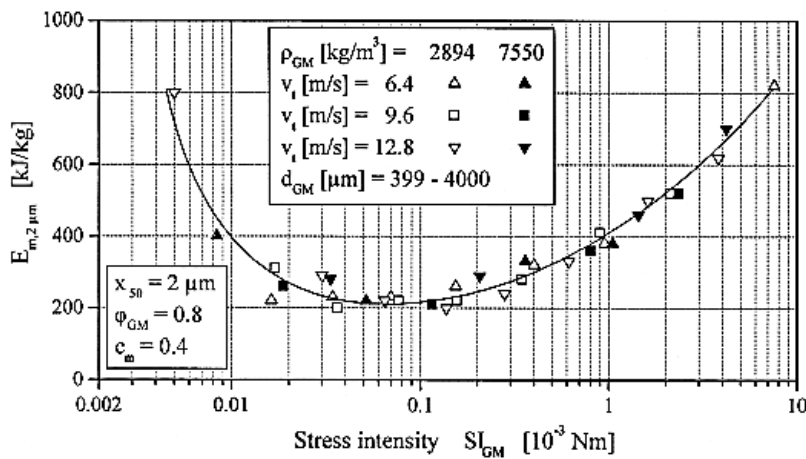


Figure 7.1. Relation Between Stress Intensity and Specific Energy [58]

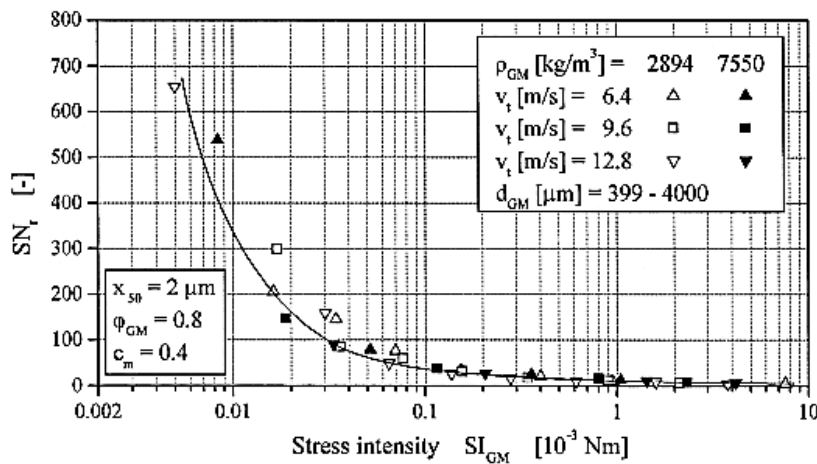


Figure 7.2. Relation Between Stress Intensity and Stress Number [58]

In 2020, the study by Prziwara investigated capturing of fine dry particles between grinding media and updated stressing equations accordingly [60]. The study shows that the motion behavior of fine particles between a static plate and a falling ball is determined by various operational parameters. An increase in the flowability and the product fineness leads to an improved displacement of the particles out of the grinding zone between the grinding media, higher impact velocities, as well as media sizes, increase the particle capturing. So that, the capturing is subsequently shown to be progressively dependent on the mentioned parameters for finer feed.

The experiments that use a sphere-sphere geometry shows that the particle capturing is nearly four times higher for the contacts of ball-plate geometry. A comparison between the results of the already existing active volume model by Schönert showed that the model yields values in the right magnitude only for the ball-plate geometry, even though Schönert was actually aiming to model the media to media contacts. For media to media contacts, however, the Schönert model overestimated the particle capturing. In addition, the model does not allow an adequate explanation of most of the parameters.

Consequently, a model extension was proposed to explain the impact of the parameters more accurately. A much more adequate definition of the active volume was achieved by

- Categorizing the flow behavior together with the fineness range of the feed powder,
- Incorporating the effect of the relative impact velocity of the grinding media and
- Considering stress geometry.

This simplification enables a very fast and precise particle capturing characterization. [60].

The equation 3 as the model which updated by Prziwara and the parameters are explained below [60].

$$m_{A,new} \propto V_A \cdot \rho \propto \frac{\pi}{4} (d_{GM} \cdot k \cdot \sin \alpha_{new})^2 \cdot 4x_{max} \cdot \rho \quad (3)$$

where;

VA: Active Volume

P: Bulk Density

dGM : Grinding media diameter

k : the particle capturing is calculated for a ball-plate contact (k = 1) or a ball-ball contact (k = 0.5)

xmax : maximum particle size in the feed material

The parameter $\sin a_{new}$ can be calculated with the following equation;

$$\sin a_{new} = a \cdot v_{impact}^b \quad (4)$$

where;

a: Contact angle

v_{impact}^b : impact velocity

2.1.3.2. Population Balance Model

The population balance model is used for modelling of the comminution equipments. Equation 5.1 gives the population balance model equation which was developed by Epstein [61].

$$p_i = f_i + \sum_{j=1}^i a_{ij} r_j s_j - r_i s_i \quad (5.1)$$

where ;

f_i : feed rate of size fraction i (t/h);

p_i : product flow of size fraction i (t/h);

a_{ij} : the mass fraction of particles of size j that appears at size i after primary breakage;

r_j : the rate of material breakage for particle size i;

s_i : amount of size i particles inside the mill (tonnes).

In a situation where the mill content data (s_i) is missing, on the assumption that the product size distribution is a function of discharge rate (d_i) and the mill content (Equation 5.2), the population balance model equation is transformed into Equation 5.3 which is named as the perfect mixing approach [62].

$$p_i = d_i s_i \quad (5.2)$$

$$f_i + \sum_{j=1}^i a_{ij} p_j \frac{r_j}{d_j} - p_i \frac{r_i}{d_i} - p_i = 0 \quad (5.3)$$

The approach of perfect mixing explains the grinding operation by the breakage rate (r or r/d parameters), which depends on the operational conditions of the mill [63] and function of breakage distribution (a_{ij}). In order for the development of a model structure of the mill, the r/d function is correlated with the operational conditions. But it requires the determination of the appearance function of the first sample [64].

In 2019, the model was used by Altun for the development of modeling for the dry stirred mill with the data obtained from the Hardgrove mill and drop weight tests with coarse cement, filter return, granulated blast furnace slag, fly ash and finished cement samples at different energy levels and size intervals. The appearance functions of each sample was calculated by using the correlation between specific comminution energy and t_{10} values or fines' generation. Calculated appearance functions were inputted to the perfect mixing model and r/d values were back-calculated. In this regard, the feed and product data from the comminution tests of a pilot-scale dry stirred mill was used. It was observed that both Hardgrove and impact bed breakage tests lead to having an agreement between the experimental and calculated product size distributions when the r/d data plots were compared. The later stage of the study focused on the development of modeling for the dry stirred mill by using the breakage function from the Hardgrove mill, which was found convenient and easier [64].

2.2. Grinding Media and Multi-Model Distribution

2.2.1. Grinding Media

Understanding the contribution of the grinding media to the grinding process has great importance because of its effects on the operation of industrial mills. As the surface area of the grinding medium expands, it provides improved contact with the ground material. In addition, capturing efficiency and density of the beads need to be considered. However, the balance of these requirements must be well adjusted because of the inverse correlation between the diameter of the grinding medium and the specific surface. Moreover, the consumption of the grinding media takes between 21 - 45% of the costs of the grinding operations (Figure 8.) [65]. However, the media and energy consumptions can be reduced by 5 - 10% with proper wear-resistant grinding media usage [2, 84]. There are other various approaches besides the wear-resistant material in the literature to reduce grinding media consumption such as using higher quality, etc.

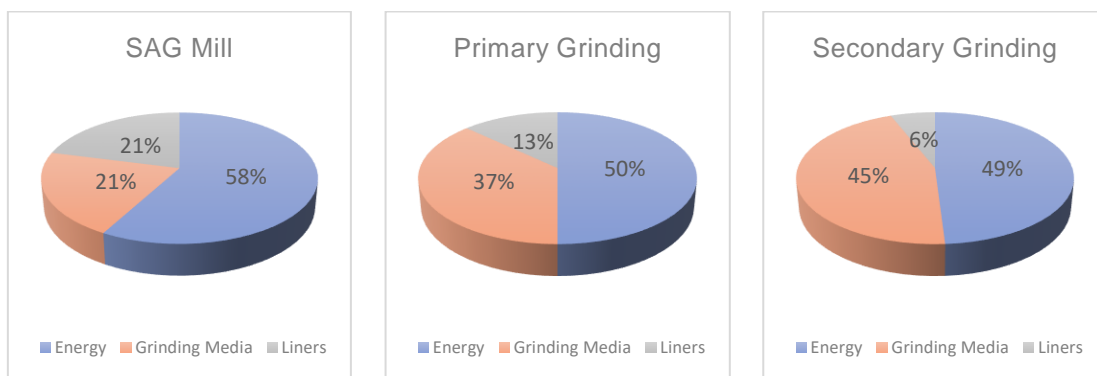


Figure 8. Typical Grinding Costs for Grinding Mill [84]

While selecting a material for grinding media the properties i.e resistance to wear, the supplier availability and the given grinding system need to be a wide range of considered materials which are available to provide wear-resistant grinding operation [66]. The abrasiveness of the ore directly affects the total wear rate of a grinding media, but the metallurgical properties for the grinding media must balance characteristics as conflicting as high hardness which maximizes abrasive wear strength and adequate ductility to avoid rapid ruptures and chipping. The main materials that used for grinding media are high-chromium white cast iron and steel.

High-chromium white cast iron and steel are widely used in the production of commercially used steel for balls. The low alloy high carbon steel is majorly used in the steel media production. High carbon steels (0.6–1.4% C) are the hardest, strongest, but the least ductile type among all steel types. They are mostly used in their hardened and tempered form, which ends up in them having expressive strength against abrasive wear as compared to other steel types. [67, 68].

One of the major operating problems for the ball milling is the make-up charge which is defined as the function of media consumption to balance the size distribution. The consumption of the grinding media takes a huge part of the grinding operational costs. The costs may reach up to 40% of the operational costs of mineral processing [69], and wear constitutes around 60% of the cost associated with ball milling [70].

It is important to determine the optimum ball size, for a given operation. As the grinding medium diameter increases, the force between the grinding surfaces increases so that larger particles can be broken [79]. Selecting a small size of balls leads to inefficient grinding due to insufficient energy. The largest and hardest particles in the feed should be taken into account when selecting the grinding media sizes. Various formulas have been proposed in the literature for the required ratio of ball size to ore size, but none of them are precise. The practice of charging balls to a tumbling mill is a matter of experience as well [80]. The capacity of a mill increases with decreasing the media diameter, due to the increase in grinding surface, to the point where the required angle of the nip between contacting balls and particles is exceeded. During the operation, grinding media are reduced in size because of wear. Due to that grinding characteristics change. The extent of wear is dependent on the characteristics of the rock present, such as density, composition, and surface hardness. It is also affected by the rotation speed, the mill diameter, the specific gravity of the mineral, and the work index of the mineral [20]. As a result of the studies, the following results had been reached in the selection of the optimum ball size for ball milling. Different approaches were considered such as feed size, mill speed, grindability, mill geometry, and some other variables (Table 3).

Table 3. Relations Between Media Diameter and Mill Parameters [81]

	Particle Size, d	Grindability W_i	Mill Speed, N	Mill Diameter D	Other Variables
Davis, 1919	-	-	important	-	-
Fahrenwald ve Lee, 1931	$d^{0.5}$	-	-	-	-
Coghill ve DeVaney, 1938	$d^{0.5}$	$W_i^{0.2}$	independent	-	-
Gow vd., 1934	$d^{0.5}$	important	important	-	-
Bond, 1958	$d^{0.5}$	$(W_i \cdot S_g)^{0.34}$	$(1/N)^{0.34}$	$(1/D)^{0.17}$	Dry - Wet, Discharge
Herdan, 1960	$d^{0.5}$	-	-	-	-
Azzaroni, 1981	$d^{0.28}$	$W_i^{0.4}$	$(1/N)^{0.26}$	$(1/D)^{0.26}$	Circulating Load
Herbst vd., 1986	dependent	dependent	independent	independent	-
Austin vd., 1984	$d^{0.5}$	-	-	$(1/d)^{0.1-0.2}$	-
Lianxiang vd., 1988	$25.8+20.4 \ln d$	-	-	-	-

For ball milling there exists different approaches defining the relationship between ball diameter and mill variables. There are mathematical expressions and these have been used in evaluations by Tarjan, Razumov, Olevsky, Papadakis, Bomble, Lianxiang, Bond and Nordberg. Since these are specific studies conducted within certain limits it is hard to reach a general conclusion.

Some approaches focused on determining the ball size distribution rather than doing mean size assessments as the materials to be ground have a wide distribution of particle size. In addition, due to the spherical shape of grinding media, the void between the balls increases with the diameter in a fixed filling volume. In this respect, it is possible to minimize the gap between the balls by using a multi-modal size distribution instead of monosized balls in order to reach the maximum grinding efficiency.

The filling ratio of balls directly affects the power drawn by the mill to a large extent. Although the energy consumption decreases at the low ball filling ratio, it requires a certain lower limit due to the increase in the amount of wear. The optimal filling rate for a certain fineness provides an increase in capacity. Detailed evaluations should be made by considering the difference, in the mill power, throughput, and product fineness [82, 83].

The literature survey shows that extensive studies have been performed to determine optimal ball size distribution for ball mills. Although approaches on media distribution for tube ball mills have been made, studies discussing the effect of the grinding medium in stirred mills are scarce.

2.2.2. Grinding Media Motion in Stirred Mills

Understanding the motion of the grinding media in a stirred mill is necessary to consider the applicability of multi-modal distributed bead composition. For media motion investigations the focus is given on the properties of the flow. Bletcher et al. [76] showed that the small size beads ($R_b/R_d=1/240$) followed a trajectory with high energy zones in contrast to larger size beads. The Re number is a function based on the particle trajectories. It is concluded that a grinding media passes through high energy zones (chamber wall and disc surface) when the Re number is between 800 and 2000. (Fig 9.1, 9.2)

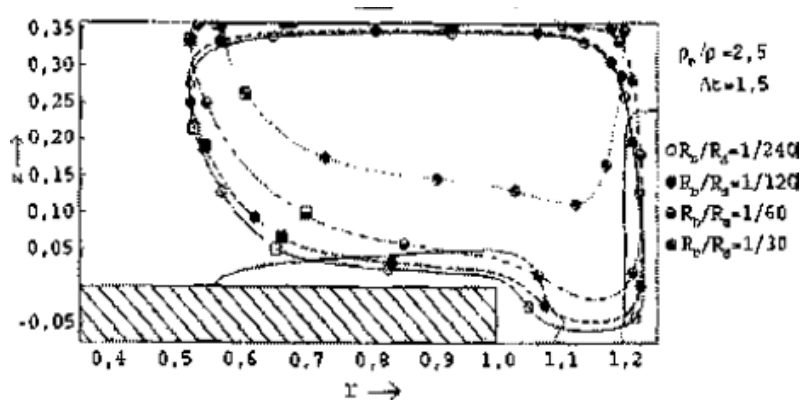


Figure 9.1. Motion of a Single Media ($R_{ball}/R_{attritor}$ diameter) [76]

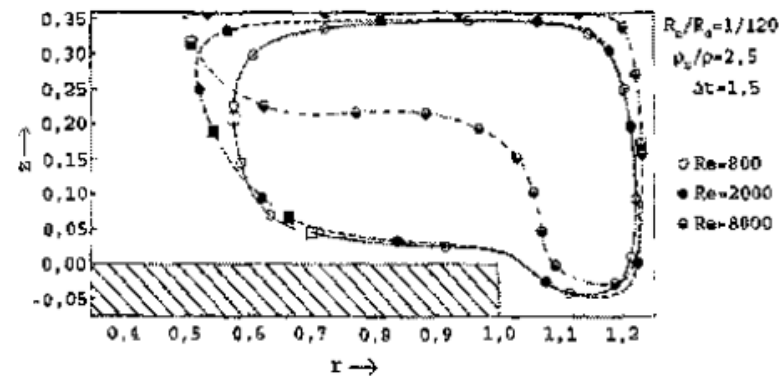


Figure 9.2. Particle Trajectory as a Function of Re [76]

The motion of a single grinding media was also investigated by Theuerkauf and Schwedes [77]. They reported that the velocity of a grinding media increases with increasing R/R_{tip} and reaches its maximum value at $R/R_{tip} = 1$ then it decreases towards the chamber Wall (Figure 10).

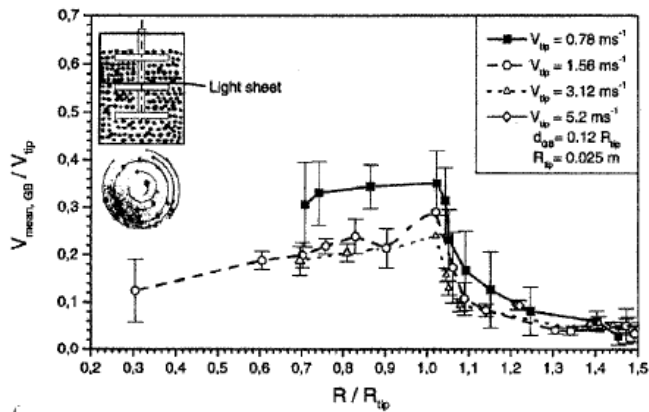


Figure 10. Circumferential Grinding Bead Velocity Distributions [77]

Eskin [78] studied analyzing the motion of a grinding media having different densities with the aid of numerical calculations. As a result, the denser media accumulated near the chamber wall while the lighter ones accumulated at the center of the chamber. The importance of the high energy zone is revealed through motion analysis of the medium and suspension mixture. It is thought that the grinding media passing through these zones provides higher grinding performance. As a result of studies on this situation, the parameter called motion index, which includes the Reynolds number, medium and stirrer size, medium density, and fluid parameters was defined by Bleacher [76]. He reported that for small values of motion index, the improved grinding performance was achieved owing to having homogeneously distributed media along with the mill chamber. Conversely, it was indicated that higher motion index values resulted in obtaining deteriorated grinding performance.

In 2015, the tests were made with 9 – 15 – 25 mm beads to carry out DEM modeling to understand the motion of media by the operation of a full-scale industrial Isamill. However, the outcomes from the DEM modeling of the media part of the study are relevant to both dry and wet operations. The fill level range of the mill was between 70% - 90% as mentioned in the literature [85, 86] The study showed that the media sizes with 15 mm and less are produced very similar flow patterns but the power draw was found to decrease in proportion to media size, in addition, for the media with wider diameters (25 mm) the flow behavior was considerably different (Figure 11.1, 11.2).

The filling rate has a strong, non-linear effect on the grinding performance with an operational range between 70–90% of the grinding chamber. The power draw increases drastically (faster than linear) with the filling rate. The functional behavior of power draw with the filling rate is very similar for media with different diameters. The collision energies also increase sharply with fill level which reflects much stronger frictional engagement with the discs, faster media speeds, and a much larger fraction of the mill charge which is strongly agitated. For media diameter with 15 mm and lower, the power draw and collision energies increase linearly with the friction coefficient and the flow patterns are qualitatively similar. For 25 mm media, bridging occurs between discs with particle jamming leading to very substantial increases in the speed of the media and in the power draw (Figure 11.3, 11.4, 11.5, 11.6) [87].

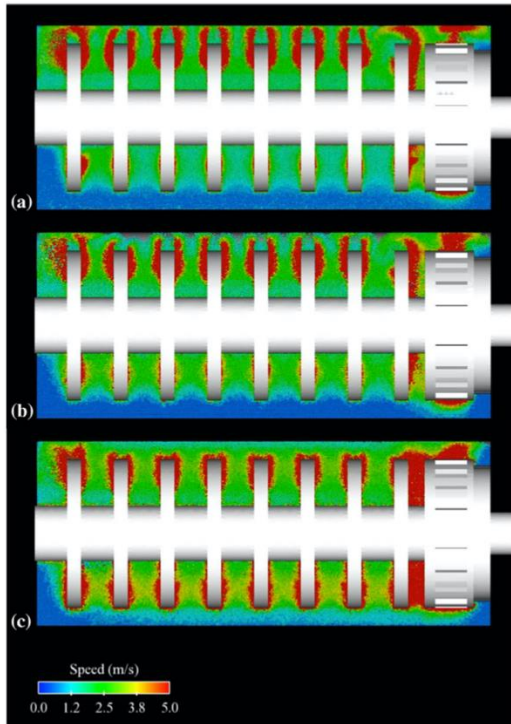


Figure 11.1. Media Distribution in a Vertical Slice of The Isamill for The 80% Operating Conditions with Media Sizes of (a) 9 mm, (b) 15 mm, And (c) 25 mm. [87].

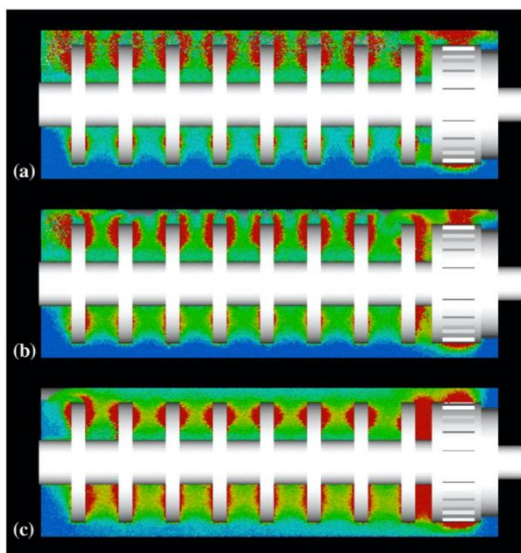


Figure 11.2. Variation of The Media Distribution and Speed for Three Fill Levels, (a) 70%, (b) 80%, And (c) 90% For 15 mm Media [87]

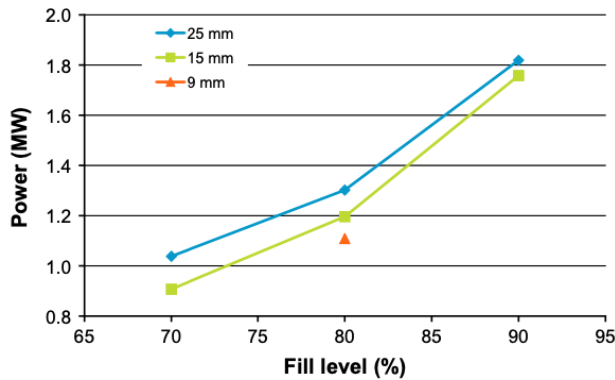


Figure 11.3. Variation of Power Draw With Fill Level for Three Different Media Sizes [87].

The reduction in the media diameter decreases the particle size distribution of the product. When the media diameter gets wider the media motion in the mill gets unsteady. On the other hand, the increasing of the fill level directly increases the grinding surface as well but the media with larger diameters have a limit on the possible smallest product compared to the smaller media while larger beads have a more stable motion in the stirred mills.

One of the aims of the thesis is to define an optimal operational range of grinding media distribution and lower energy consumption without losing the grinding efficiency and product quality. In this regard, multi-modal distributions were also considered. The larger beads were used to provide a stable motion in the stirred mill which also have enough energy to crush coarser particles. The smaller beads were used to increase the grinding surface and ground the particles finer compared to the wider beads. To define an optimal range between both monosized and a mixture of 2 or 3 different sizes of beads in different percentages were used in the study.

3. EXPERIMENTAL STUDIES and INITIAL TEST WORKS

In this section, the materials and methods used in the study are explained. The chemical contents, particle size distributions of the ores, also the information about the media compositions used in the batch grinding tests are summarized in this section.

3.1. Laboratory Equipments and Test Procedures

3.1.1. Laboratory Scale Dry Vertical Stirred Mill

A dry vertical stirred mill was used in the study. Technical specifications of the mill are given in Figure 12 and Table 4.

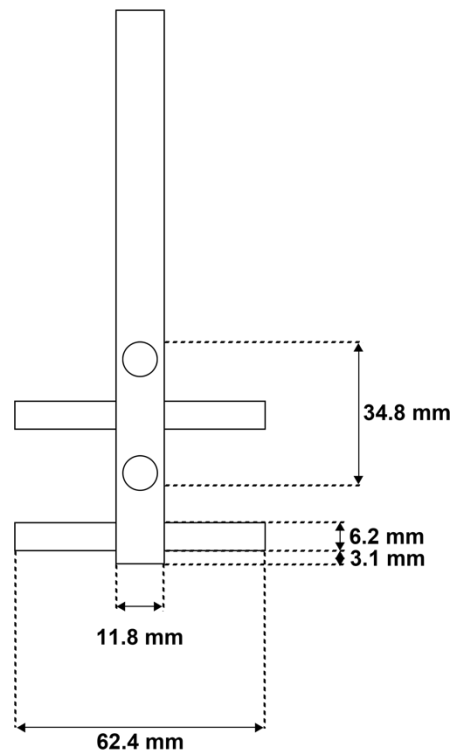


Figure 12. Laboratory Scale Vertical Stirred Mill and Stirrer Geometry

Table 4. Technical Characteristics of Dry Stirred Mill

Active Chamber Diameter (mm)	118
Active Chamber Height (mm)	192
Active Volume (cm ³)	1750
Top Speed (m/s)	4,48

3.1.2. Sympatec Helos Lazer

Size distribution measurement is the main characterization technique in size reduction processes. In this context, the laser scattering method [12] was used and dry measurements were made with the Sympatec device (Figure 13) with a Helos sensor. As a result of the measurements, all size distributions of the samples were determined from 600 μm to 1.8 μm .

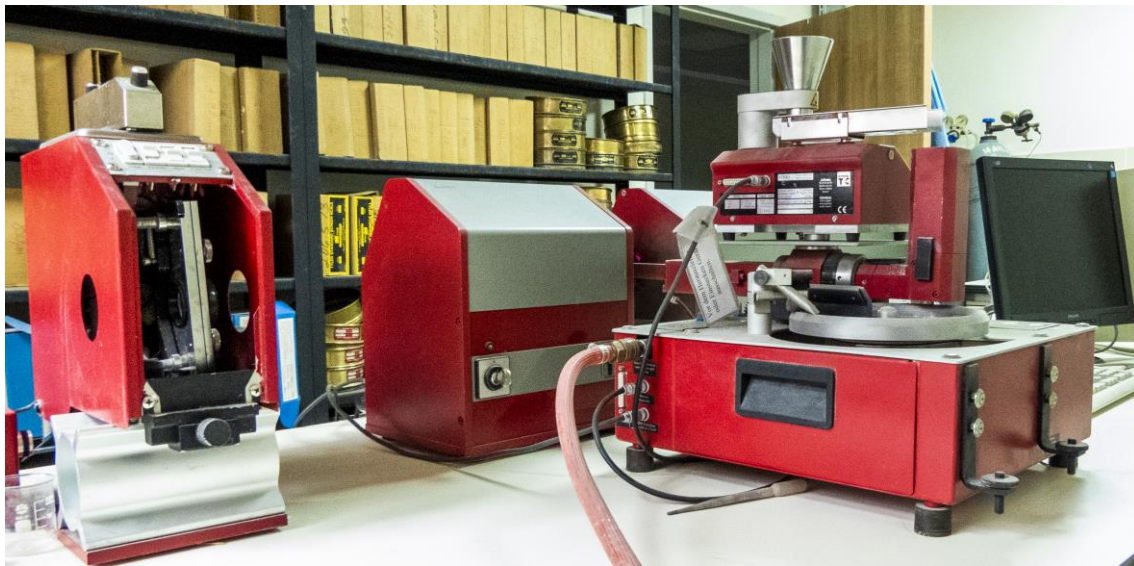


Figure 13. Sympatec Helos Lazer

3.2. Laboratory Studies

3.2.1. Experimental Test Matrice

In the tests performed with the batch grinding procedure within the scope of the study, 8 different ball compositions were used in calcite, clinker, and copper grinding processes in a vertical chamber dry-mixed mill with monosized, bi-modal, and tri-modal distributions. Grinding operations were carried out at 3 different RPM values (Table 6) and representative samples were taken at 1, 5, and 10 minutes of the grinding time. The experimental study matrix including the grinding media compositions and the distribution percentage of these compositions are shown in Table 5. During the tests, mechanical limits due to the mills filling ratio were observed. This limit is defined by the fact that the stirrer cannot take off consistently and the test cannot be performed for some compositions at a 50% filling ratio for grinding with material and 70% for grinding without material. For this reason, material grinding tests were performed at a 40% filling rate, while no data could be obtained for some compositions for 70% filling rate in power measurements. The experimental matrix has been prepared considering these limits.

Table 5. Experimental Study Test Matrice

Type	Code	Average	Size			Grinding Time		
			1,5 mm	2,5 mm	4 mm	1"	5"	10"
Monosized	C1	1.5 mm	100%	0%	0%			
	C2	2.5 mm	0%	100%	0%			
	C3	4 mm	0%	0%	100%			
Bi-modal	C4	3.25 mm	0%	50%	50%			
	C5	2.75 mm	50%	0%	50%			
	C6	2 mm	50%	50%	0%			
Tri-modal	C7	2.66 mm	33%	33%	33%			
	C8	3.375 mm	10%	25%	65%			

Table 6. Dry Stirred Mill Stirrer Speed Information

Code	m/s
RPM 1	4.48
RPM 2	4.06
RPM 3	3.36

3.2.2. Preparation of Samples

The stirred mill chamber is filled with water to calculate the active volume. As a result of this process, the active volume value was determined as 1750cc. The amount of material to be charged to the mill was calculated to provide a 40% filling ratio and 100% material filling for this filling rate. In order to calculate the amount of media and materials to be charged, the amount of media void was measured, this process was calculated over the amount of water added, after charging 200cc (40% by volume) media into a 500cc cylinder, completing with water up to 200cc. Bulk densities of the materials were calculated on the basis of volume measured with graduated cylinder and their weight measured with a precision scale. These values were measured as 1.75 g/cm³ for calcite, 2.05 g/cm³ for clinker, and 1.55 g/cm³ for copper. Bulk density values, ball to void ratios, and the amount of media and materials required for each composition were calculated.

Table 7. Media to Material Void Ratios

Composition	Media	Material
C1	57.53%	42.47%
C2	56.07%	43.93%
C3	55.90%	45.10%
C4	47.09%	52.90%
C5	51.49%	48.51%
C6	53.50%	46.95%
C7	51.30%	49.70%
C8	54.25%	45.75%

3.2.2.1. Calcite

Calcite mineral which is stated to be 98.97% purity by the facility was reduced to below 600 µm by a jaw crusher, a roller crusher, and a russel sieve respectively. The particle size distribution of the calcite mineral, which was examined after the size reduction processes, was calculated as 222 µm for d₈₀ and 101µm for d₅₀. The particle size distribution measured for calcite feed is shown in Figure 14.

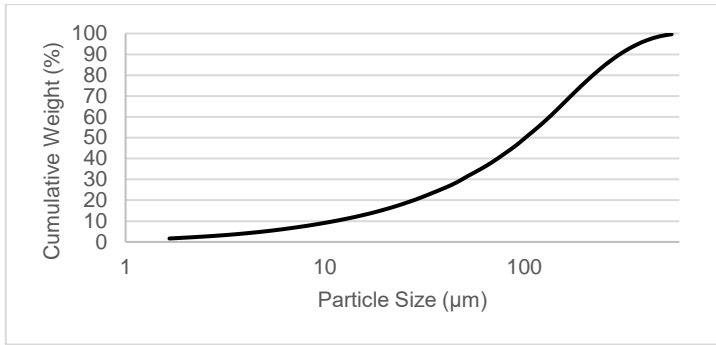


Figure 14. Particle Size Distribution of Calcite Feed

3.2.2.2. Clinker

The clinker was sieved through a 600 µm Russel sieve. Afterwards, the particle size distribution was measured. For clinker, the d_{80} value was calculated as 237 µm and the d_{50} value as 101 µm. The particle size distribution measured for clinker feed is shown in Figure 15.

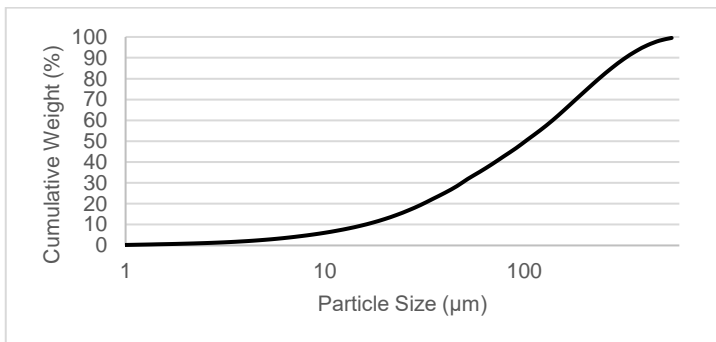


Figure 15. Particle Size Distribution of Clinker Feed

3.2.2.3. Copper

The copper ore which is stated to be 0.7% grade by the facility obtained from the hydrocyclone overflow working in a closed circuit with a primary ball mill was subjected to the sieving process and the top size value was checked by sieving it through a 600 µm wide sieve. The d_{80} value for copper was calculated as 99 µm and the d_{50} value as 12 µm. The particle size distribution measured for the copper feed is shown in Figure 16.

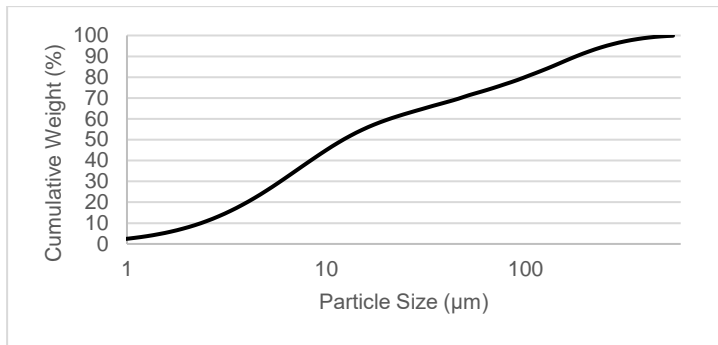


Figure 16. Particle Size Distribution of Copper Feed

With 8 different compositions, batch grinding operations at 3 different RPMs were completed by taking samples at 1, 5, and 10 minutes from each grinding. The particle size distributions of representative samples were measured by Sympatec Helos laser, as in feed samples. Size reduction ratios were calculated by comparing the d_{80} and d_{50} values obtained with these measurements. In order to evaluate the correlation between reduction ratio and specific energy for each grinding, the power amount of the dry vertical stirred mill during all grinding processes were recorded.

3.2.3. Media Wear Tests

In order to discuss the effects of media distributions on a plant scale milling operation, the results should also be evaluated on an economic basis. Therefore, tests were carried out to examine the effects of media compositions on wear. C2, C3, and C4 compositions were charged without material at a 40% filling ratio and weighed for 10 and 20 minutes. Then the amount of wear was calculated size-by-size as a percentage.

3.2.4. Energy Consumption Tests

Another data needed in the study in order to make comments about the economy on a plant scale is specific energy consumption. For this reason, during the grinding tests with calcite, clinker and copper the power consumption data as kW which were provided from an electric meter connected to the power line of the mill were recorded at 1, 5, and 10 minutes. The specific energy consumption data were calculated as kWh/t with the data of power consumption as kW, grinding time as hour and the material weight as metric ton.

3.2.5. Grinding Aid Dosage

Triethanolamine (TEA) was used in all the grinding tests as grinding aid which is mostly used to reduce the agglomeration and improve the grinding efficiency during the cement grinding [89, 94]. In addition, studies shown that the use of triethanolamine in grinding limestone and quartz raw materials has an improvement in grinding efficiency [91, 91, 92, 93]. The optimum dosage amount is stated as 1000g/t for cement in the literature [94]. However, to prevent coating of the material, a different amount of dosage has used in the experiments. The amount of dosage used in the tests is given in Table 8.

Table 8. Grinding Aid Dosage Amount

Minute	Amount
0" (0 – 1)	1000g/t
1" (1 – 5)	250g/t
5" (5 – 10)	250g/t

3.2.6. Rosin Rammler Size Distribution

In the scope of the study, the effect of the used media compositions on the product size steepness was examined. In order to make this evaluation, the n value which expresses the slope of the particle size distribution plot mathematically were calculated for each sample. The Rosin Rammler Size Distribution method is used for this calculation which is first used by Rosin & Rammler to define particle size distributions in milling processes which is shown in equation 6 [88].

$$R = \left(1 - \exp \left[- \left(\frac{x}{x'} \right)^n \right] \right) \quad \text{Eq.6}$$

Where;

R : Cumulative passing %

x : Particle Size

x' : Passing Size

n : Slope value

4. RESULTS and DISCUSSIONS

In this section, the data obtained from the experiments conducted within the scope of the thesis study are presented and discussed. In summary, the product particle size distributions obtained by applying the test methods given under the title of Experimental Studies and Initial Testworks; product particle size values have been evaluated considering the mill energy consumption and steepness of the size distribution.

4.1. Batch Test Results

In order to examine the effects of monosized, bi-modal, and tri-modal media compositions on grinding, batch grinding tests were performed at different stirrer speeds. D_{80} and d_{50} values were calculated from the particle size distribution data obtained by representative samples from the compositions with percentage distributions specified in the above-mentioned study matrix.

4.1.1. Results of Calcite Grinding

Within the scope of the study, 8 different media compositions were used in calcite grinding tests in 3 different stirrer speeds. The calcite used in the tests has a d_{80} value of 222 μm and a d_{50} value of 101 μm . Specific energy and reduction ratio comparison plots were drawn using the energy consumption and particle size distribution data obtained from these tests. The outcomes obtained from these plots are discussed in the following section.

4.1.1.1. Monosized Composition Tests

The batch grinding tests were performed with compositions C1, C2, and C3 consisting of 1.5 mm, 2.5 mm, and 4 mm diameter beads respectively. Particle size distribution plots of the products obtained with composition C1, C2, and C3 are shown in Figures 17, 18, and 19.

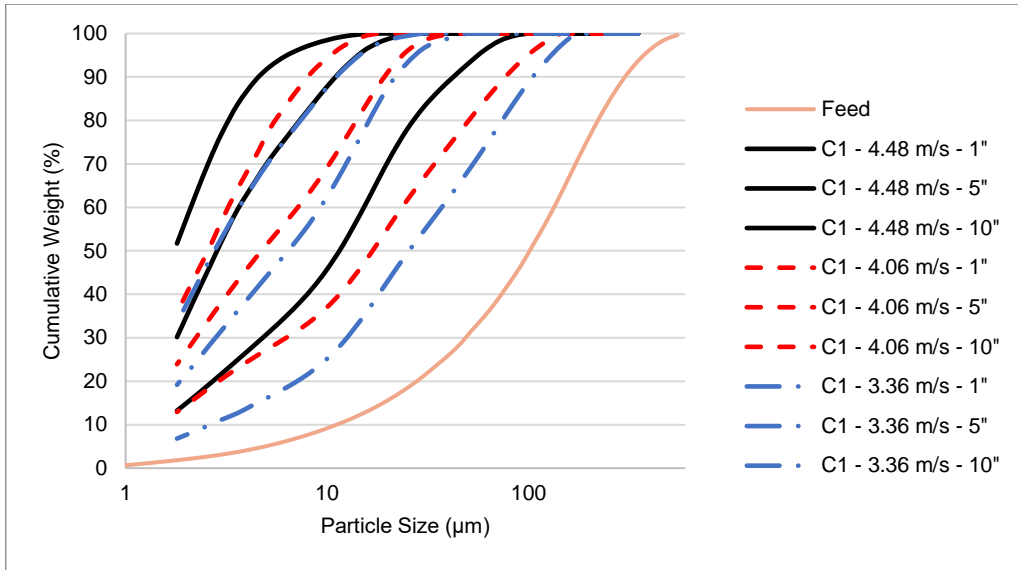


Figure 17. Particle Size Distribution Plots of Calcite Tests with C1

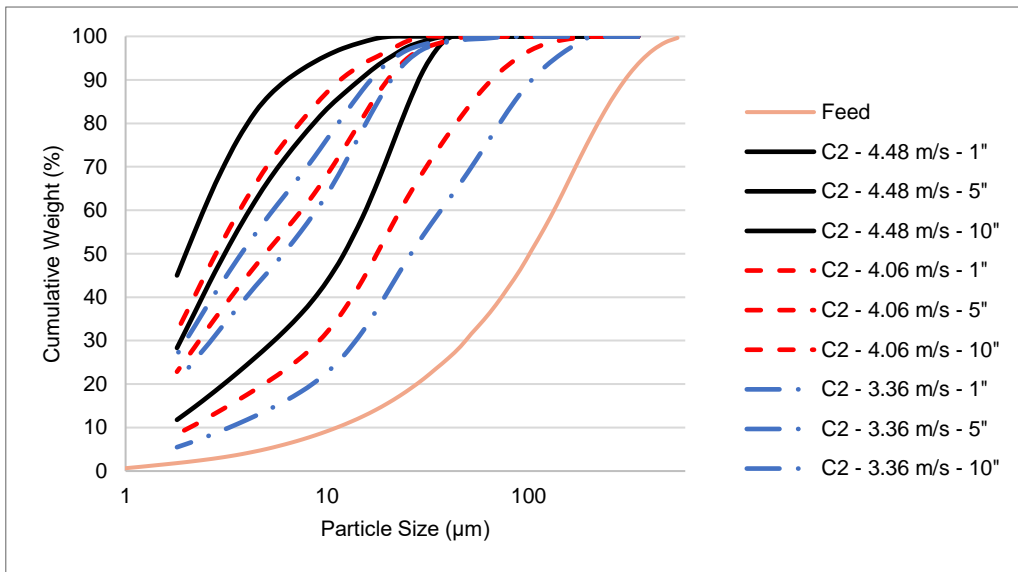


Figure 18. Particle Size Distribution Plots of C2

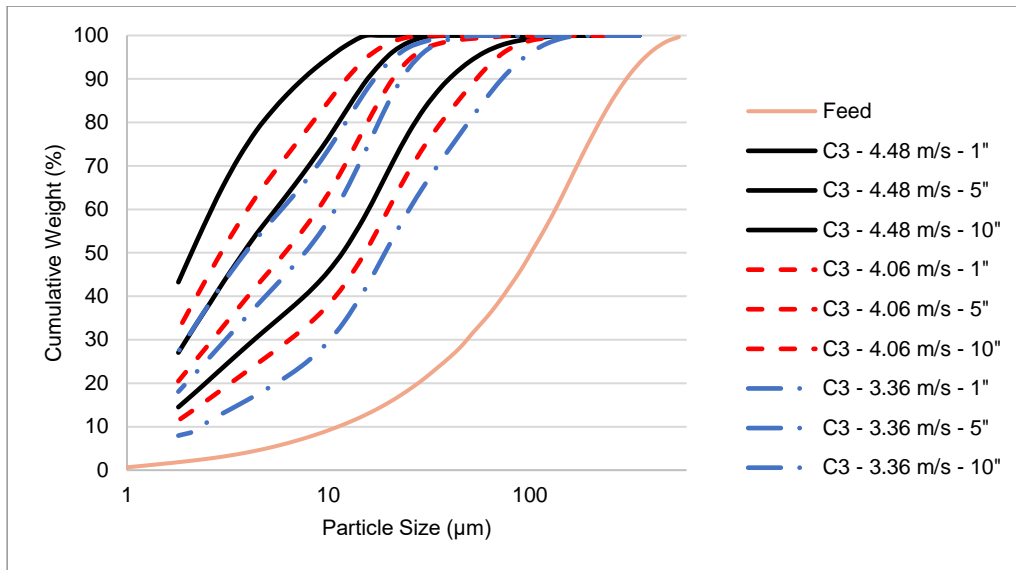


Figure 19. Particle Size Distribution Plots of Calcite Tests with C3

Specific energy and reduction ratio relationship plots of compositions C1, C2, and C3 are shown in Figure 20.

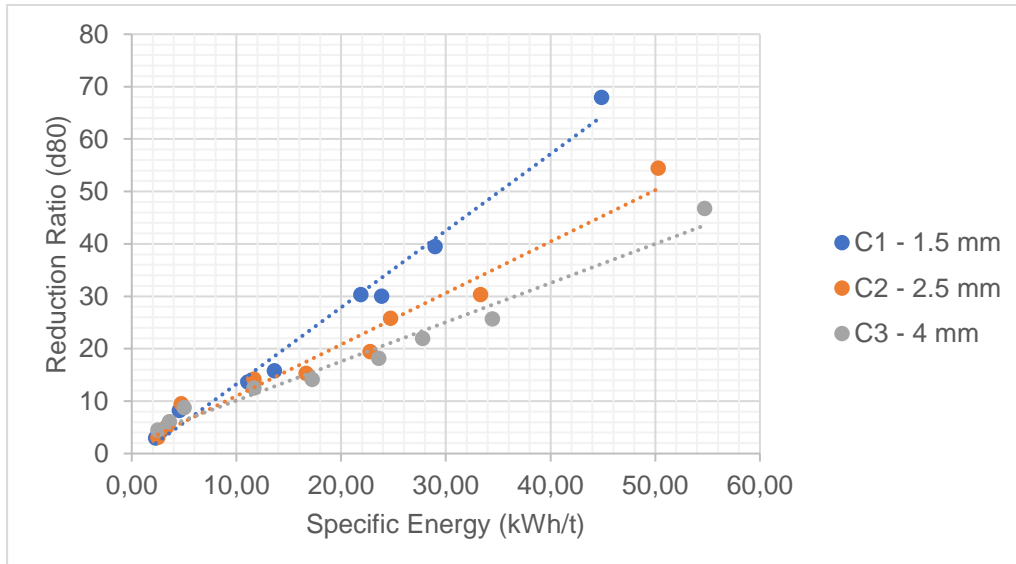


Figure 20. Specific Energy and Reduction Ratio Relationship of C1, C2 and C3 for Calcite

The effects of stirrer speed and media surface area on product particle size have been reported in the literature. The increase in the stirrer speed provides an increase in stress intensity. The smaller media requires a higher agitator speed to improve grinding efficiency. The reduction in the diameter of the media results in an increase in the media surface area [5].

When the results obtained from the tests performed with the monosized compositions were compared, for the same energy levels, an inverse relationship was observed between the media diameter and the size reduction. 1.5 mm media appears to provide the most efficient grinding for both low and high energy levels. This is followed by 2.5 mm media. Although 4 mm media has the same effect at low energy levels as 2.5 mm media, it cannot maintain the same effect at high energy levels. For the same reduction ratio, C1 provides 33% more efficient grinding operation compared to C2 and 66% compared to C3 on the energy consumption basis. In this context, the data obtained are in agreement with the literature.

The particle size distribution plots of the products obtained as a result of 10 minute grinding tests with compositions C1, C2, and C3 were also examined in terms of slope values. In order to make this evaluation, the value of n , which enables the steepness to be expressed mathematically, was calculated with the RRSB method. These data is shown in Table 9.

Table 9. n Values of C1, C2, and C3 for Calcite

10"	C1	C2	C3
4.48 m/s	1.18	1	0.94
4.06 m/s	1.08	0.89	0.88
3.36 m/s	0.9	0.84	0.82

The slope value evaluation was made over the data obtained at the end of 10 minutes of grinding. The reason for this situation is that no significant effect could be observed in the data obtained at 1 and 5 minutes. The slope values of the products obtained after 10 minutes of grinding for compositions C2 and C3 are similar. Compared to the other two monosized compositions, composition C1 has

a higher slope value. The difference in slope values may be up to 0.26 for 4.48 m/s stirrer speed, 0.16 for 4.06 m/s stirrer speed, and 0.12 for 3.36 m/s stirrer speed.

The study is continued with bi-modal media compositions. In the following section, the results obtained with these compositions are discussed and compared with monosized media compositions.

4.1.1.2. Bi-Modal Composition Tests

Within the scope, 3 different bi-modal distributions were tested. Composition C4 consists of 50% 2.5 mm media and 50% 4 mm media while C5 consists of 50% 1.5 mm media and 50% 4 mm media and C6 consist of 50% 1.5 mm media and 50% 2.5 mm media. The average media diameter values are 3.25 mm for C4, 2.75 mm for C5, and 2 mm for C6. The particle size distribution plots for the products obtained from the grinding tests performed with C4, C5, and C6 compositions are shown in Figures 21, 22, and 23.

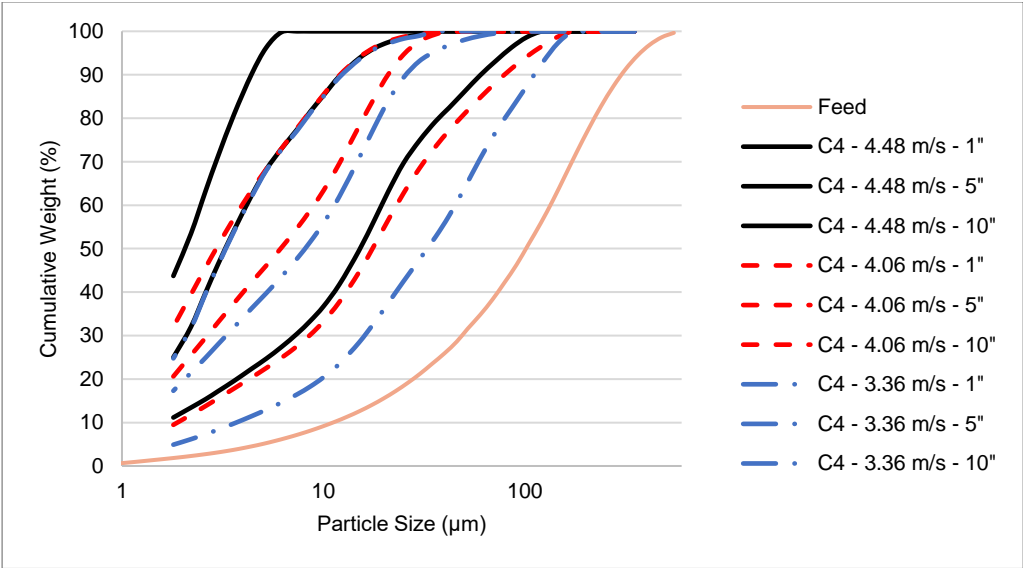


Figure 21. Particle Size Distribution Plots of Calcite Tests with C4

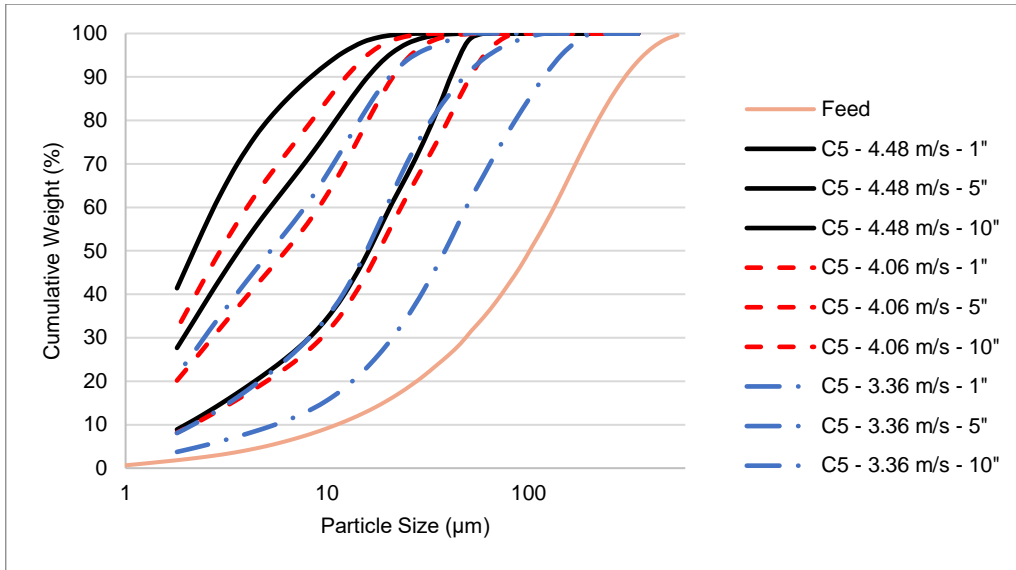


Figure 22. Particle Size Distribution Plots of Calcite Tests with C5

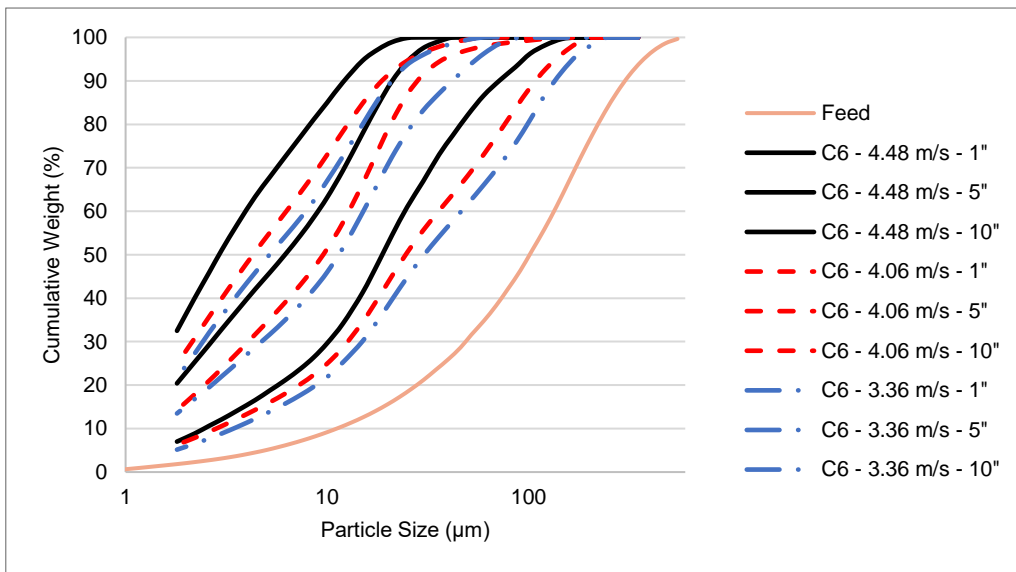


Figure 23. Particle Size Distribution Plots of Calcite Tests with C6

Specific energy and reduction ratio relationship of compositions C1, C2, and C3 are shown in Figure 24.

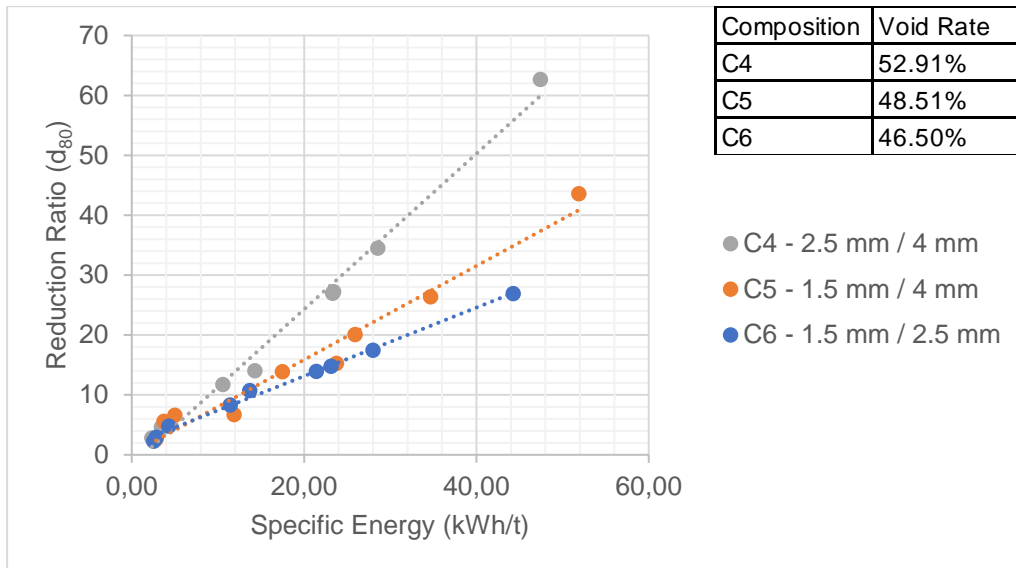


Figure 24. Specific Energy and Reduction Ratio Relationship of C4, C5, C6 for Calcite, and The Void Rates

Evaluations on bi-modal compositions have shown that composition C4 provides a finer product at the same energy levels. When bi-modal compositions were compared, for the same reduction ratio, C4 provides 41% more efficient grinding operation compared to C5 and 83% more compared to C6 on the energy consumption basis. The reduced void between the media negatively affects the flow in the milling environment. This relationship between media diameter and flow irregularity was reported by Cleary in the literature [87]. The data show that there is a linear relationship between the size reduction and the media void volumes of the compositions.

Specific energy and size reduction values obtained from tests performed with composition C4 were compared to 2.5 mm and 4 mm diameter media. This comparison is shown in Figure 25.

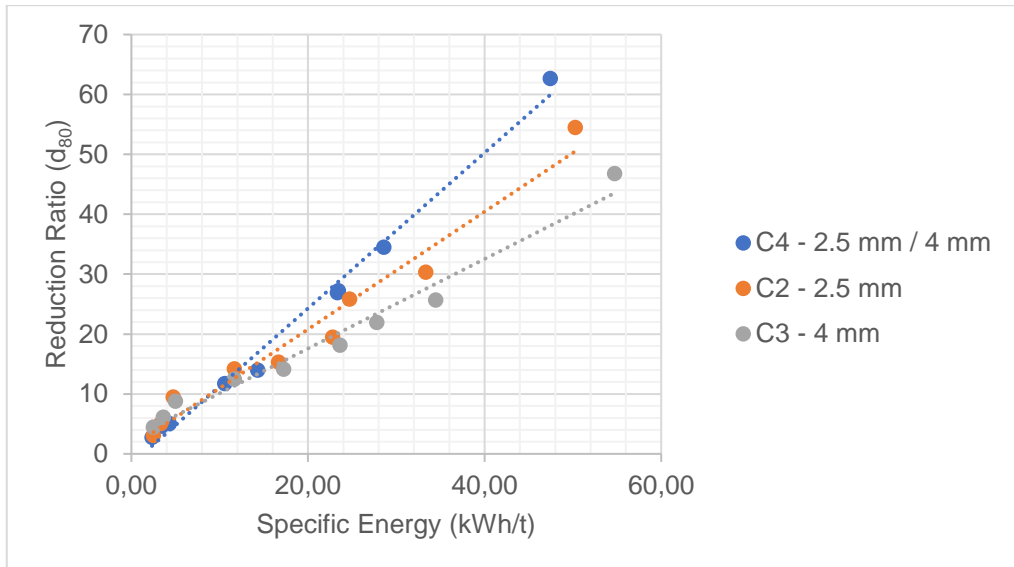


Figure 25. Specific Energy and Reduction Ratio Relationship of C2, C3 and C4 for Calcite

When the data interpretation was done, it was observed that the bi-modal media composition provides higher reduction ratio rates than monosized compositions at the same energy levels. At lower energy levels (<10 kWh/t), all compositions have the same size reduction effect. Composition C4 provides a 25% decrease in energy consumption compared to 2.5 mm diameter media and a 56% compared to 4 mm diameter media. In other words, the effect of the bi-modal media composition increases with the increase of energy level.

The comparison of composition C5 and the monosized media it contains are shown in Figure 26.

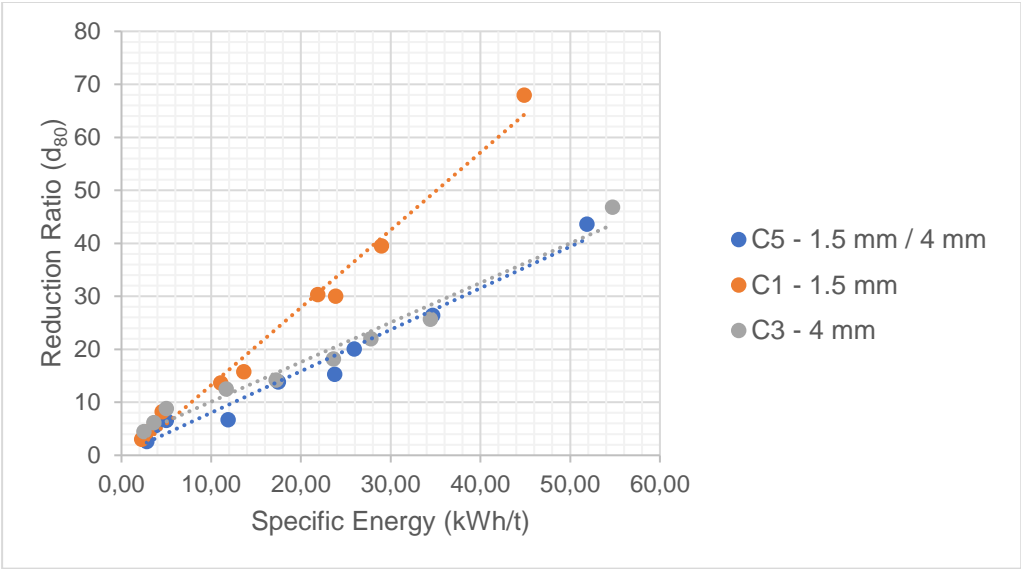


Figure 26. Specific Energy and Reduction Ratio Relationship of C1, C3, and C5 for Calcite

Composition C5 when compared to compositions C1 (1.5 mm) and C3 (4mm) at the same energy levels, has the same reduction ratio as composition C3, which provides the most coarse product among monosized compositions. In other words, no effect on size reduction was observed for composition C5.

The comparison of composition C6 with compositions C1 and C2 is shown in Figure 27.

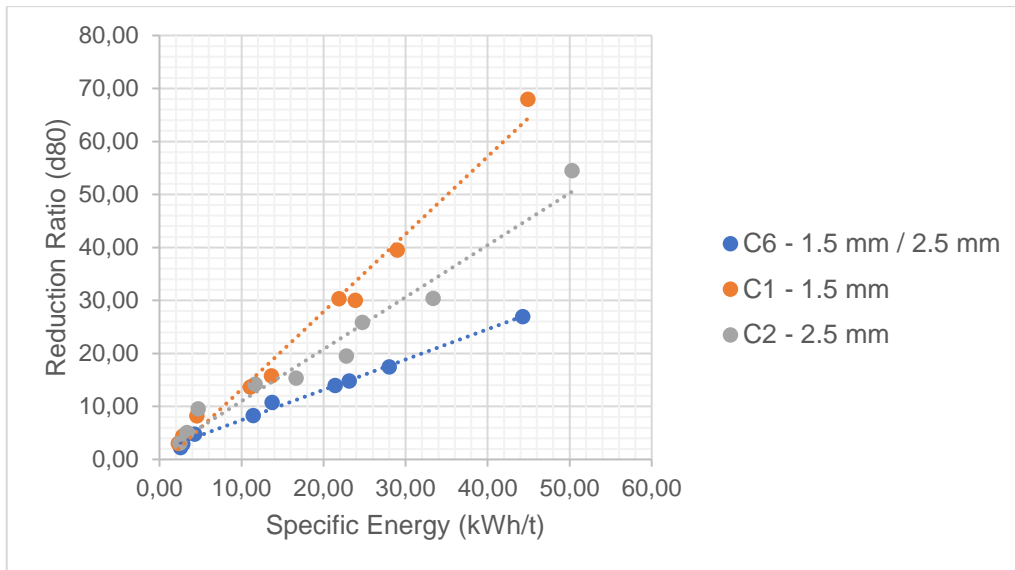


Figure 27. Specific Energy and Reduction Ratio Relationship of C1, C2, and C6 for Calcite

Composition C6 has a lower reduction ratio when compared to the monosized media compositions it contains. For the same reduction ratio value, C6 provides a grinding operation with a need of 83% more energy consumption compared to C2 and 144% more compared to C1.

The slope values of the bi-modal and monosized compositions are shown in Table 10.

Table 10. *n* Values of Monosized and Bi-modal Compositions for Calcite

10"	C1	C2	C3	C4	C5	C6
4.48 m/s	1.18	1	0.94	1.6	0.89	0.88
4.06 m/s	1.08	0.89	0.88	0.88	0.87	0.83
3.36 m/s	0.9	0.84	0.82	1.03	0.85	0.83

Composition C4 provides a more steep size distribution compared to C2 and C3. The difference between the composition C4 and monosized compositions may be up to 0.66 at 4.48 m/s stirrer speed. When the slope value changes of the products obtained with C1, C3, and C5 were examined, no difference was

observed between these compositions. Composition C6 provides a less steep size distribution compared to composition C1 and C2 at all stirrer speeds.

4.1.1.3. Tri-Modal Composition Tests

There tested 2 different tri-modal distribution. Compositions C7 and C8 are tri-modal compositions obtained by mixing media with 3 different diameters at different rates. The purpose of the tests performed with these compositions is to observe how the effects observed in bi-modal compositions aiming to increase the grinding performance by increasing the media surface area change when the surface area is increased even more. In this context, C7 composition contains 3 different sizes of media in 33% of each other with a 2.66 mm average media diameter. This ratio changes as 10% 1.5 mm, 25% 2.5mm, and 65% 4 mm for composition C8 which has an average media diameter of 3.375 mm. The particle size distribution plots of the products obtained from the tests performed with composition C7 and C8 are shown in Figures 28 and 29.

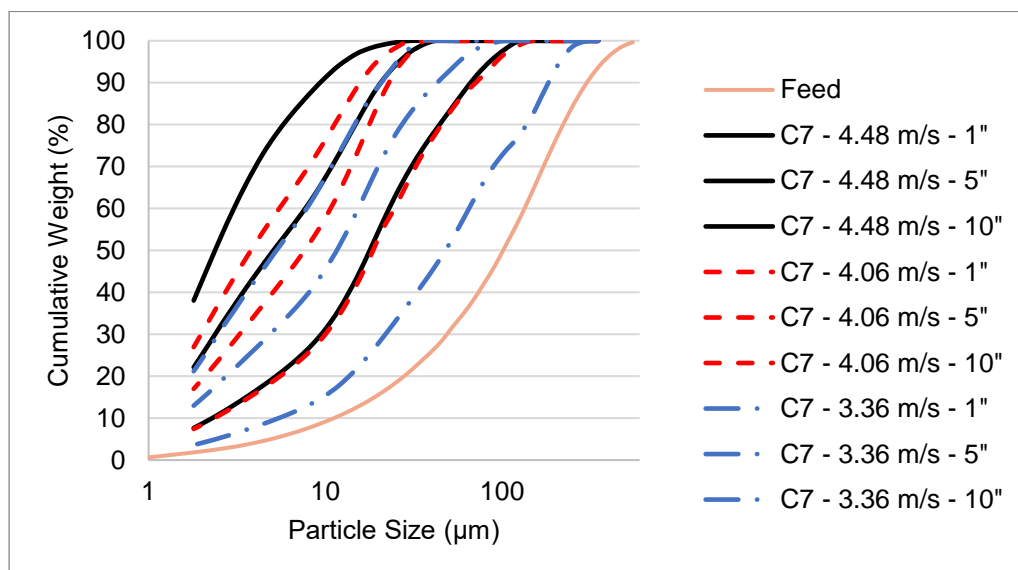


Figure 28. Particle Size Distribution Plots of Calcite Tests with C7

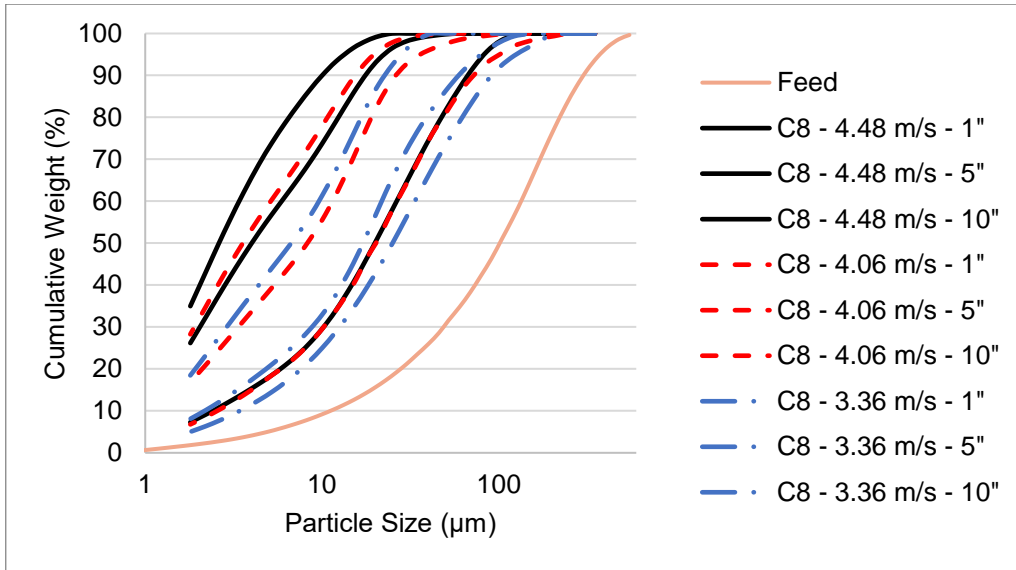


Figure 29. Particle Size Distribution Plots of Calcite Tests with C8

The comparison of tri-modal and monosized compositions are shown in Figure 30.

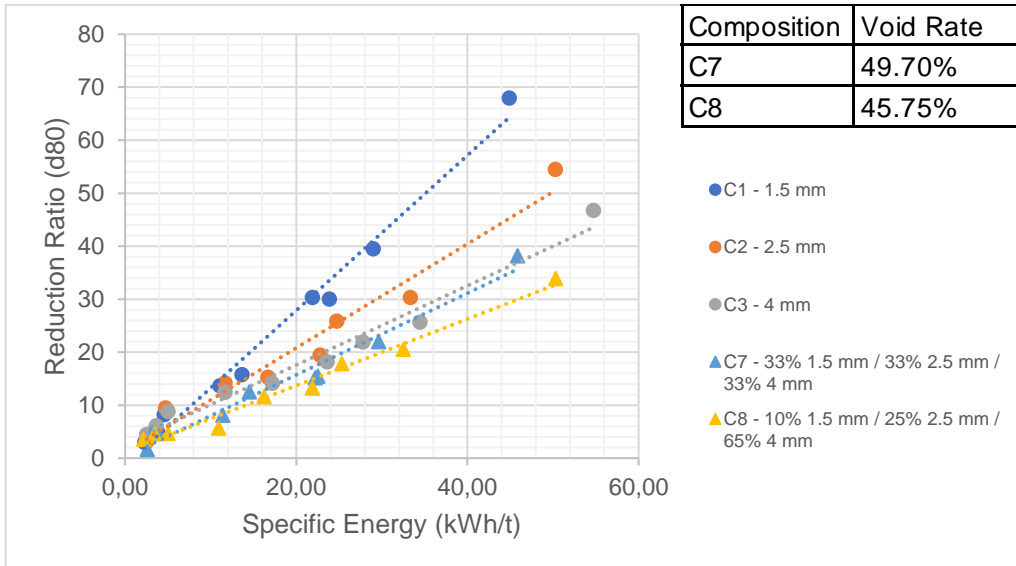


Figure 30. Specific Energy and Reduction Ratio Relationship of Tri-modal and Monosized Compositions for Calcite and the Void Rates of C7 and C8

Compositions C7 and C8, when compared to the monosized compositions cannot provide an efficient grinding process in terms of reduction ratio. Composition C7 provides similar reduction ratios to composition C3 which contains 4 mm media. Although composition C8 provides the same effect as composition C7 at low energy levels, on the other hand, composition C8 provides a %20 less energy-efficient operation compared to composition C7 for the same reduction ratio value.

When the reduction ratios and the volume rates were compared, it was seen that composition C7 has less void between beads. Therefore composition C8, which has a higher average diameter is thought to have more irregular flow. This irregularity also increases with different flow characteristics of 3 different types of media.

To discuss the steepness of the size distribution of tri-modal compositions, *n* values of monosized and tri-modal compositions are shown in Table 11.

Table 11. *n* Values of Monosized and Tri-modal Compositions for Calcite

10"	C1	C2	C3	C7	C8
4.48 m/s	1.18	1	0.94	0.9	0.93
4.06 m/s	1.08	0.89	0.88	0.87	0.85
3.36 m/s	0.9	0.84	0.82	0.87	0.89

When composition C7 and C8 were examined in terms of the slope values, compared to monosized media, they could not provide a steep size distribution at any stirrer speed. However, when the slope values were compared to the slope values of C2 and C3, it showed similar effects.

Specific energy and size reduction data obtained from all of the grinding tests performed with calcite are shown together in Figure 31.

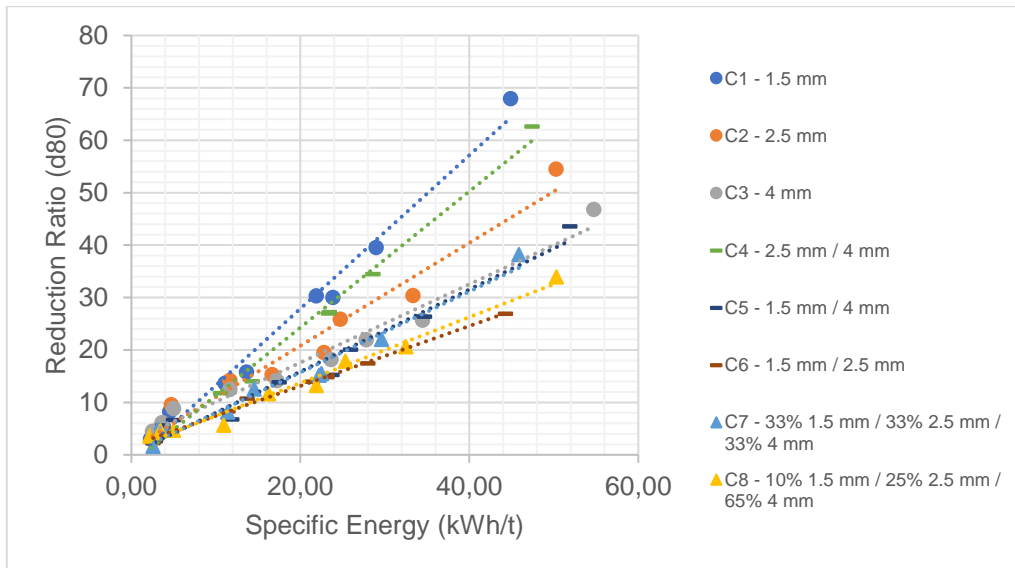


Figure 31. Specific Energy and Reduction Ratio Relationship of All Compositions

The compositions that were evaluated in defined groups as monosized, bi-modal, and tri-modal on the basis of particle size distribution, reduction ratios, specific energy values, and slope values, were also examined in general terms. The order of the energy consumption amount for the same size reduction is $C1 < C4 < C2 < C3 \approx C5 \approx C7 < C8 < C6$ for both low and high energy levels.

As a result of batch grinding tests with calcite, several conclusions may be drawn.

- Composition C4 provides an energy-efficient grinding operation for the same size reduction. This efficiency may be up to 25% compared to C2 and 56% compared to C3
- The slope value can be changed by the composition C4 between 0.13 and 0.66 to provide a more steep size distribution
- Tri-modal compositions had led to higher specific energy consumption when compared to other configurations.

In the following section, the data obtained from the grinding tests performed with clinker are discussed and the repeatability of the data obtained in the grinding tests performed with calcite with clinker is examined.

4.1.2. Results of Clinker Grinding

Clinker with a d_{80} value of 237 μm and a d_{50} value of 101 μm were used in the tests with the same configurations as calcite. The data obtained from the grinding tests made with clinker are discussed in the following section.

4.1.2.1. Monosized Composition Tests

The batch grinding tests were performed with compositions, C1, C2, and C3 consisting of 1.5 mm, 2.5 mm, and 4 mm diameter media respectively. Particle size distribution plots of the products obtained with composition C1, C2, and C3 are shown in Figures 32, 33, and 34.

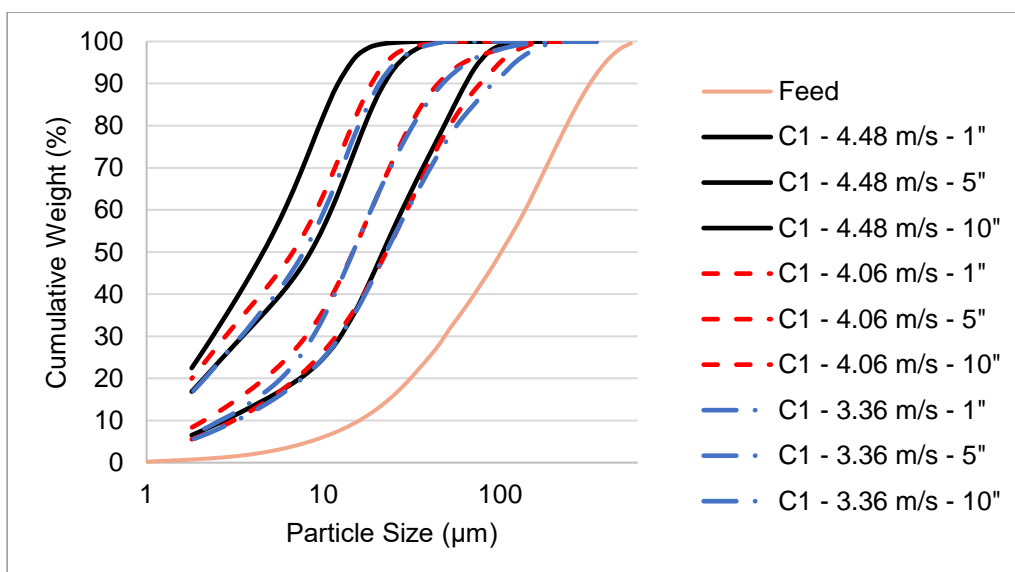


Figure 32. Particle Size Distribution Plots of Clinker Tests with C1

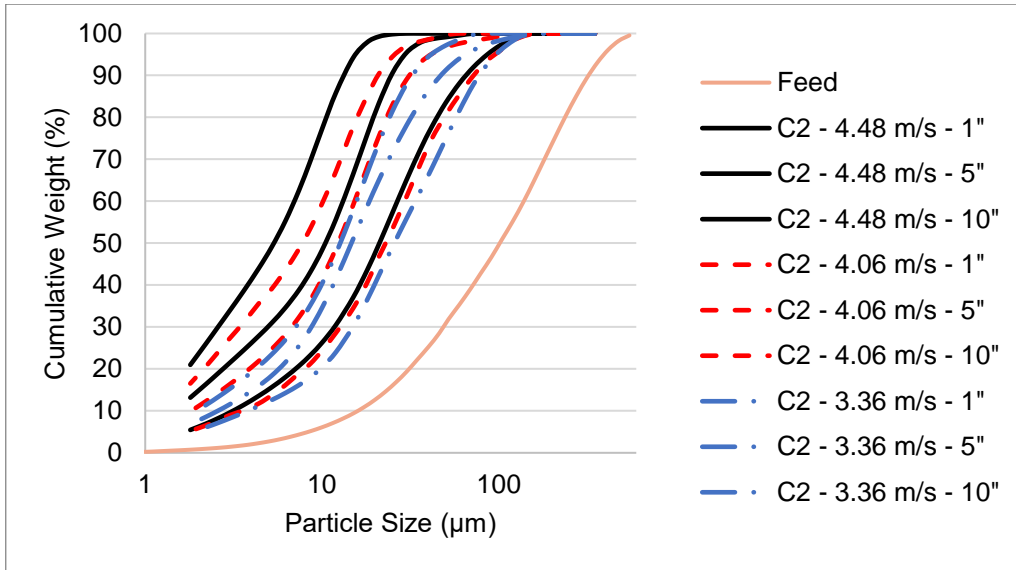


Figure 33. Particle Size Distribution Plots of Clinker Tests with C2

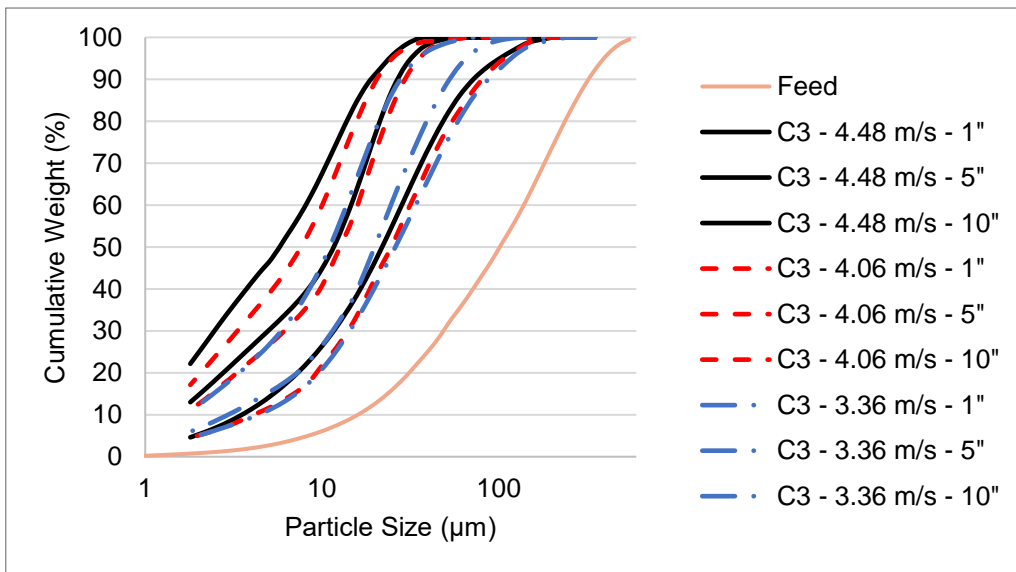


Figure 34. Particle Size Distribution Plots of Clinker Tests with C3

Specific energy and reduction ratio relationship plots of compositions C1, C2, and C3 are shown in Figure 35.

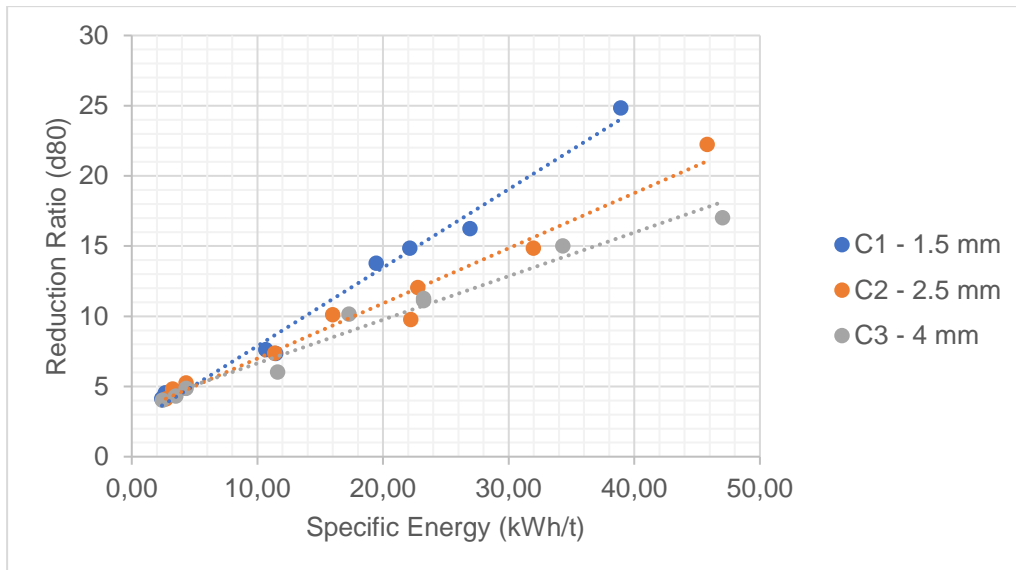


Figure 35. Specific Energy and Reduction Ratio Relationship of C1, C2 and C3 for Clinker

When the results obtained from the tests performed with compositions C1, C2 and C3 were compared, the outcomes obtained in the tests performed with calcite; for the same energy levels, an inverse relationship between the diameter of the media and reduction ratio was also observed for clinker. For the same reduction ratio, C1 provides 42% more efficient grinding operation compared to C2 and 76% compared to C3 on the energy consumption basis.

The particle size distribution graphs of the products obtained as a result of 10 minute grinding tests at different stirrer speeds with compositions C1, C2, and C3 and the n values are shown in Table 12.

Table 12. n Values of C1, C2, and C3 for Clinker

10"	C1	C2	C3
4.48 m/s	1.11	1.1	0.9
4.06 m/s	0.95	0.99	0.99
3.36 m/s	1.1	1.15	1.12

When 3 monosized compositions were compared, the only difference obtained was that 4 mm C3 composition at 4.48 m/s stirrer speed was 0.2 less steep compared to C1 and C2.

Grinding tests were continued with bi-modal and tri-modal compositions. In the following section, the results obtained with these compositions are discussed and compared with monosized media compositions.

4.1.2.2. Bi-Modal Composition Tests

Within the scope, 3 different bi-modal distributions were tested. The particle size distribution plots for the products obtained from the grinding tests performed with C4, C5, and C6 compositions are shown in Figures 36, 37, and 38.

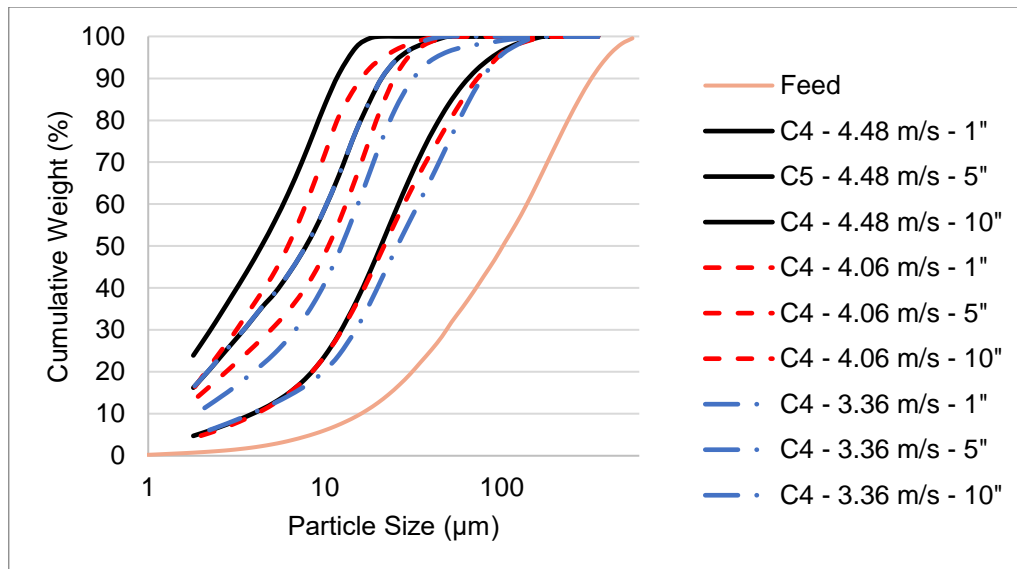


Figure 36. Particle Size Distribution Plots of Clinker Tests with C4

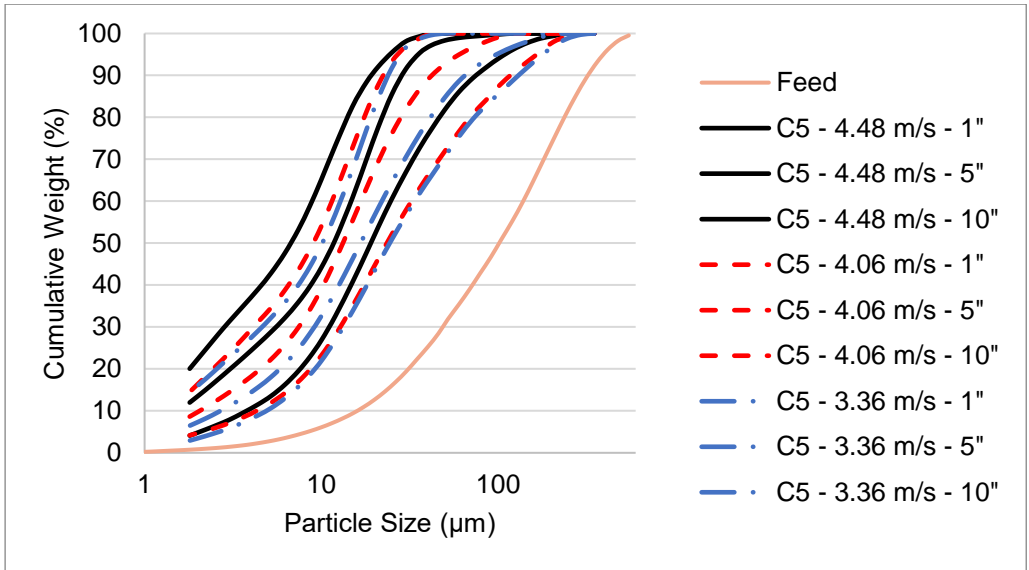


Figure 37. Particle Size Distribution Plots of Clinker Tests with C5

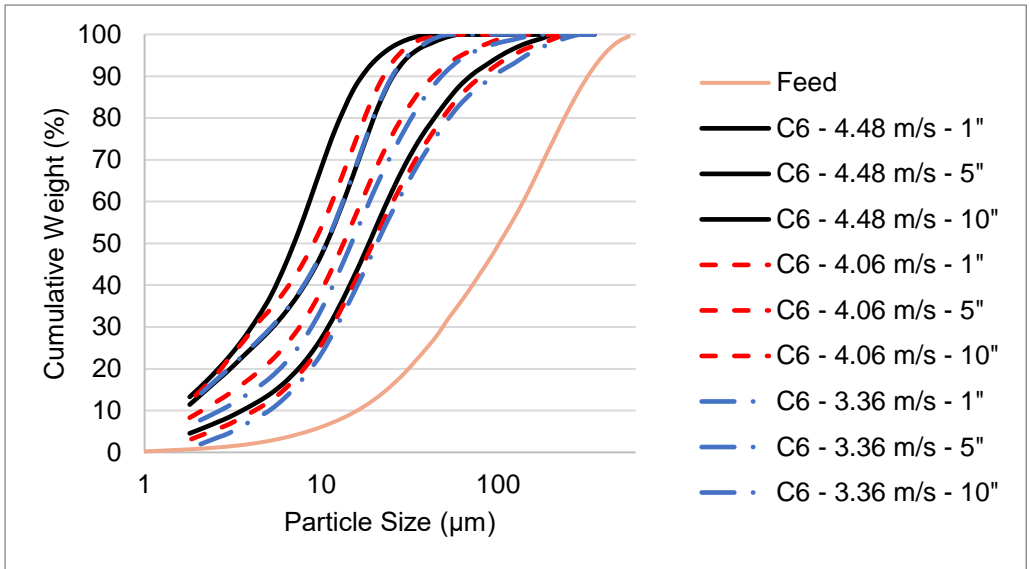


Figure 38. Particle Size Distribution Plots of Clinker Tests with C6

Specific energy and reduction ratio relationship plots of compositions C1, C2, and C3 are shown in Figure 39.

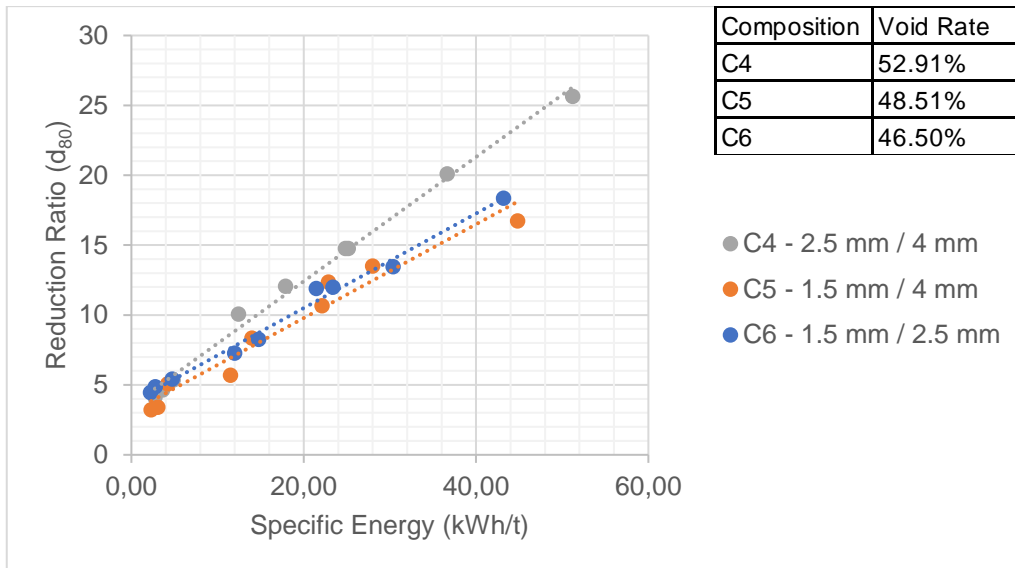


Figure 39. Specific Energy and Reduction Ratio Relationship of C4, C5, C6 for Clinker, and the Void Rates

The evaluations made on bi-modal compositions are in agreement with the tests performed with calcite. The tests have shown that composition C4 has a finer final product at the same energy levels. However, compositions C5 and C6, which have a significant reduction ratio difference between them in tests performed with calcite, show similarity in grinding tests with clinker. When composition C4 was compared with composition C5 and C6, it provides a 37% reduction in energy consumption for the same size reduction. The correlation with the reduction ratio and the void ratios of compositions obtained in the calcite tests also obtained in the clinker tests.

Specific energy and size reduction values obtained from tests performed with composition C4 were compared to 2.5 mm and 4 mm diameter media. This comparison is shown in Figure 40.

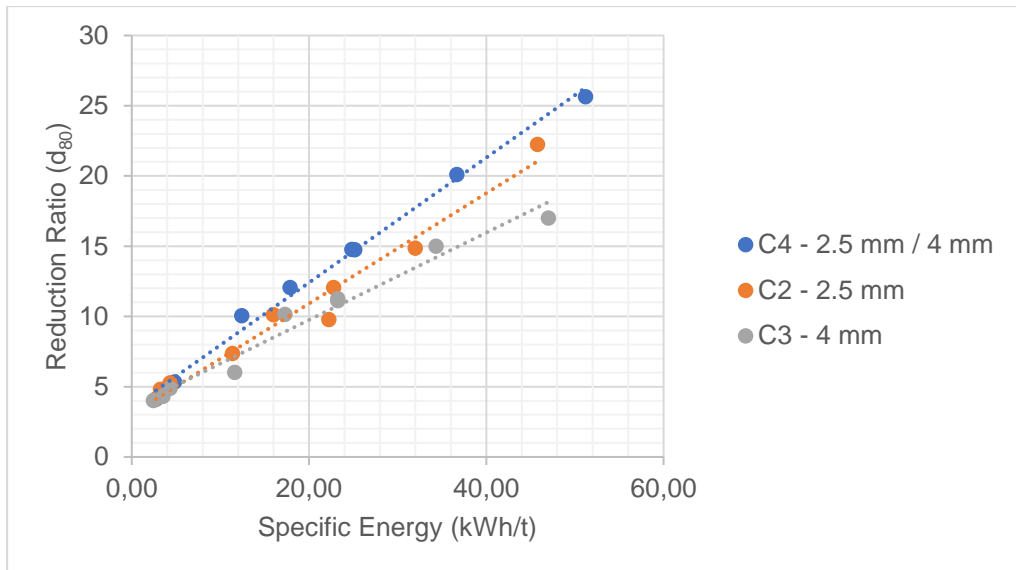


Figure 40. Specific Energy and Reduction Ratio Relationship of C2, C3 and C4 for Clinker

When the data were examined, at the same energy levels, it can be said that compared to C2 and C3, composition C4 produces a finer product with the same specific energy. In other words, the data are in agreement with the data obtained from the grinding tests of calcite. When the results observed for clinker are expressed mathematically, with composition C4, for the same reduction ratio value, a 32% decrease in energy consumption is possible compared to C2, and 50% compared to C3.

The comparison of composition C5 and the monosized media it contains are shown in Figure 41.

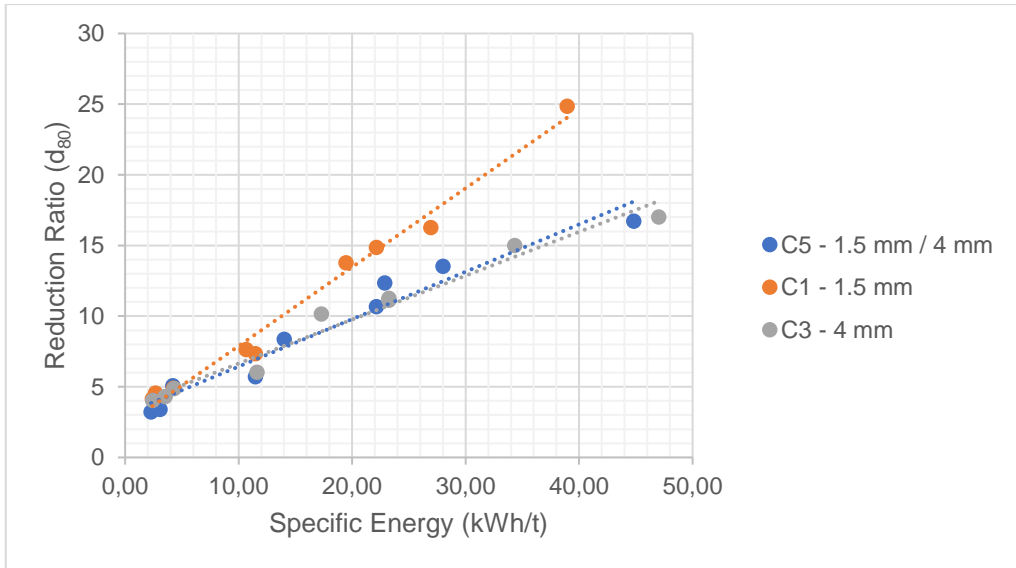


Figure 41. Specific Energy and Reduction Ratio Relationship of C1, C3, and C5 for Clinker

Composition C5 provides the same reduction ratios as composition C3 at the same energy levels when compared to composition C1 (1.5 mm) and composition C3 (4 mm). Similar to the effect observed for calcite, no size reduction effect was observed for composition C5 in the tests with clinker. The comparison of composition C6 with compositions C1 and C2 is shown in Figure 42.

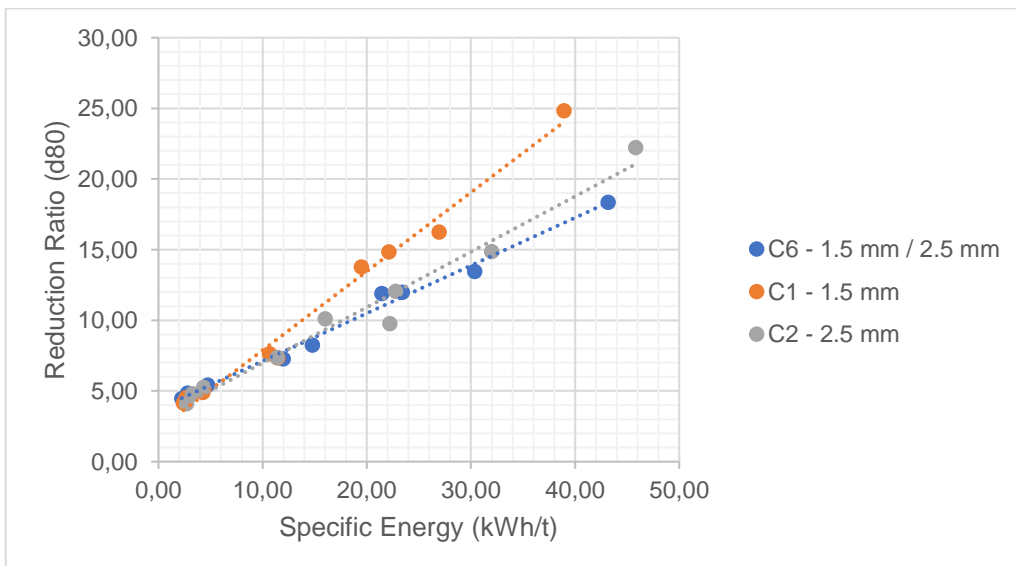


Figure 42. Specific Energy and Reduction Ratio Relationship of C1, C2, and C6 for Clinker

When composition C6 was compared to the other monosized media compositions, it was seen that at 10 kWh/t, they all have the same reduction ratio. However, the change in reduction ratio depending on the energy levels is in parallel with the data obtained from the tests performed with calcite. At high energy levels, for the same reduction ratio value, C6 provides a grinding operation with a need of 10% more energy consumption compared to C2 and 50% more compared to C1.

The slope values of the bi-modal and monosized compositions are shown in Table 13.

Table 13. *n* Values of Monosized and Bi-modal Compositions for Clinker

10"	C1	C2	C3	C4	C5	C6
4.48 m/s	1.11	1.1	0.9	1.11	0.96	0.88
4.06 m/s	0.95	0.99	0.99	1.13	1.05	0.83
3.36 m/s	1.1	1.15	1.12	1	1.05	0.83

Composition C4 provides a more steep size distribution compared to C2 and C3. Unlike the calcite results, this steepness difference only occurs at the 4.06 m/s stirrer speed. C4 provides a 0.14 more steep size distribution compared to C2 and C3 at 4.06 m/s stirrer speed. When compared to the slope value changes of compositions C5 and C6, these compositions couldn't provide a more steep size distribution compared to monosized compositions. This result was obtained with calcite tests as well.

4.1.2.3. Tri-Modal Composition Tests

There tested 2 different tri-modal distribution. Particle Size Distribution graphs of the products obtained as a result of tests performed with composition C7 which contains 3 different sizes of media in 33% of each other and composition C8 which contains 10% 1.5 mm, 25% 2.5mm, and 65% 4 mm are shown in Figure 43 and 44.

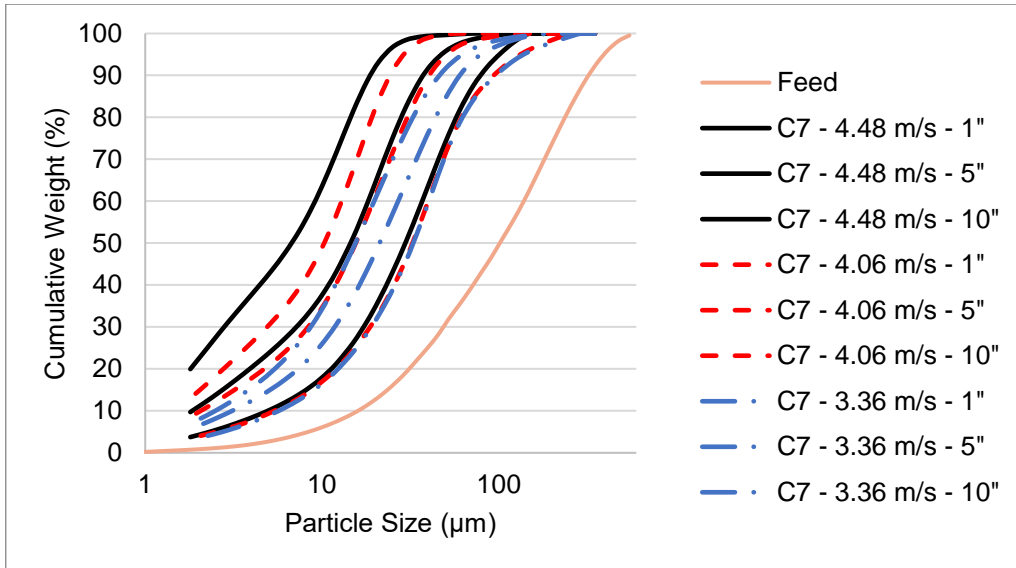


Figure 43. Particle Size Distribution Plots of Clinker Tests with C7

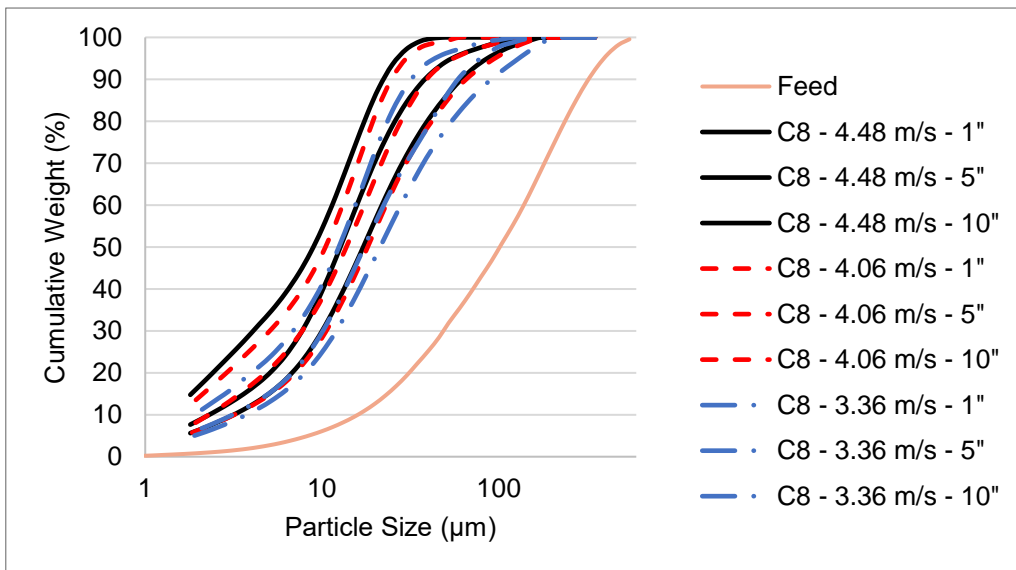


Figure 44. Particle Size Distribution Plots of Clinker Tests with C8

The comparison of tri-modal and monosized compositions are shown in Figure 45.

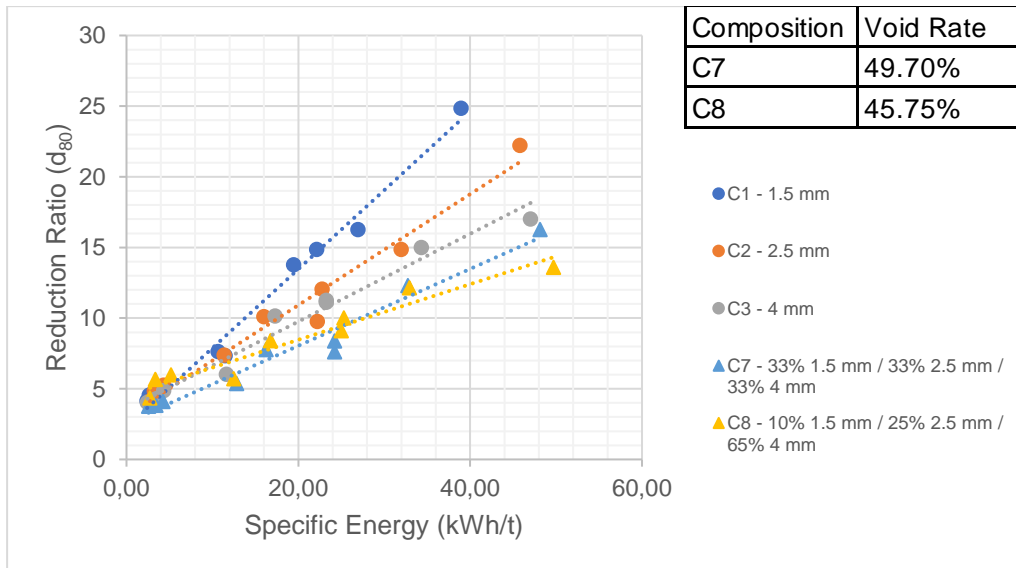


Figure 45. Specific Energy and Reduction Ratio Relationship of Tri-modal and Monosized Compositions for Clinker and the Void Rates of C7 and C8

Compositions C7 and C8, when compared to monosized compositions cannot provide an efficient grinding process in terms of reduction ratio, these results are in agreement with the tests performed with calcite. When tri-modal compositions were examined, C7 needs 25% more energy and C8 needs 50% more compared to composition C3 for the same size reduction rates. When the reduction ratios and the volume rates were compared, the effect observed with calcite was also observed for the clinker tests.

To discuss the steepness of the size distribution of tri-modal compositions, n values of monosized and tri-modal compositions are shown in Table 14.

Table 14. n Values of Monosized and Tri-modal compositions for Clinker

10"	C1	C2	C3	C7	C8
4.48 m/s	1.11	1.1	0.9	0.95	1.04
4.06 m/s	0.95	0.99	0.99	1.07	1.08
3.36 m/s	1.1	1.15	1.12	1.09	1.13

Composition C7 and C8 were examined in terms of the slope values, compared to monosized media. Composition C7 provides a less steep size distribution at

4.48 m/s compared to monosized media. The difference may be up to 0.16. However, this composition provides a slope value increase with a range between 0.8 to 1.2 at 4.06 m/s. At 3.36 m/s stirrer speed, C7 has the same steepness as monosized compositions. As the only difference, at 4.48 m/s stirrer speed which is a 0.9 increase compared to the C7, composition C8 has a similar steepness effect at all stirrer speeds.

Specific energy and size reduction data obtained from all of the grinding tests performed with clinker are shown together in Figure 46.

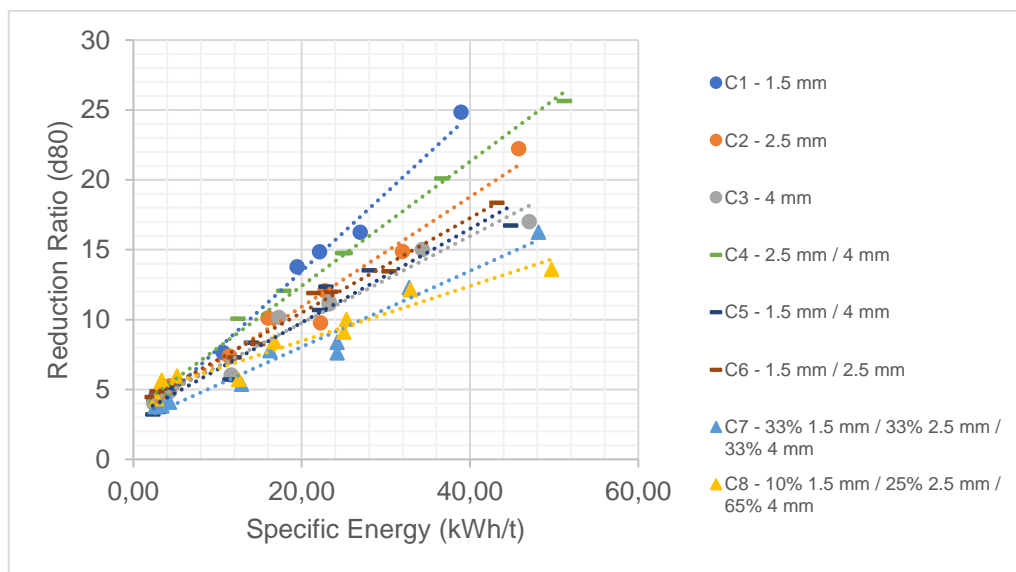


Figure 46. Specific Energy and Reduction Ratio Relationship of All Compositions for Clinker

When the 8 compositions used in the tests were evaluated and compared for specific energy values for the same reduction ratio, they have the same order for both low and high energy levels as $C1 < C4 < C2 < C3 \approx C5 \approx C6 < C7 < C8$. Although there are differences observed in the general evaluation due to the material characteristics, in the tests performed with the bi-modal and tri-modal compositions compared with the monosized compositions associated with them, the results which were observed for clinker has a similarity with results of tests performed with calcite.

As a result of batch grinding tests with clinker, several conclusions may be drawn.

- Composition C4 provides an energy-efficient grinding operation for the same size reduction. This efficiency may be up to 28% compared to C2 and 50% compared to C3
- The steepness can be adjusted with both bi-modal and tri-modal compositions, however, the compositions' size reduction effects should be considered.
- Tri-modal compositions provide coarser products compared to monosized and bi-modal compositions.

In the following section, the data obtained from the grinding tests performed with copper ore are discussed. Also, the data of the tests with copper ore were examined for its similarity to the results of the grinding tests performed with calcite and clinker.

4.1.3. Results of Copper Grinding

The study was carried out with the grinding tests performed at 3 different stirrer speeds with a d_{80} value of 99 μm , and d_{50} value of 12 μm copper ore, and 8 different media compositions that were also applied for calcite and clinker. The data obtained from these tests are discussed in the following section.

4.1.3.1. Monosized Composition Tests

The batch grinding tests were performed with compositions, C1, C2 and C3. Particle size distribution plots of the products obtained with composition C1, C2, and C3 are shown in Figures 47, 48, and 49.

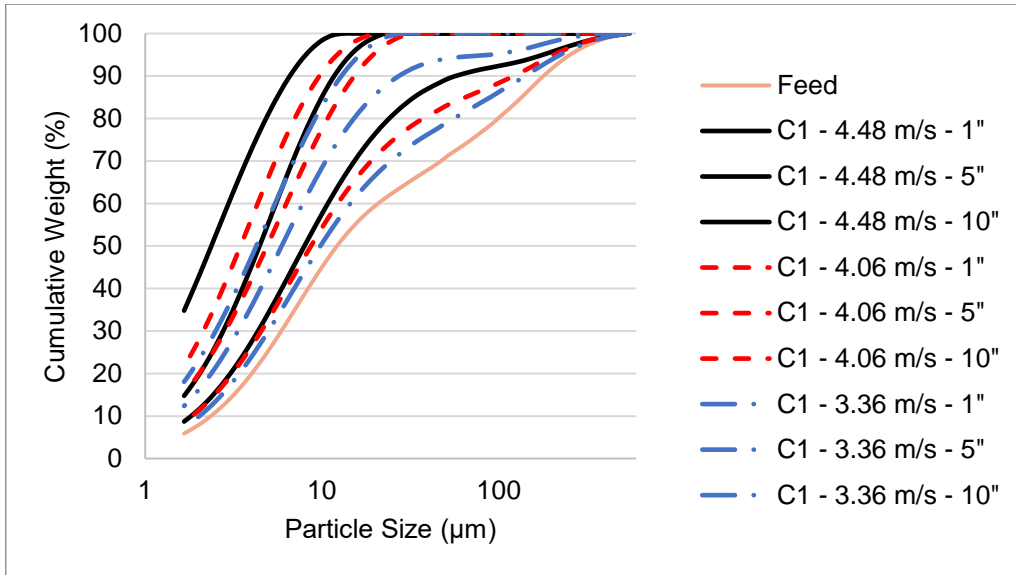


Figure 47. Particle Size Distribution Plots of Copper Tests with C1

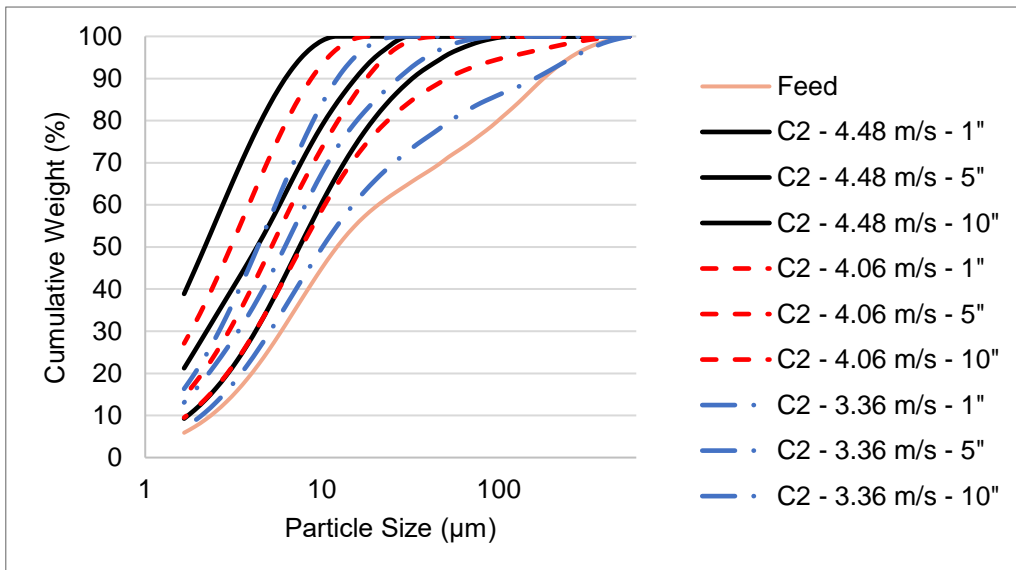


Figure 48. Particle Size Distribution Plots of Copper Tests with C2

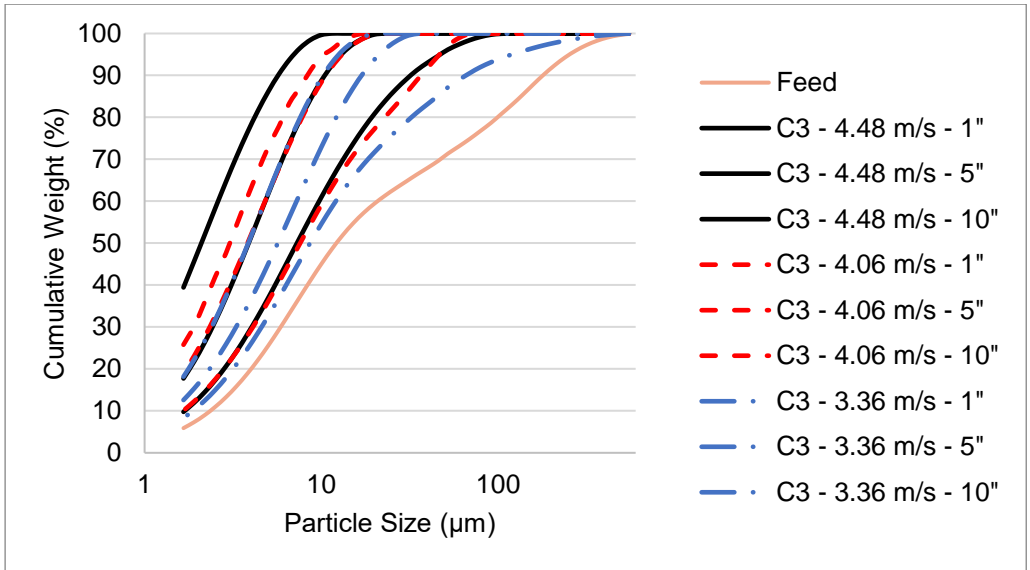


Figure 49. Particle Size Distribution Plots of Copper Tests with C3

Specific energy and reduction ratio relationship plots of compositions C1, C2, and C3 are shown in Figure 50.

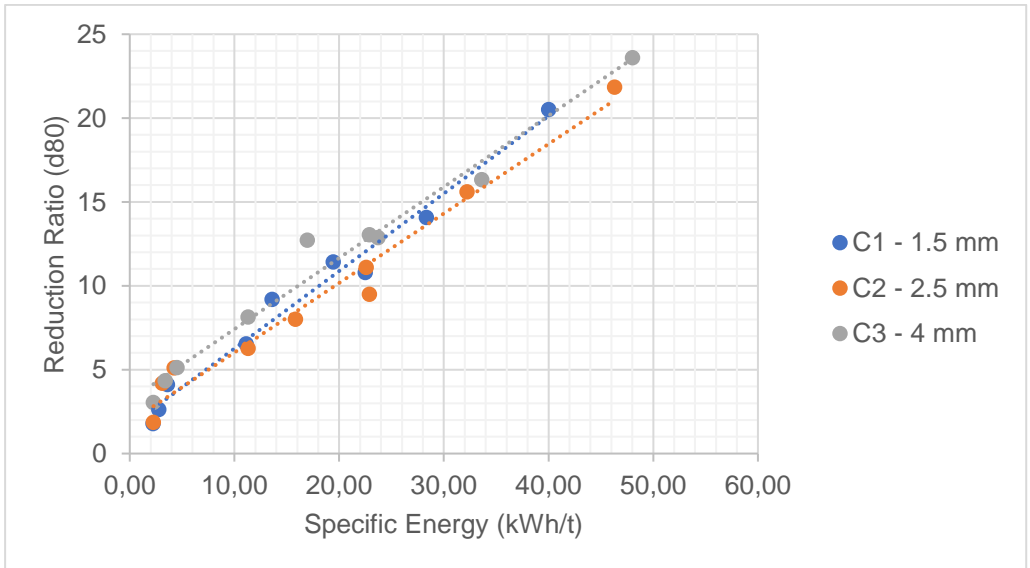


Figure 50. Specific Energy and Reduction Ratio Relationship of C1, C2 and C3 for Copper

When the results of the tests with composition C1, C2, and C3 were compared, no media diameter dependent effects were observed for the same energy levels. Although there is a $C3 > C1 > C2$ relationship between the monosized compositions, the reduction ratio change between the compositions is less than 7%. The reason why the inverse correlation between reduction ratio and media diameter obtained from the test performed with calcite and clinker cannot be said for copper is thought to be in relation to the feed particle size distribution. It has also been reported in the literature that the effect on the reduction rate appears to be more rapid for coarse feed compared to thin feed [32].

The effects of compositions C1, C2, and C3 which have the same reduction ratios at the same energy levels, on the slope value for particle size distribution over the n values were discussed. The n values for the monosized compositions are shown in Table 15.

Table 15. n Values of C1, C2 and C3 for Copper

10"	C1	C2	C3
4.48 m/s	1.35	1.29	1.4
4.06 m/s	1.35	1.27	1.37
3.36 m/s	1.24	1.31	1.39

When the slope values of the products obtained after 10 minutes of grinding with compositions C1, C2, and C3 were examined, it was observed that relatively similar results with a difference range between 0.1 – 0.15 at different stirrer speeds were obtained.

The study was carried out with bi-modal compositions. In the following section, the results obtained with these compositions are discussed and compared with the monosized media compositions.

4.1.3.2. Bi-Modal Composition Tests

Within the scope, 3 different bi-modal distributions were tested. The particle size distribution plots for the products obtained from the grinding tests performed with C4, C5, and C6 compositions are shown in Figures 51, 52, and 53.

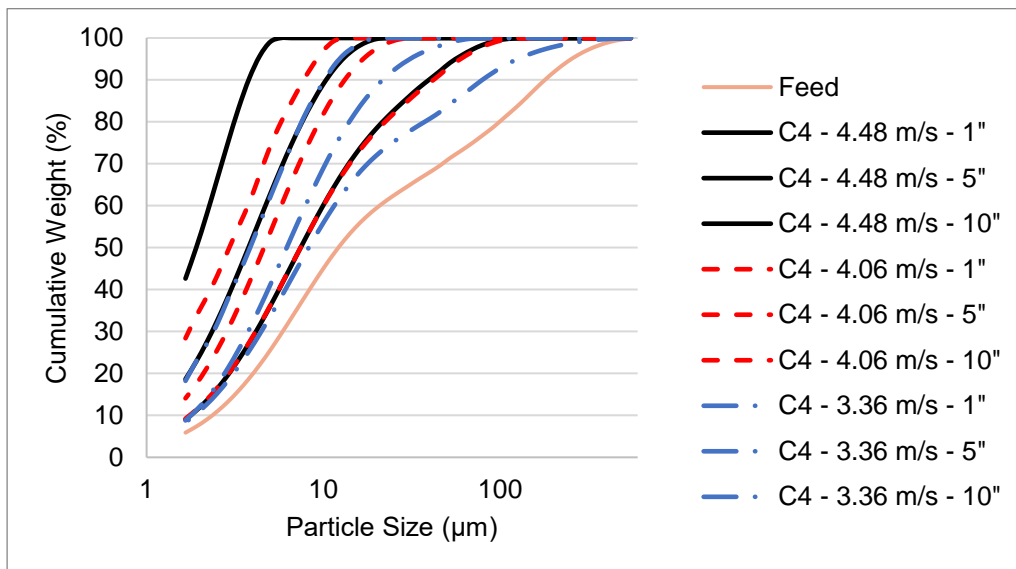


Figure 51. Particle Size Distribution Plots of Copper Tests with C4

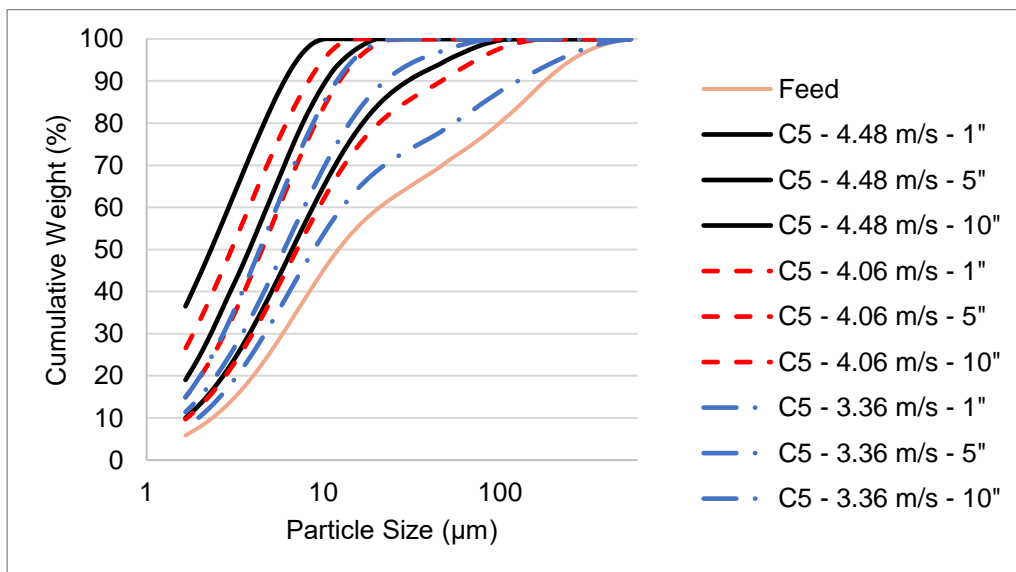


Figure 52. Particle Size Distribution Plots of Copper Tests with C5

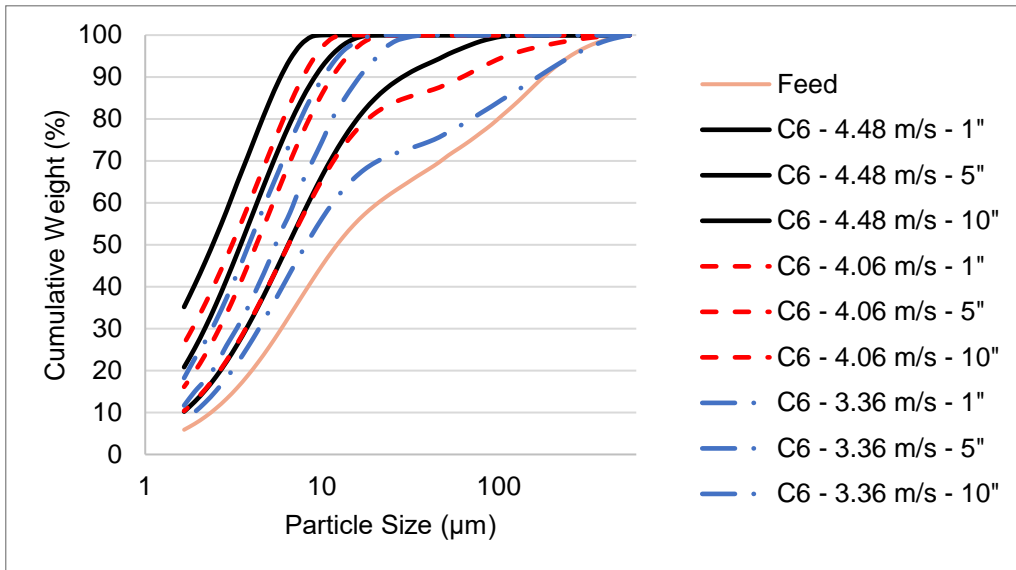


Figure 53. Particle Size Distribution Plots of Copper Tests with C6

Specific energy and reduction ratio relationship plots of compositions C4, C5, and C6 are shown in Figure 54.

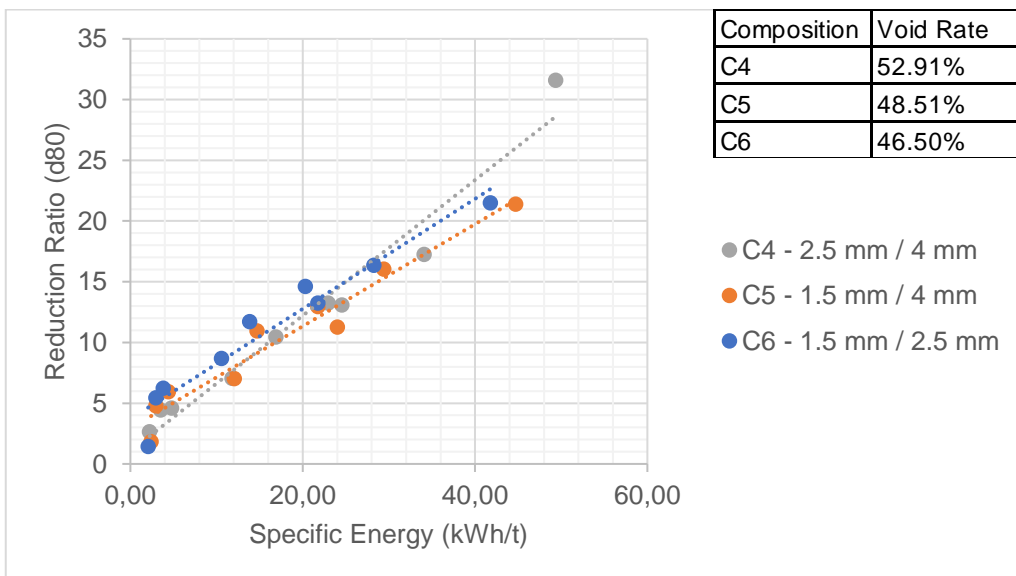


Figure 54. Specific Energy and Reduction Ratio Relationship of C4, C5, C6 for Copper, and the Void Rates

When bi-modal compositions were compared, for the same reduction ratio, C4 provides a 9% more efficient grinding operation compared to C5 and 21% more compared to C6 on the energy consumption basis. A relatively different effect was observed among the bi-modal compositions from the results obtained from the grinding tests with calcite and clinker. The difference is based on the fact that the bi-modal compositions have similar effects on copper ore, unlike calcite and clinker. A similar situation was observed with monosized compositions that provide the same effects with each other regarding the change of the feed rate.

Specific energy and size reduction values obtained from tests performed with composition C4 were compared to 2.5 mm and 4 mm diameter media. This comparison is shown in Figure 55.

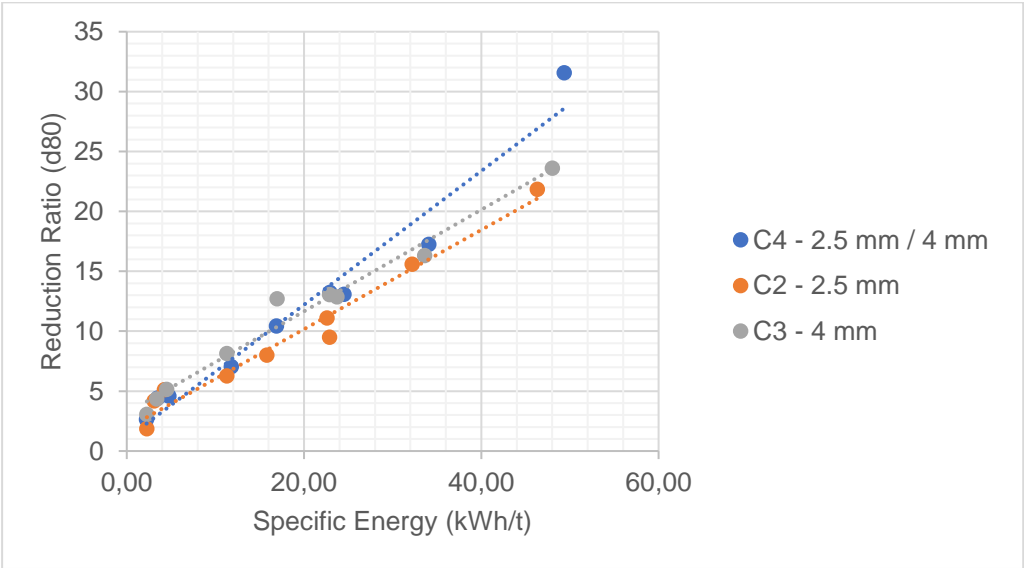


Figure 55. Specific Energy and Reduction Ratio Relationship of C2, C3 and C4 for Copper

When the data were examined, it was observed that the bi-modal media composition provides higher reduction ratios than monosized compositions at high energy levels. At lower energy levels (<10 kWh/t), all compositions have the same size reduction effect as calcite and clinker tests. Composition C4 provides a 22% decrease in energy consumption compared to 2.5 mm diameter media and a 33% compared to 4 mm diameter media.

The comparison of composition C5 and the monosized media it contains are shown in Figure 56.

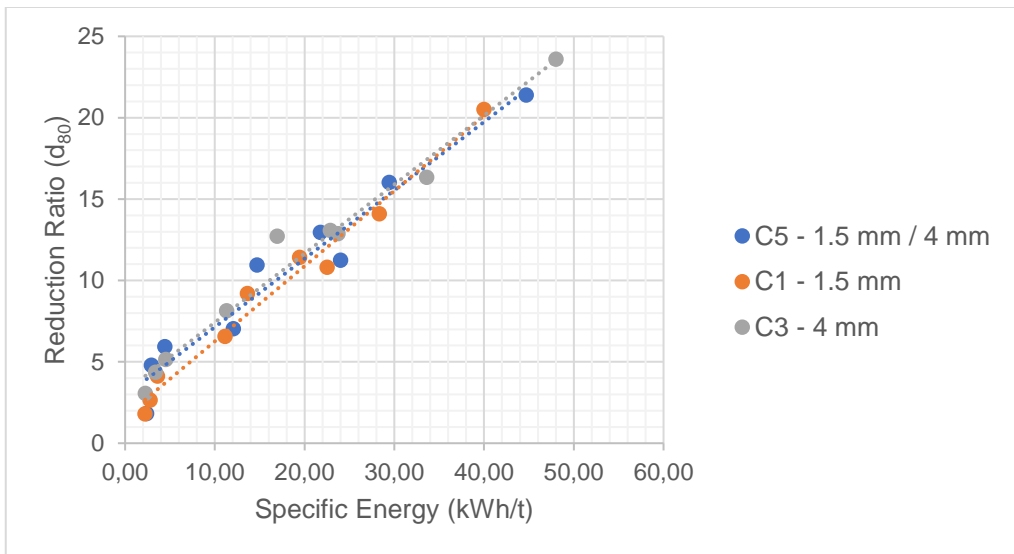


Figure 56. Specific Energy and Reduction Ratio Relationship of C1, C3, and C5 for Copper

Composition C5 has the same reduction ratio as the monosized compositions it contains for all energy levels. This situation was also obtained with calcite and clinker tests. The comparison of composition C6 with compositions C1 and C2 is shown in Figure 57.

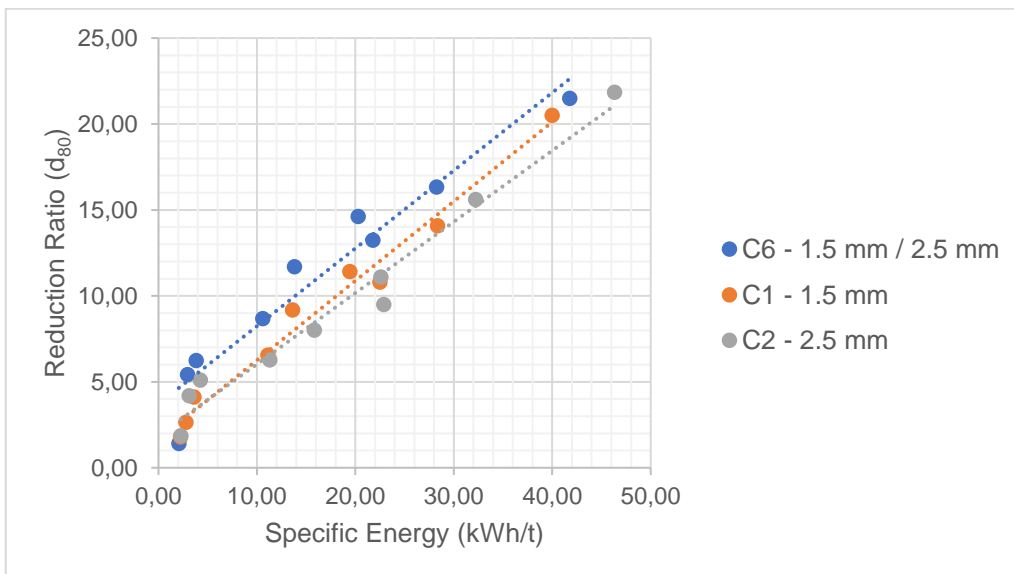


Figure 57. Specific Energy and Reduction Ratio Relationship of C1, C2, and C6 for Copper

Unlike the results of calcite and clinker tests, composition C6 provided a finer product compared to C1 and C2. For the same size reduction values, C6 provides an energy-efficient grinding operation with a 25% decrease in energy consumption compared to C1 and a 50% decrease compared to C2.

The slope values of the bi-modal and monosized compositions are shown in Table 16.

Table 16. *n* Values of Monosized and Bi-modal Compositions for Copper

10 ⁿ	C1	C2	C3	C4	C5	C6
4.48 m/s	1.35	1.29	1.4	1.6	1.32	1.35
4.06 m/s	1.35	1.27	1.37	1.28	1.33	1.33
3.36 m/s	1.24	1.31	1.39	1.38	1.38	1.44

Compared to compositions C2 and C3 which have similar slope characteristics, the product obtained from the grinding tests for composition C4, has a more steep size distribution. This difference may be up to 0.31 for C4 when compared to monosized compositions. When the steepness changes were examined, no differences were observed between C5 and monosized compositions. When the effect of composition C6 on the slope value was examined, no effects were observed for 4.48 m/s and 4.06 m/s stirrer speeds compared to monosized compositions. However, when compared to composition C2 at 3.36 m/s stirrer speed, composition C6 has a 0.2 more steep size distribution compared to C1 and 0.13 more compared to C2.

4.1.3.3. Tri-Modal Composition Tests

There tested 2 different tri-modal distribution. The particle size distribution plots of the products obtained from the tests performed with composition C7 and C8 are shown in Figures 58 and 59.

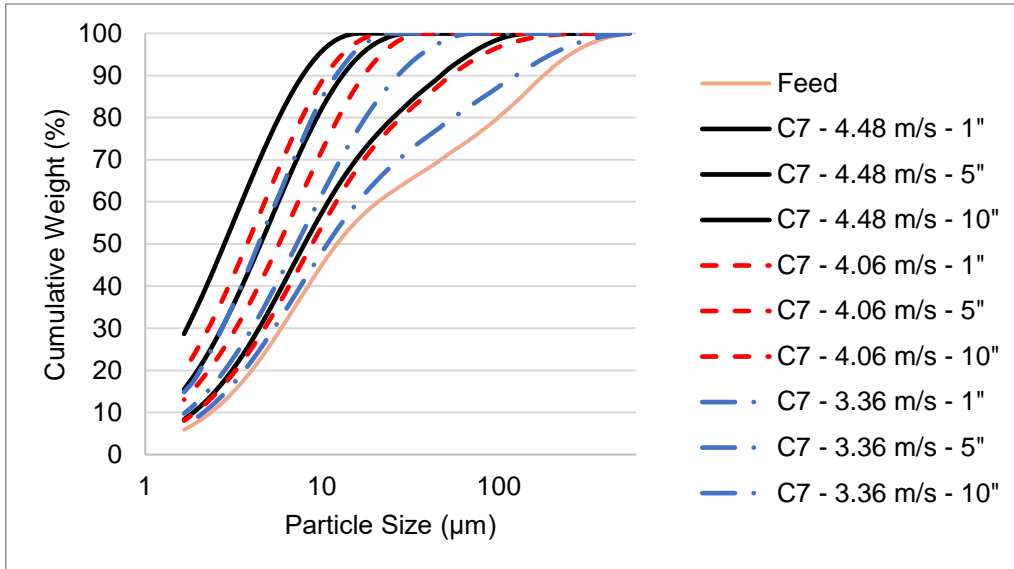


Figure 58. Particle Size Distribution Plots of Copper Tests with C7

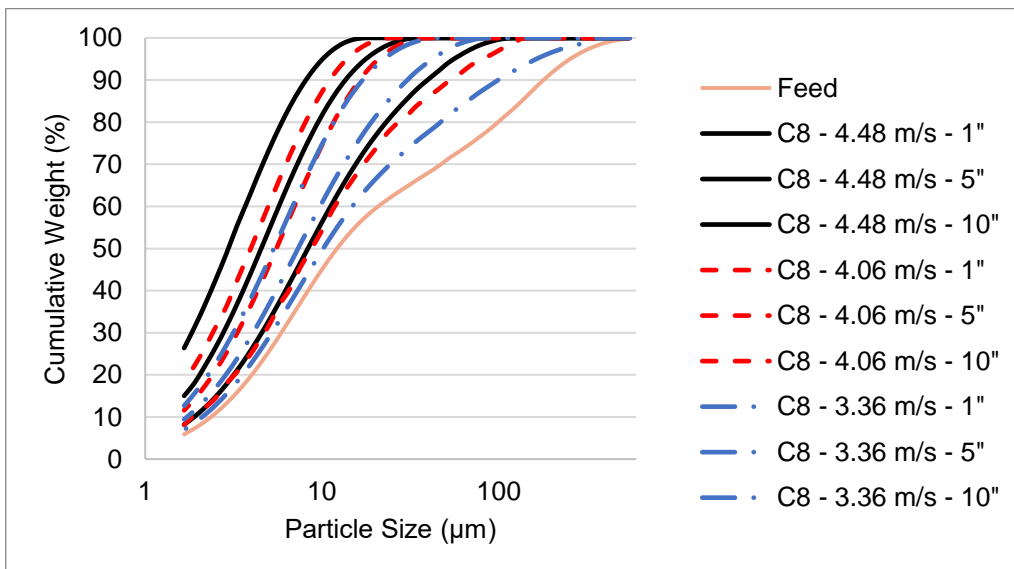


Figure 59. Particle Size Distribution Plots of Copper Tests with C8

The comparison of tri-modal and monosized compositions are shown in Figure 60.

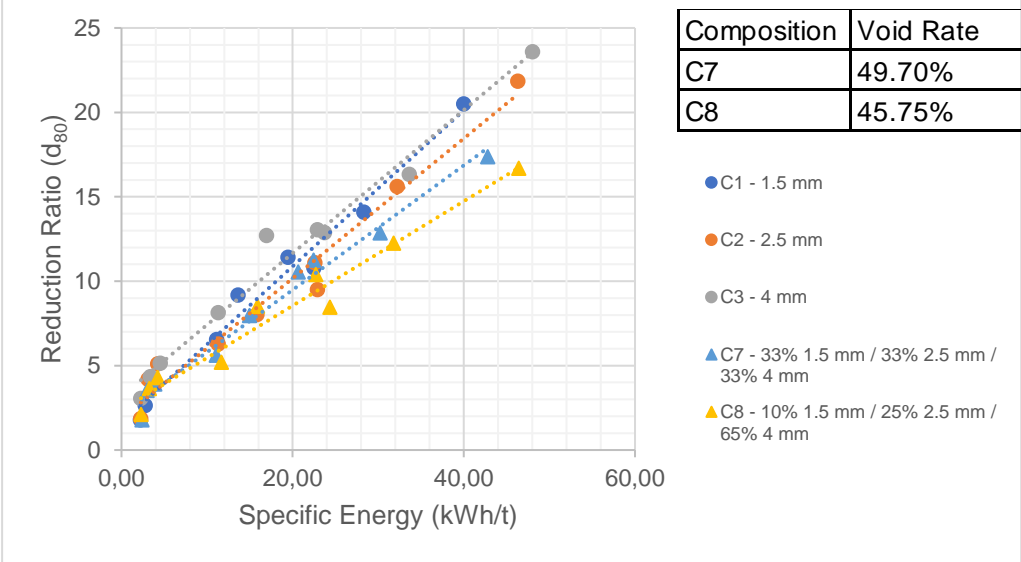


Figure 60. Specific Energy and Reduction Ratio Relationship of Tri-modal and Monosized Compositions for Copper and the Void Rates of C7 and C8

When compositions C7 and C8 were compared with the monosized compositions, it was seen that an efficient grinding process in terms of reduction ratio could not be provided, similar to the results observed with tests performed with calcite and clinker. Composition C7 provides a 12% more energy-consuming grinding operation while C8 provides 25% more compared to C2 for the same reduction ratio value. When the reduction ratios and the volume rates were compared, the effect which could be observed with calcite and clinker tests also observed with copper tests.

To discuss the steepness of the size distribution of tri-modal compositions, *n* values of monosized and tri-modal compositions are shown in Table 17.

Table 17. *n* Values of Monosized and Tri-modal compositions for Copper

10"	C1	C2	C3	C7	C8
4.48 m/s	1.35	1.29	1.4	1.34	1.36
4.06 m/s	1.35	1.27	1.37	1.35	1.33
3.36 m/s	1.24	1.31	1.39	1.38	1.24

When compositions C7 and C8 were examined in terms of slope value, compared to monosized media, no effects on steepness were examined at any stirrer speeds. Specific energy and size reduction data obtained from all of the grinding tests performed with copper are shown together in Figure 61.

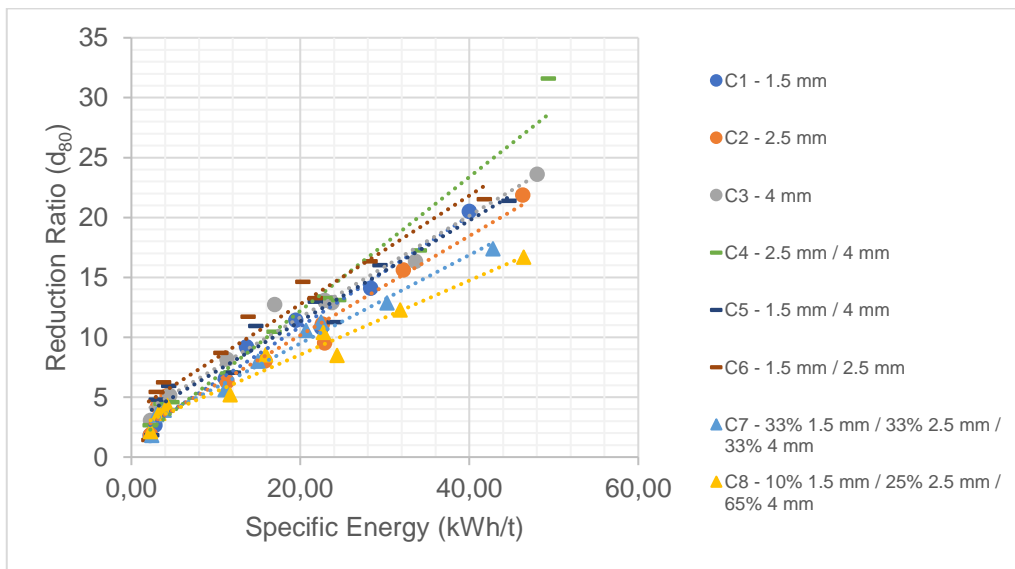


Figure 61. Specific Energy and Reduction Ratio Relationship of All Compositions for Copper

When the compositions were evaluated for the high energy levels in general terms, the order is $C4 < C1 \approx C2 \approx C3 \approx C5 \approx C6 < C7 < C8$, by the specific energy values that were observed for the same reduction ratio values. This order changes as $C6 < C1 \approx C3 \approx C4 \approx C5 < C2 < C7 < C8$ at low energy levels. It is thought that the effect occurs due to the fact that the feed particle size is much finer than calcite and clinker.

Below some important points are summarized;

- Composition C4 provides an energy-efficient grinding operation for the same size reduction. This efficiency may be up to 22% compared to C2 and 33% compared to C3
- Composition C5 couldn't increase the grinding efficiency for copper, like calcite and clinker. However, C6 could provide a finer product compared to monosized compositions due to the finer feed particle size. It is thought, in the absence of the coarse particles that calcite and clinker contain, the effect of the grinding surface that increases due to the decreasing media diameter provides a finer product unlike the grinding tests with calcite and clinker that operated with composition C6.
- The slope value can be changed by the composition C4 between 0.07 and 0.31 to provide a more steep size distribution.
- Tri-modal compositions had led to higher specific energy consumption when compared to other configurations.

4.2. Wear Tests Results

The wear data were analyzed to discuss the economic impact of composition C4, which provides finer products and a more steep size distribution. The wear values for composition C2, C3, and C4 are shown in Figure 62.

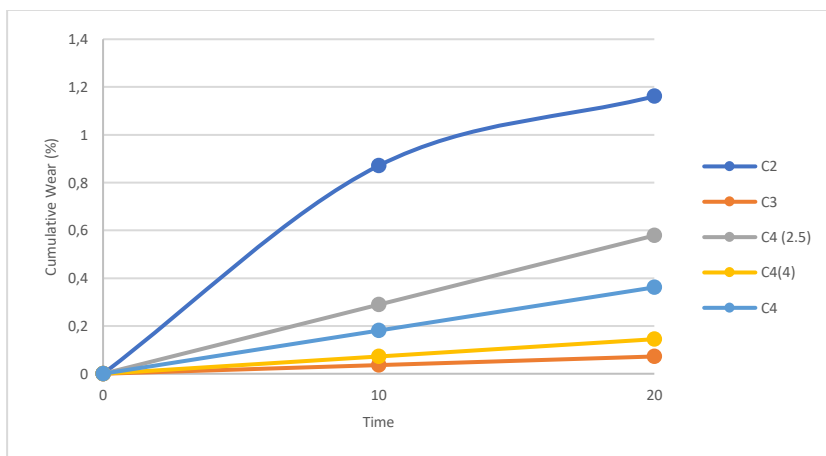


Figure 62. Wear rates of C2, C3 and C4

Tests performed to show that 2.5 mm diameter media have much lower durability compared to 4 mm diameter media due to the linear correlation between the media strength and diameter. However, this effect is reduced when 2.5 mm diameter media is mixed with 4 mm diameter media as a bi-modal composition. This is thought to be due to the high-stress intensity, which causes the 2.5 mm diameter media to be easily deformed. When two media with different diameters are used together, this effect can be absorbed by the durable 4 mm diameter media. To express this reduction mathematically, it is possible to reduce the wear rate by 2.5 mm up to 50% by using bi-modal composition.

5. CONCLUSION

The study aimed to provide an insight on energy optimization in the stirred mills by investigating the influences of the bead composition on grinding results. In this regard, Mono, bi-modal, tri-modal distributions were prepared and tested for different operating conditions and materials. It is also aimed to provide valuable information for continuous operated dry stirred milling as the application is steadily increasing within the recent years.

It has been observed that different bi-modal compositions had improved grinding efficiency at high and low energy levels, for different materials and at different tip speeds compared to the monosized compositions that bi-modal composition contains. For the mixture of 2.5 mm and 4 mm beads, this effect can be defined as an increase in reduction ratio and a reduction in the energy consumption, steep size distribution, and the provision of a 50% wear reduction for the grinding media. For such a grinding media composition energy saving of 56% was achieved when compared to mono sizes.

The steepness of the distributions can be adjusted with both bi-modal and tri-modal compositions. Composition C4 provides a more steep size distribution up to 0.7 (n number of RRSB) while producing finer products compared to monosized compositions.

The breakage possibility of coarse particles directly affects the grinding efficiency and the steepness. Steep size distribution can be provided with bi-modal compositions at stirrer speeds that enable the coarse media to break down the material in the calcite and clinker tests. However, bi-modal compositions couldn't produce a finer product than monosized compositions in the calcite and clinker tests. But, in the grinding tests with copper which has a finer feed particle size, for the high energy levels, the bi-modal composition C4 increases the reduction ratio and decreases the energy consumption compared to 1.5 mm media composition.

The wear is an important issue for a grinding operation. Within the study, grinding media wear measurements were conducted for the most efficient bead composition (mix of 2.5 and 4). The measurements proved that it was possible to reduce the wear up to 50% in case the bi-modal distribution was preferred. Further studies on this subject will provide a more consistent economic evaluation of the subject at an industrial scale.

The flow characteristics of different sized compositions have vital importance to achieve a positive effect on the grinding operation with bi-modal compositions. Still, it may be possible to achieve similar effects with tri-modal distributions by conducting further studies on the flow characteristics of multi-modal distributions. To investigate that, further studies about the stirrer type should be conducted. Similar tests should also be carried out on continuous mills in order to observe the economic and performance effects of such a study on an operational scale.

It is recommended to link the knowledge gained within the study to the subsequent enrichment processes or end use applications. In this regard, influences of the shape of size distribution on cement strength properties, flotation or other beneficiation methods can be studied and valuable contribution can be made to the literature.

REFERENCES

- [1] C.C. Harris, On the Rate of Energy in Comminution, A review of Physical and Mathematical Principles, Transaction IMM, 37-57, **1965**.
- [2] N.A. Madloul, R. Saidur, M.S. Hossain, N.A. Rahim, Renewable and Sustainable Energy Reviews, A Critical Review on Energy Use Savings in the Cement Industries, 15 (**2011**) 2042-2060.
- [3] Y.H. Huang, Y.L. Chang, T. Fleiter, Energy Policy, A Critical Analysis of Energy Efficiency Improvement Potentials in Taiwan's Cement Industry, 96 (**2016**) 14-26.
- [4] T.J. Napier-Munn, S. Morrell, R.D. Morrison, T. Kojovic, Mineral Comminution Circuits: Their Operation and Optimisation, Vol. 2, Brisbane, **1996**.
- [5] A. Jankovic, Minerals Engineering, Variables Affecting the Fine Grinding of Minerals Using Stirred Mills, 16 (**2003**) 337-345.
- [6] A.G. Doll, Fine Grinding, a Refresher, 49th Annual Canadian Mineral Processors Operators Conference, Ottawa, Canada, **2017**.
- [7] A. Gupta, D.S. Yan, in Mineral Processing Design and Operations: An Introduction (Second Edition), A. Gupta, D.S. Yan (Eds.), Elsevier, Chapter 10, **2016**.
- [8] H. Cho, J. Kwon, K. Kim, M. Mun, Powder Technology, Optimum choice of the make-up ball sizes for maximum throughput in tumbling ball mills, 246 (**2013**) 62--634.
- [9] T. Yokoyama, Y. Inoue, in Handbook of Powder Technology, A.D. Salman, M. Ghadiri, M.J. Hounslow (Eds.), Vol. 12, Elsevier, Chapter 10, **2007**
- [10] B.D. Burford, E. Niva, Comparing energy efficiency in grinding mills, Metallurgical Plant Design and Operating Strategies Conference (MetPlant 2008), Perth, Australia, 18--19 August, **2008**.
- [11] A. Jankovic, Journal of Mining and Metallurgy A: Mining, Fine grinding in Australian Minerals Industry, 36 (**2000**) 51-61.

- [12] L. Taylor, D. Skuse, S. Blackburn, R. Greenwood, Powder Technology, Stirred Media Mills in the Mining Industry: Material Grindability, Energy-Size Relationships, and Operating Conditions, 369 (2020) 1-16.
- [13] A. Jankovic, W. Valery, G. Clarke, Design and Implementation of an AVC Grinding Circuit at BHP Billiton Cannington, 4th International Conference on Autogenous and Semigenous Grinding Technology (SAG 2006), Vancouver, 23-27 September 2006, University of British Columbia, 2006.
- [14] O.D. Neikov, Handbook of Non-Ferrous Metal Powders (Second Edition), Elsevier, 2019.
- [15] A. Jankovic, Mathematical Modelling of Stirred Mills, Ph. D Thesis, University of Queensland, Brisbane, 1999.
- [16] M. Gao, M. Young, P. Allum, IsaMill Fine Grinding Technology and Its Industrial Applications at Mount Isa Mines, Proc. 34th Annual Meeting of the Canadian Mineral Processors, Ottawa, 22-24 January 2002, The Canadian Mineral Processors, Ottawa, 2002, p. 171-188.
- [17] Union Process, The Evolution of Milling Technology, Union Process Corporate Brochure, <https://unionprocess.com/pdfs/up-corporate-brochure.pdf> (Erişim tarihi: 17 Kasım 2020).
- [18] A. Kwade, J. Schwedes, in Handbook of Powder Technology, A.D. Salman, M. Ghadiri, M.J. Hounslow (Eds.), Vol. 12, Elsevier, Chapter 6, 2007.
- [19] Metso, VERTIMILL® Grinding Mills & Stirred Media Detritor Brochure, <https://pdf.directindustry.com/pdf/metso-corporation/vertimill-grinding-mills-stirred-media-detritor-brochure/9344-774345-2.html> (Erişim Tarihi: 18 Kasım 2020)
- [20] A. Gupta, D.S. Yan, Mineral Processing Design and Operation: An introduction (2nd Edition), Elsevier, 2006.
- [21] B.A. Wills, J.A. Finch, in Wills' Mineral Processing Technology (8th Edition)- An Introduction to the Practical Aspects of Ore Treatment and Mineral Recovery, B.A. Wills, J.A. Finch (Eds.), Butterworth-Heinemann, Chapter 7, 2016.
- [22] C.H. Lofthouse, F.E. Johns, Minerals Engineering, The Svedala (ECC International) Detritor and the Metals Industry, 12 (2) (1999) 205-217.

- [23] S. Hochberg, E.I. du Pont de Nemours & Company, Process for Dispersing Pigments in Film-Forming Materials, **1948**.
- [24] Glencore Technology, IsaMill™: Breaking the Boundaries, IsaMill Brochure, <http://www.isamill.com/EN/Downloads/Brochures/IsaMillBrochure.pdf> (**Erişim Tarihi: 13 Kasım 2020**).
- [25] A.J. Lynch, C.A. Rowland, The History of Grinding, Society for Mining, Metallurgy, and Exploration, **2005**.
- [26] J.D. Pease, M.F. Young, D.C. Curry, Fine Grinding as Enabling Technology- The IsaMill, Proc. 6th Annual Crushing and Grinding Conference, Perth, 29-30 March **2004**.
- [27] N. Stehr, International Journal of Mineral Processing, Recent Developments in Stirred Ball Milling, 22 (**1988**) 431-444.
- [28] Svedala, Zement-Kalk-Gips, Energy-Saving Ultra Fine Grinding with SALA Agitated Mill. 46 (9) (**1993**) 600-601.
- [29] M. Becker, J. Schwedes, Powder Technology, Comminution of Ceramics in Stirred Media Mills and Wear of Grinding Beads, 105 (1-3) (**1999**) 374-381.
- [30] M. Gao, E. Forssberg, Powder Technology Prediction of Product Size Distributions for a Stirred Ball Mill, 84 (**1995**) 101-106.
- [31] J. Zheng, C.C. Harris, P. Somasundaran, Powder Technology, A study on Grinding and Energy Input in Stirred Media Mills, 86 (2) (**1996**) 171-178.
- [32] O. Altun, Investigation of Dry Horizontal Stirred Milling Applications for Cement Grinding Circuits, Doktora Tezi, Hacettepe Üniversitesi Fen Bilimleri Enstitüsü, Ankara, **2013**.
- [33] Y. Wang, E. Forssberg, J. Sachweh, International Journal of Mineral Processing, Dry Fine Comminution in a Stirred Media Mill- MaxxMill, 74 (**2004**) 64-75.
- [34] S. Dikmen, Modelling of the Performance of Stirred Media Mills in Regrinding Circuits, Ph. D Thesis, Hacettepe University, Ankara, **2008**.
- [35] H. Fadhel, C. Frances, Powder Technology, Wet Batch Grinding of Alumina in a Stirred Bead Mill, 119 (2-3) (**2001**) 257-268.

- [36] C.C. Pilevneli, S. Kizgut, T. Toroglu, D. Cuhadaroglu, E. Yigit, Powder Technology, Open and Closed Circuit Dry Grinding of Cement Mill Rejects in a Pilot Scale Vertical Stirred Mill, 139 (2) (**2004**) 165-174.
- [37] L.Y. Sadler III, D.A. Stanley, D.R. Brooks, Powder Technology, Attrition Mill Operating Characteristics, 12 (1) (**1975**) 19-28.
- [38] P. Prziwara, S. Breitung-Faes, A. Kwade, Minerals Engineering, Impact of the Powder Flow Behavior on Continuous Fine Grinding in Dry Operated Stirred Media Mills, 128 (**2018**) 215-223.
- [39] Y.B. Farber, B. Durant, N. Bedesi, Minerals Engineering, Effect of Media Size and Mechanical Properties on Milling Efficiency and Media Consumption, 24 (3-4) (**2011**) 367-372.
- [40] M.J. Mankosa, G.T. Adel, R.H. Yoon, Powder Technology, Effect of Media Size in Stirred Ball Mill Grinding of Coal, 49 (1) (**1986**) 75-82.
- [41] A. Kwade, L. Blecher, J. Schwedes, Powder Technology, Motion and Stress Intensity of Grinding Beads in Stirred Media Mill Part 2: Stress Intensity and Its Effect on Comminution, 86 (1) (**1996**) 69-76.
- [42] S. Mende, F. Stenger, W. Peukert, J. Schwedes, Journal of Materials Science, Production of Sub Micron Particles by Wet Comminution in Stirred Media Mills, 39 (16-17) (**2004**) 5223-5226.
- [43] H. Persson, E. Forssberg, Aufbereitungs Technik, Fine Grinding of a Magnetite Ore with a Stirred Ball Mill, 35 (6) (**1994**) 307-320.
- [44] A.E. Schollbach, Aufbereitungs Technik, Influence of the Grinding Media Size on Comminution in Stirred Ball Mills with Additional Introduction of Vibrations, 40 (6) (**1999**) 259-267.
- [45] Y. Wang, E. Forssberg, Minerals Engineering, Product Size Distribution in Stirred Media Mills, 13 (4) (**2000**) 459-465.
- [46] W. Gao, E. Forssberg, International Journal of Mineral Processing, A Study on the Effect of Parameters in Stirred Ball Milling, 37 (1-2) (**1993**) 45-59.
- [47] R. Sivamohan, P. Vachot, Powder Technology, A Comparative Study of Stirred and Vibratory Mills for the Fine Grinding of Muscovite, Wollastonite and Kaolinite, 61 (2) (**1990**) 518-523.

- [48] S. Strasser, R.A. Somani, A.K. Dembla, Zement-Kalk-Gips, Improvements in the Production of Raw Meal and Cement by the Combined Use of Roller Press and V-Separator, 3 (50) (1997) 140-146.
- [49] R.R. Klimpel, W. Manfroy, Industrial and Engineering Chemistry Process Design and Development, Chemical Grinding Aids for Increasing Throughput in the Wet Grinding of Ores, 17 (4) (1978) 518-523.
- [50] P.A. Rehbinder, N.A. Kalinkovskaya, J. Tech. Phys., Decrease in The Surface Energy of Solid-Bodies and The Work of Dispersion During Formation of an Adsorption Layer, (2) (1932) 726-755.
- [51] J. Zheng, C.C. Harris, P. Somasundaran, Powder Technology, The Effect of Additives on Stirred Media Milling of Limestone, 91 (3) (1997) 173-179.
- [52] P.C. Kapur, T.W. Healy, P.J. Scales, D.V. Boger, D. Wilson, International Journal of Mineral Processing, Role of Dispersant in Kinetics and Energetics of Stirred Ball Mill Grinding, 47 (1-2) (1996) 141-152.
- [53] H. Choi, W. Lee, D.U. Kim, S. Kumar, S.S. Kim, H.S. Chung, J.H. Kim, Y.C. Ahn, Minerals Engineering, Effect of the Grinding Aids on the Grinding Energy Consumed During Grinding of Calcite in a Stirred Ball Mill, 23 (1) (2010) 54-57.
- [54] P. Prziwara, S. Breitung-Faes, A. Kwade, Minerals Engineering, Comparative Study of the Grinding Aid Effects for Dry Fine Grinding of Different Materials, 144 (2019).
- [55] A. Kwade, C.T. Jayasundara, R.Y. Yang, B.Y. Guo, A.B. Yu, I. Govender, A. Mainza, A. Westhuizen, J. Rubenstein, Powder Technology, 105 (1-4) (1999) 382-388.
- [56] A. Kwade, H. Stender, Aufbereitungs Technik, Constant Grinding Results at Scale-up of Stirred Media Mills, 39 (8) (1998) 373-382.
- [57] A. Jankovic, Minerals Engineering, Media Stress Intensity Analysis for Vertical Stirred Mills, 14 (10) (2001) 1177-1186.
- [58] A. Kwade, Powder Technology, Wet Comminution in Stirred Media Mills - Research and Its Practical Application 105 (1-3) (1999) 14-20.
- [59] A. Kwade, Chemical Engineering Technology, A Stressing Model for the Description and Optimization of Grinding Process, 26 (2) (2003) 199-205.

- [60] P. Prziwara, L.D. Hamilton, S. Breitung-Faes, A. Kwade, Powder Technology, Evaluation of the Capturing of Dry Fine Particles Between Grinding Media by Drop-Weight Tests, 363 (2020) 326-336.
- [61] B. Epstein, Journal of the Franklin Institute, The Material Description of Certain Breakage Mechanisms Leading to the Logarithmic - Normal Distribution, 244 (1947) 471-477.
- [62] A.J. Lynch, Mineral Crushing and Grinding Circuits: Their Simulation, Optimization, Design and Control, Elsevier Scientific, 1977.
- [63] M. Hasan, S. Palaniandy, M. Hilden, M. Powell, Minerals Engineering, Calculating Breakage Parameters of a Batch Vertical Stirred Mill, 111 (2017) 229-237.
- [64] D. Altun, O. Altun, S. Zencirci, Minerals Engineering, Developing a Methodology to Model and Predict the Grinding Performance of the Dry Stirred Mill, 139 (2019).
- [65] P. Radziszewski, Minerals Engineering, Exploring Total Media Wear, 15 (2002) 1073-1087.
- [66] C. Aldrich, Minerals Engineering, Consumption of Steel Grinding Media in Mills- A Review, 49 (2013) 77-91.
- [67] E. Albertin, F. Beneduce Neto, I.O. Teixeira, Tecnologia em Metalurgia e Materiais, Adequação da Composição Química e do Tratamento de Ferros Fundidos de Alto Cromo Utilizando Termodinâmica Computacional, 8 (4) (2011) 223-229.
- [68] I. Fernández, F.J. Belzunce, Materials Characterization, Wear and Oxidation Behavior of High-Chromium White Cast Irons, 59 (6) (2008) 669-674.
- [69] E. Roveri, A.P. Chaves, Tecnologia em Metalurgia, Materiais e Mineração, Mecanismos de Desgaste de Corpos Moedores em Moinhos de Bolas, 8 (4) (2011) 261-266.
- [70] A.R. Sayadi, M.R. Khalesi, M.K. Borji, Minerals Engineering, A Parametric Cost Model for Mineral Grinding Mills, 55 (2014) 96-102.
- [71] J.D. Gates, M.S. Dargusch, J.J. Walsh, S.L. Field, M.J.P. Hermand, B.G. Delaup, J.R. Saad, Wear, Effect of Abrasive Mineral on Alloy Performance in the Ball Mill Abrasion Test, 265 (2008) 865-870.

- [72] A.K. Gangopadhyay, J.J. Moore, *Wear*, The Role of Abrasion and Corrosion in Grinding Media Wear, 104 (**1985**) 49-64.
- [73] F.C. Bond, *Metal Wear in Crushing and Grinding*, Proc. 54th Annual Meeting of American Institute of Chemical Engineers, 3 December 1963, Allis-Chalmers Manufacturing Company, Houston, **1963**.
- [74] I. Iwasaki, R.L. Pozzo, K.A. Natarajan, K. Adam, J.N. Orlich, *International Journal of Mineral Processing*, Nature of Corrosive and Abrasive Wear in Ball Mill Grinding, 22 (1-4) (**1988**) 345-360.
- [75] T.W. Chenje, D.J. Simbi, E. Navara, *Minerals Engineering*, The Role of Corrosive Wear During Laboratory Milling, 16 (7) (**2003**) 619-624.
- [76] L. Blecher, A. Kwade, J. Schwedes, *Powder Technology*, Motion and Stress Intensity of Grinding Beads in Stirred Media Mill. Part I: Energy Density Distribution and Motion of Single Grinding Beads, 86 (1) (**1996**) 59-68.
- [77] J. Theuerkauf, J. Schwedes, *Chemical Engineering and Technology*, Investigation of Motion in Stirred Media Mills, 23 (3) (**2000**) 203-209.
- [78] D. Eskin, O. Zhupanska, R. Hamey, B. Moudgil, B. Scarlett, *Powder Technology*, Microhydrodynamics of Stirred Media Milling, 156 (23) (**2005**) 95-102.
- [79] E.G. Kelly, D.J. Spottiswood, *Introduction to Mineral Processing*, John Wiley & Sons Inc, New York, **1982**.
- [80] F. Concha, L. Magne, L.G. Austin, *International Journal of Mineral Processing*, Optimization of the Make-up Ball Charge in a Grinding Mill, 34 (**1992**) 231-241.
- [81] R.E. Mclvor, *The Effect of Media Sizing on Ball Milling Efficiency*, Comminution Practices, SME Society for Mining, Metallurgy and Exploration, Kawatra, Colorado, 279-292, **1997**.
- [82] L.G. Austin, *Concepts in Process Design of Mills*, *Mining Engineering*, 628-635, **1984**.
- [83] W.H. Duda, *Cement Data Book Volume 1 and Volume 2*, Bauverlag GmbH, Wiesbaden and Berlin, **1985**.

- [84] Metso Inc, Basics in Mineral Processing Handbook, **2002**
- [85] C.T. Jayasundara, R.Y. Yang, A.B. Yu, J. Rubenstein, International Journal of Mineral Processing, Effects of Disc Rotation Speed and Media Loading on Particle Flow and Grinding Performance in a Horizontal Stirred Mill, 96 (1) **(2010)** 27–35.
- [86] O. Altun, H. Benzer, U. Enderle, Minerals Engineering, Effects of Operating Parameters on the Efficiency of Dry Stirred Milling, 43 **(2013)** 58-66.
- [87] P.W. Cleary, M. D. Sinnott, G.G. Pereira, Minerals Engineering, Computational Prediction of Performance for a Full Scale Isamill: Part 1 - Media Motion and Energy Utilisation in a Dry Mill, 79 **(2015)** 220-238
- [88] P. Rosin, E. Rammler, Journal of the Institute of Fuel, The Laws Governing the Fineness of Powdered Coal, 7 **(1933)** 29–36
- [89] A.A. Jeknavorian, E.F. Barry, F. Serafin, Determination of Grinding Aids in Portland Cement by Pyrolysis Gas Chromatography-Mass Spectrometer. Cement and Concrete Research, 28 **(1998)** 1335-1345.
- [90] L.G. Austin, R.R. Klimpel, P.T. Luckie, Process engineering of size reduction: Ball milling, **(1984)** 561
- [91] H. El-Shall, P. Somasundaran, Powder Technology, Physico-Chemical aspects of grinding: a review of use of additives, 38 **(1984)** 275-293
- [92] D.W. Fuerstenau, Grinding aids, Kona, 13, **(1995)** 5-18.
- [93] M. Hasegawa, M. Kimata, M. Shimane, T. Shoji, M. Tsuruta, Powder Technology, The effect of liquid additives on dry ultrafine grinding of quartz, 114 **(2001)** 145-151

[94] N.A. Toprak, O. Altun, H. Benzer, Construction and Building Materials, The effects of grinding aids on modelling of air classification of cement, 160 (2018) 564-573.